# Octa carboxy metal (II) phthalocyanine covalent films as pH sensitive electrochemical sensor for neurotransmitters

**A thesis submitted in fulfilment of the requirements**

**for the degree of**

**MASTER OF SCIENCE**

**of**

**RHODES UNIVERSITY**

**by**

**IPHITHULI MOYO**

**January 2023**

**Acknowledgements**

I would like to express my sincere gratitude to my supervisor, Prof. Philani N. Mashazi for the opportunity to pursue my MSc studies in his research group and assistance to secure funding for the studies. I am grateful for his exceptional guidance, patience and great support while sharing his remarkable knowledge. I wish to thank Dr. Daniel Mwanza for being my day one both in Grahamstown and in the laboratory. I am thankful for his mentorship from the start of defining a phthalocyanine to the end of this Masters road. To all my friends, thank you for making Grahamstown a home away from home. A warm thanks to Charles, Mojahi, Ridge, Tumelo and my entire fellow F3/F5 family for the unwavering assistance and words of encouragement always. To the Chemistry Department at Rhodes University, thank you for the opportunity to be part of your family. I also wish to express my appreciation to the Sandisa Imbewu for the financial assistance.

My deepest gratitude goes to my parents, Mr. George and Mrs. Virginia Moyo for their unconditional love, unending support and their prayers that saw me through. Many thanks go to Vitalis and Brighton for your constant love, standing by me and everyday motivation, and to all my siblings for being there for me and always checking up on me. A reserved special thanks to my precious baby girl Lwandile Cherry for her warm smile that inspired me always and kept me going.

Last but certainly not least, I thank the Lord Almighty through His son Jesus Christ for the gift of life and His steadfast love and blessings on me. He always makes a way where there seems to be no way because He loves us.

**Abstract**

Octa acyl chloride metallophthalocyanines of cobalt (CoOAClPc) and iron (FeOAClPc) were synthesized and characterized using spectroscopic and electrochemical techniques. The metallophthalocyanines were fabricated as thin films onto phenylethylamine (PEA) pre-grafted Au electrode following a covalent amide reaction. The spectroscopic and electrochemical characterization confirmed the modification of the bare Au with PEA monolayer thin film (Au-PEA) and the covalent immobilization of MOAClPc to yield Au-PEA-MOAClPc (where M is Co and Fe). The acyl chloride functional groups were hydrolyzed forming pH sensitive thin films of terminal carboxylic acid (-COOH) functional groups (Au-PEA-MOCAPc). The Au-PEA-MOCAPc electrode exhibited pH selectivity and sensitivity properties towards the negatively charged $[Fe(CN)_6]^{3-/4-}$ and positively charged $[Ru(NH_3)_6]^{2+/3+}$ redox probes.

The Au-PEA-MOCAPc electrodes were studied for their electrocatalytic and electroanalytical properties towards the detection of catecholamine neurotransmitters; dopamine (DA), epinephrine (EP) and norepinephrine (NOR). The electrodes were further investigated in the screening of ascorbic and uric acids by means of pH sensitive functional groups. The modification process exhibited good reproducibility. Excellent electrocatalytic and electroanalytical properties were observed. The limits of detection (LOD) determined using 3σ/m was found to be 64 nM, 0.22 μM and 0.17 μM for DA, EP and NOR respectively using Au-PEA-CoOCAPc. For Au-PEA-FeOCAPc, the LOD was found to 0.24 μM, 0.45 μM and 0.34 μM for DA, EP and NOR respectively. The Au-PEA-MOCAPc electrodes screened off the strong interferents, ascorbic and uric acid. The Au-PEA-FeOCAPc electrode was evaluated for its potential application in real sample analysis using new born calf serum, and it showed excellent percentage recoveries.

**Table of contents**

Acknowledgements ..... i

Abstract ..... ii

Table of contents ..... iii

List of abbreviations ..... ix

List of figures ..... xii

List of tables ..... xvi

List of schemes ..... xvii

List of publications ..... xviii

Chapter 1 ..... 1

1 Justification ..... 1

1.1 Electrode modification ..... 1

1.1.1 Covalent electrografting ..... 2

1.2 Metallophthalocyanines ..... 4

1.2.1 Substituted MPcs ..... 5

1.2.2 MPcs synthesized in this study ..... 7

1.2.3 Synthesis of MOAClPc in this study ..... 8

1.2.4 Electrocatalytic properties of MPcs ..... 9

1.2.5 Spontaneous immobilization of MPc ..... 10

1.3 Catecholamine neurotransmitters detection and interferences ..... 12

1.4 Aims and objectives of this thesis ..... 13

1.5 Chapter layout ..... 14

1.6 References ..... 15

Chapter 2 ..... 24

2 Literature review ..... 24

2.1 Neurotransmitters ..... 24

2.2 Classification of neurotransmitters ..... 25

2.3 Catecholamine neurotransmitters ..... 25

2.3.1 Dopamine ..... 26

2.3.2 Norepinephrine ..... 27

2.3.3 Epinephrine ..... 27

2.3.4 Synthesis of catecholamine neurotransmitters ..... 28

2.4 Current methods for determining and detection of catecholamine NTs ..... 28

2.5 Fundamentals of electrochemistry ..... 30

2.6 Current methods of electrode modification and challenges faced ..... 34

2.7 Phthalocyanines ..... 37

2.7.1 Nomenclature of phthalocyanines ..... 38

2.7.2 Synthesis of MPcs ..... 39

2.7.3 Electronic properties of MPcs ..... 40

2.8 Applications of MPcs ..... 41

2.8.1 MPcs as electrocatalysts ..... 42

2.9 References ..... 43

Chapter 3 ..... 52

3 Novel covalent immobilization of cobalt (II) octa acyl chloride phthalocyanines onto phenylethylamine pre-grafted gold via spontaneous amidation..... 52

Abstract..... 52

3.1 Introduction ..... 53

3.1.1 Aims..... 56

3.2 Experimental..... 56

3.2.1 Chemicals and reagents ..... 56

3.2.2 Apparatus and instrumentations..... 57

3.2.3 Synthesis of cobalt (II) octa carboxylic acid phthalocyanine (CoOCAPc, **3**) ..... 58

3.2.4 Synthesis of cobalt (II) octa acyl chloride phthalocyanine (CoOAClPc, **4**). ..... 59

3.2.5 Electrode pre-modification and immobilization of CoOAClPc, **4**..... 59

3.3 Results and discussion..... 61

3.3.1 Synthesis of cobalt (II) octa acyl chloride phthalocyanine (CoOAClPc, **4**). ..... 61

3.3.2 Characterization of CoOCAPc (**3**) and CoOAClPc (**4**)..... 62

3.3.3 Electrografting of AEBD onto Au electrode and immobilization of CoOAClPc (**4**) to form Au-PEA-CoOCAPc, Scheme 3.2. ..... 65

3.3.4 Electrochemical characterization of the bare Au, Au-PEA and Au-PEA-CoOCAPc surfaces..... 67

3.3.5 XPS characterization of modified electrodes ..... 74

3.3.6 Effect of pH on the negatively or positively charged redox probes ..... 77

3.3.7 Electrocatalysis of the catecholamine NTs at Au, Au-PEA and Au-PEA-CoOCAPc ..... 80

3.3.8 Effect of scan rate on catecholamine NT ..... 83

3.3.9 Interference studies ..... 85

3.3.10 Analytical studies of neurotransmitters at Au-PEA-CoOCAPc ..... 86

3.4 Conclusions ..... 90

3.5 References ..... 91

Chapter 4 ..... 98

4 pH sensitive thin films of iron phthalocyanines as electrocatalysts for screening of ascorbic and uric acids and selective detection of neurotransmitters ..... 98

Abstract ..... 98

4.1 Introduction ..... 99

4.1.1 Aims ..... 102

4.2 Experimental ..... 102

4.2.1 Chemical and reagents ..... 102

4.2.2 Synthesis of iron (II) octa carboxylic acid phthalocyanine (FeOCAPc, **1**) ..... 102

4.2.3 Synthesis of iron (II) octa acyl chloride phthalocyanine (FeOAClPc, **2**) ..... 103

4.2.4 Electrode pre-modification and immobilization of FeOAClPc, Scheme 4.2 ..... 103

4.3 Results and discussion ..... 105

4.3.1 Synthesis of iron (II) octa acyl chloride phthalocyanine (FeOAClPc, **2**) ..... 105

4.3.2 Characterization of FeOCAPc (**1**) and FeOAClPc (**2**) ..... 105

4.3.2.1 FT-IR analysis ..... 105

4.3.2.2 UV-vis and MCD spectroscopy ..... 106

4.3.2.3 Mass spectroscopy ..... 107

4.3.2.4 Raman spectroscopy ..... 108

4.3.3 Electrode pre-modification of PEA and immobilization of FeOAClPc ..... 109

4.3.4 Characterization of the bare and modified gold surfaces ..... 112

4.3.5 Effect of pH of Au-PEA-FeOCAPc towards $[Fe(CN)_6]^{3-/4-}$ and $[Ru(NH_3)_6]^{2+/3+}$ ..... 116

4.3.6 Electrochemical detection of the neurotransmitters at Au-PEA-FeOCAPc ..... 118

4.3.7 Effect of scan rate on redox probes ..... 120

4.3.8 Screening of the interferents ..... 122

4.3.9 Effect of AA and UA as interferents ..... 123

4.3.10 Electroanalysis of catecholamine neurotransmitters ..... 125

4.3.11 Simultaneous and mixed detection of catecholamine NTs ..... 129

4.3.12 Real sample analysis ..... 129

4.3.13 Mechanism of electrocatalysis ..... 132

4.3.14 Reproducibility, stability, and repeatability ..... 133

4.4 Conclusions ..... 134

4.5 References ..... 135

Chapter 5 ..... 144

5 Discussions ..... 144

5.1 Electrografting ..... 144

5.2 pH sensitivity of the electrochemical sensors ..... 145

5.3 Detection of catecholamine NTs at Au-PEA-CoOCAPc and Au-PEA-FeOCAPc ..... 146

5.4 References ..... 148

Chapter 6 ..... 150

6 Conclusions and future perspectives ..... 150

6.1 Conclusions ..... 150

6.2 Future perspectives ..... 151

## List of abbreviations

| | |
|---|---|
| AA | Ascorbic acid |
| ACN | Acetonitrile |
| ADHD | Attention deficit hyperactivity disorder |
| AEBD | 4-(2-aminoethyl) benzene diazonium |
| Ag | Silver |
| AgCl | Silver chloride |
| Au | Gold |
| Au-C | Gold carbide bond |
| Au-S | Gold sulphur bond |
| C-C | Carbon carbon bond |
| CE | Counter electrode |
| CNS | Central nervous system |
| COCl | Acyl chloride |
| CoOAClPc | Cobalt (II) octa acyl chloride phthalocyanine |
| CoOCAPc | Cobalt (II) octa carboxylic acid phthalocyanine |
| COOH | Carboxylic acid |
| CV | Cyclic voltammetry |
| DA | Dopamine |
| DCC | Dicyclohexyl carbodiimide |
| DCM | Dichloromethane |
| DMF | Dimethylformamide |
| DMSO | Dimethyl sulfoxide |
| DPV | Differential pulse voltammetry |

| | |
|---|---|
| EIS | Electrochemical impedance spectroscopy |
| EP | Epinephrine |
| FeOAClPc | Iron (II) octa acyl chloride phthalocyanine |
| FeOCAPc | Iron (II) octa carboxylic acid phthalocyanine |
| FT-IR | Fourier Transform Infrared |
| HOMO | Highest occupied molecular orbital |
| L-DOPA | L-3,4-dihydroxyphenylalanine |
| LOD | Limit of detection |
| LOQ | Limit of quantification |
| LUMO | Lowest unoccupied molecular orbital |
| M-C | Metal-carbon bond |
| MCD | Magnetic circular dichroism |
| MDD | Major depressive disorder |
| MPc | Metallophthalocyanine |
| NDDs | Neurodegenerative disorders |
| NHS | N-hydroxysuccinimide |
| NOR | Norepinephrine |
| NT | Neurotransmitter |
| PBS | Phosphate buffer solution |
| Pc | Phthalocyanine |
| PEA | Phenylethylamine |
| PMDA | Pyromellitic dianhydride |
| $R_{CT}$ | Charge transfer resistance |
| RE | Reference electrode |
| SAM | Self-assembled monolayer |

| | |
|---|---|
| $TBABF_4$ | Tetrabutylammonium tetrafluoroborate |
| UA | Uric acid |
| UV-vis | Ultraviolet-visible spectroscopy |
| WE | Working electrode |
| XPS | X-ray photoelectron spectroscopy |

**List of figures**

**Figure 1.1**: Molecular structure of metallophthalocyanine showing α- and β- positions and the notations. ..... 5

**Figure 1.2**: Chemical structure of cobalt (CoOAClPc) and iron (FeOAClPc) octa acyl chloride phthalocyanines. ..... 9

**Figure 2.1**: The general action of neurotransmitters through the synaptic cleft. ..... 25

**Figure 2.2**: Chemical structure of (a) DA, (b) NOR, and (c) EP. ..... 26

**Figure 2.3**: A diagrammatic representation of a three-electrode electrochemical cell ..... 32

**Figure 2.4**: Schematic diagram for an Ag|AgCl electrode ..... 33

**Figure 2.5**: Chemical structures of (a) metal-free ($H_2Pc$) and (b) metallated phthalocyanines, where M represents the central metal. ..... 37

**Figure 2.6**: Nomenclature of metallophthalocyanine ..... 38

**Figure 2.7**: Typical absorption spectrum of a metallophthalocyanine. ..... 40

**Figure 2.8**: Gouterman's four-orbital model showing electron transitions and origins of B and Q bands. ..... 41

**Figure 3.1**: FT-IR spectra of (i) pyromellitic dianhydride (PMDA, **1**), (ii) cobalt (II) octa carboxylic acid phthalocyanine (CoOCAPc, **3**) and (iii) cobalt (II) octa acyl chloride phthalocyanine (CoOAClPc, **4**). ..... 63

**Figure 3.2**: (i) UV-vis and (ii) MCD spectra of (a) cobalt (II) octa carboxylic acid phthalocyanine (CoOCAPc) and (b) cobalt (II) octa acyl chloride phthalocyanine (CoOAClPc) in dry DMF. ..... 64

**Figure 3.3**: Mass-spectra and the corresponding chemical structure of (a) CoOCAPc and (b) CoOAClPc ..... 65

**Figure 3.4**: CVs for the electrografting of ACN containing 1.0 mM AEBD salt and 0.10 M $TBABF_4$ on Au electrode. Scan rate = 50 $mV.s^{-1}$. ..... 66

**Figure 3.5**: CVs and Nyquist plots of (i) bare Au, (ii) Au-PEA and (iii) Au-PEA-CoOCAPc measured in 2.0 mM (a) $[Fe(CN)_6]^{3-/4-}$ and (b) $[Ru(NH_3)_6]^{2+/3+}$ containing 0.10 M KCl. Scan rate = 50 $mV.s^{-1}$. ..... 68

**Figure 3.6**: CVs of (i) bare Au, (ii) Au-PEA and (iii) Au-PEA-CoOCAPc measured in (a) 0.010 M KOH and (b) 1.0 mM $CuSO_4$ in 0.50 M $H_2SO_4$ solution. Scan rate = 50 $mV.s^{-1}$ ..... 72

**Figure 3.7**: XPS spectra of Au-PEA, (a) survey spectrum and high-resolution core-level spectra of (b) C 1s and (c) N 1s. ..... 75

**Figure 3.8**: (a) Survey spectrum and the high resolution core-level spectra of (b) C 1s, (c) N 1s and (d) O 1s. ..... 76

**Figure 3.9**: (a) and (b) CVs, (a') and (b') Nyquist plots and (c) correlation of ΔE and RCT vs pH of Au-PEA-CoOCAPc measured in 2.0 mM (a) $[Fe(CN)_6]^{3-/4-}$ and (b) $[Ru(NH_3)_6]^{2+/3+}$ containing 0.10 M KCl in different pH solutions ranging from (i) pH 3.0 to (viii) pH 10. Scan rate = 50 $mV.s^{-1}$ for (n = 3). ..... 78

**Figure 3.10**: CVs of Au-PEA-CoOCAPC in (i) absence (ii) presence of 1.0 mM (a) DA, (b) NOR, (c) EP and (d) 0.10 mM AA in 0.010 M PBS (pH 7.4). Scan rate = 50 $mV.s^{-1}$ ..... 80

**Figure 3.11**: CVs for electrochemical oxidation of 1.0 mM (a) DA, (b) NOR, (c) EP and (d) 0.10 mM AA in 0.010 M PBS (pH 7.4) at (i) bare Au, (ii) Au-PEA and (iii) Au-PEA-CoOCAPc. Scan rate = 50 $mV.s^{-1}$. ..... 82

**Figure 3.12**: CVs of Au-PEA-CoOCAPc measured in PBS (pH 7.4) containing 0.10 mM (a) DA, (b) NOR and (c) EP at different scan rates (i) 25 – (v) 125 $mV.s^{-1}$ and their

corresponding calibrations curves. The electrolyte solution was 0.010 M PBS (pH 7.4). ..... 84

**Figure 3.13**: (a) DPVs of Au-PEA-CoOCAPc in (i) 0.010 M PBS (pH 7.4), (ii) 0.10 mM AA, (iii) 0.50 mM GA, (iv) 0.25 mM DA and (v) mixture (0.25 mM DA + 0.50 mM GA + 0.10 mM AA) all in 0.010 M PBS (pH 7.4). (b) CVs in the (i) absence and (ii) presence of 0.50 mM GA in 0.010 M PBS (pH 7.4). Scan rate = 50 $mV.s^{-1}$. ..... 85

**Figure 3.14**: DPVs and calibration curves of Au-PEA-CoOCAPc from 0.10 µM – 50 µM of (a) DA, (b) NOR and (c) EP in 0.010 M PBS (pH 7.4). Scan rate = 50 $mV.s^{-1}$. ..... 87

**Figure 4.1**: FT-IR spectra of (i) pyromellitic dianhydride (PMDA), (ii) iron (II) octa carboxylic acid phthalocyanine (FeOCAPc, **1**) and (iii) iron (II) octa acyl chloride phthalocyanine (FeOAClPc, **2**). ..... 106

**Figure 4.2**: (i) UV-vis and (ii) MCD spectra for (a) iron (II) octa carboxylic acid phthalocyanine (FeOCAPc) and (b) iron (II) octa acyl chloride phthalocyanine (FeOAClPc) in dry DMF. ..... 107

**Figure 4.3**: Mass spectra and corresponding chemical structure of (a) FeOCAPc and (b) FeOAClPc. ..... 108

**Figure 4.4**: Raman spectrum of FeOCAPc ..... 109

**Figure 4.5**: CVs for the electrografting of 1.0 mM AEBD salt in ACN solution containing 0.10 M $TBABF_4$ onto the Au electrode, from (i) scan 1, (ii) scan 2, and (iii) scan 3. Scan rate = 50 $mV.s^{-1}$ ..... 111

**Figure 4.6**: CVs and Nyquist plots of (i) bare Au, (ii) Au-PEA and (iii) Au-PEA-FeOCAPc measured in 2.0 mM (a) $[Fe(CN)_6]^{3-/4-}$ and (b) $[Ru(NH_3)_6]^{2+/3+}$ containing 0.10 M KCl. Scan rate = 50 $mV.s^{-1}$. ..... 113

**Figure 4.7**: CVs, Nyquist plots and (a'') correlation of ΔE and $R_{CT}$ vs pH of Au-PEA-FeOCAPc measured in 2.0 mM (a) $[Fe(CN)_6]^{3-/4-}$ and (b) $[Ru(NH_3)_6]^{2+/3+}$ containing 0.10 M KCl in different pH values ranging from (i) 2.0 to (vii) 8.0. (c) $E_{pa}$ vs pH for Au-PEA-FeOCAPc in $[Fe(CN)_6]^{3-/4-}$. Scan rate 50 $mV.s^{-1}$..... 117

**Figure 4.8**: CVs of Au-PEA-FeOCAPc in (i) PBS (pH 7.4) alone and (ii) PBS (pH 7.4) containing 1.0 mM (a) DA, (b) NOR, (c) EP, and (d) overlaid CVs of NTs. Scan rate = 50 $mV.s^{-1}$..... 120

**Figure 4.9**: CVs of Au-PEA-FeOCAPc measured in PBS (pH 7.4) containing 0.10 mM (a) DA, (b) NOR and (c) EP at different scan rates (i) 25 to (vi) 150 $mV.s^{-1}$ and their corresponding linear regression. ..... 121

**Figure 4.10**: CVs of (i) bare Au, (ii) Au-PEA and (iii) Au-PEA-FeOCAPc in (a) 0.10 mM AA and (b) 10 μM UA. ..... 122

**Figure 4.11**: DPVs of Au-PEA-FeOCAPc in (a) 50 μM DA, (b) 50 μM NOR and (c) 50 μM EP, with 50 μM AA and 50 μM UA in PBS (pH 7.4). Scan rate = 50 $mV.s^{-1}$..... 124

**Figure 4.12**: DPVs and calibration curves of Au-PEA-FeOCAPc in 1.0 – 50 μM of (a) DA, (b) NOR, and (c) 1.0 – 30 μM EP in PBS (pH 7.4). Scan rate = 50 $mV.s^{-1}$..... 126

**Figure 4.13**: Simultaneous detection of the 1.0 μM DA and 1.0 μM EP and increasing concentrations of NOR (1.0 – 40.0 μM) in pH 7.4 PBS solution. ..... 129

**Figure 4.14**: DPVs and calibration curves of Au-PEA-FeOCAPc in linear range 1.0 μM – 50 μM of (a) DA, (b) NOR and (c) EP in 10% new-born calf serum in PBS (pH 7.4). Scan rate = 50 $mV.s^{-1}$..... 131

**Figure 4.15**: Variation of peak current of individual DPVs of 10 μM DA in PBS (pH 7.4) at Au-PEA-FeOCAPc. ..... 133

**List of tables**

**Table 3.1**: Summary of CV and EIS parameters of Au-PEA-CoOCAPc in 2.0 mM $[Fe(CN)_6]^{3-/4-}$ and $[Ru(NH_3)_6]^{2+/3+}$ both containing 0.10 M KCl at pH 3.0 to pH 10..... 79

**Table 3.2**: Comparison of analytical parameters of electrochemical sensors reported for detection of DA, EP and NOR. ..... 89

**Table 4.1**: Summary of parameters obtained from EIS in 2.0 mM $[Fe(CN)_6]^{3-/4-}$ containing 0.10 M KCl. RCT values in brackets are for $[Ru(NH_3)_6]^{2+/3+}$. ..... 115

**Table 4.2**: Comparison of analytical parameters of electrochemical sensors reported for the detection of DA, EP and NOR. ..... 128

**Table 4.3**: Determination of DA, NOR and EP in 10% new-born calf serum, (n = 3). ..... 130

**Table 5.1**: Summary of oxidation potentials of AA and UA. ..... 145

**Table 5.2**: Comparison of electrocatalysis of Au-PEA-CoOCAPc and Au-PEA-FeOCAPc towards the detection of DA, NOR and EP..... 147

**List of schemes**

**Scheme 1.1**: Electrochemical grafting of 4-(2-aminoethyl) benzene diazonium salt (AEBD) onto gold electrode. ..... 3

**Scheme 1.2**: Synthesis route for metallophthalocyanine, (a) tetra-substituted, (b) octa-substituted, where R = substituents. ..... 6

**Scheme 1.3**: Nucleophilic addition/elimination reaction between acyl chlorides and amines. ..... 11

**Scheme 2.1**: Biological synthesis of the catecholamine neurotransmitters. ..... 29

**Scheme 2.2**: Electrochemical oxidation and/or reduction process of dopamine to dopamine-o-quinone. ..... 30

**Scheme 2.3**: General synthesis scheme for metallophthalocyanine from different precursors. ..... 39

**Scheme 3.1**: Synthesis of cobalt (II) octa acyl chloride phthalocyanine (CoOAClPc, **4**). ..... 62

**Scheme 3.2**: Electrografting of AEBD to form Au-PEA and immobilization of CoOAClPc thin monolayer film onto Au-PEA electrode to form Au-PEA-CoOCAPc. ..... 67

**Scheme 4.1**: Synthesis of iron (II) octa acyl chloride phthalocyanine (FeOAClPc, **2**) ..... 105

**Scheme 4.2**: Electrografting of AEBD to form Au-PEA and immobilization of FeOAClPc on Au-PEA electrode surface to form Au-PEA-FeOCAPc. ..... 110

**List of publications**

---

**List of papers published that form part of the thesis (not cited):**

1. **Iphithuli Moyo**, Daniel Mwanza, Philani Mashazi, Novel covalent immobilization of cobalt (II) octa acyl chloride phthalocyanines onto phenylethylamine pre-grafted gold via spontaneous amidation. *Electrochimica Acta* 422 (2022) 140550.

   **Own contribution**: study conception and design, data collection: analysis and interpretation of results, and draft manuscript preparation.

2. **Iphithuli Moyo**, Daniel Mwanza, Philani Mashazi, pH sensitive thin films of iron phthalocyanines as electrocatalysts for screening of ascorbic and uric acids and selective detection of neurotransmitters. *Journal of Organometallic Chemistry* 990 (2023) 122662.

   **Own contribution**: study conception and design, data collection: analysis and interpretation of results, and draft manuscript preparation.

---

**Article published as co-author and does not form part of this manuscript.**

3. Charles Luhana, **Iphithuli Moyo**, Keamogetse Tshenkeng, Philani Mashazi, In-sera selectivity detection of catecholamine neurotransmitters using covalent composite of cobalt phthalocyanine and aminated graphene quantum dots. *Microchemical Journal* 180 (2022) 107605.

   **Own contribution**: Methodology, Formal analysis, Investigation.

# Chapter 1

## 1 Justification

### 1.1 Electrode modification

In the recent years, the development of new electrochemical sensors is continuously growing [1–3]. The electrochemical sensors are widely applied in research laboratories, industries as well as health care centers. They are more common when compared to other instrumental techniques such as fluorimetry, chromatography, capillary electrophoresis, fluorescence [4]. This is because of their fast response, easy to operate with simpler instrumentation requirements leading to cost effectiveness, and they are portable and suitable for on-site monitoring and needing small sample volumes for successful analysis [4,5]. The development of electrochemical sensors involves electrode modification with materials that seek to improve and impart properties such as sensitivity, specificity and selectivity towards the analytes of interest. There is also a need for a method used to be simple for the electrode functionalization towards an electrochemical sensor fabrication and to minimize costs. Electrode functionalization is a method used in the design of electrochemical sensors and affords the attachment of a molecule with excellent electron transfer properties for improved electrocatalytic properties towards analytes of interest. It is a crucial process since surface chemistry drives the interaction of the analytes with the sensor/electrode surface [6]. Several approaches have been studied for electrode functionalization and these can be grouped into four classes namely (i) electrostatic approach, (ii) non-specific adsorption, (iii) non-covalent and (iv) covalent approach [6,7]. Covalent electrode modification exhibits better selectivity, reproducibility of the surface

functionalization and completely avoids non-specific adsorption when compared to other approaches [7].

Thiolated surfaces have been reported to form an orderly self-assembled monolayer (SAM) on gold surfaces [3,8]. However, SAMs have several drawbacks; (i) they can easily be oxidized in the atmosphere, (ii) they undergo place exchange and (iii) they energetically move around on the gold surface [9]. Additionally, the thiolate (Au-S) bond is thermally unstable and has a short shelf-life [10]. Due to the instability of the thiol SAMs, research continues to seek alternative methods to form stable thin monolayer films on gold electrode surfaces.

Alternatively, the electrografting method has received much attention in research over the conventional strategies mainly due to high stability, simplicity, rapid electro-reduction, and less time consumption [9,11,12]. The electrochemical grafting results in environmentally and electrical stable gold carbide (Au-C) bond. The Au-C bond has a bond energy of 317 kJ/mol [13] which is relatively stronger than the gold-sulphur (Au-S) bond of 154 kJ/mol in SAMs [14]. Electrografting of phenylethylamine on a gold electrode has been investigated and reported to be stable [13,15].

### 1.1.1 Covalent electrografting

Electrografting is defined as the electrochemical reaction that allows organic layers to be covalently attached to solid conducting substrates [11]. The mechanism involves the reduction of an aryl diazonium salt. Aryl diazonium salts are easily and rapidly prepared from primary aromatic amines with sodium nitrite in the presence of excess acid. An aryl radical is generated at the electrode/solution interface by a single electron

reduction process of the corresponding aryl diazonium salt. The radical generated covalently binds on the surface of either carbon or gold substrate. The resulting modification is a strong and stable covalent C-C or Au-C bond [11,16]. The electrografting method also allows for the covalent attachment of aryl groups having different terminal functional groups such as methoxy, thiol, nitro, carboxylic acid, cyanide, including amines, on various substrates for many potential applications [9]. For the reasons mentioned above, this study will electrochemically graft phenylethylamine onto a gold electrode using 4-(2-aminoethyl) benzene diazonium (AEBD) salt in acetonitrile (ACN) using tetrabutylammonium tetrafluoroborate ($TBABF_4$) as the supporting electrolyte. A stable gold carbide (Au-C) bond was formed. **Scheme 1.1** shows the mechanism for the one electron process in electrografting. Modification with aryl diazonium salt brings about low capacitance and a high rate of electron transfer on gold electrode [17].

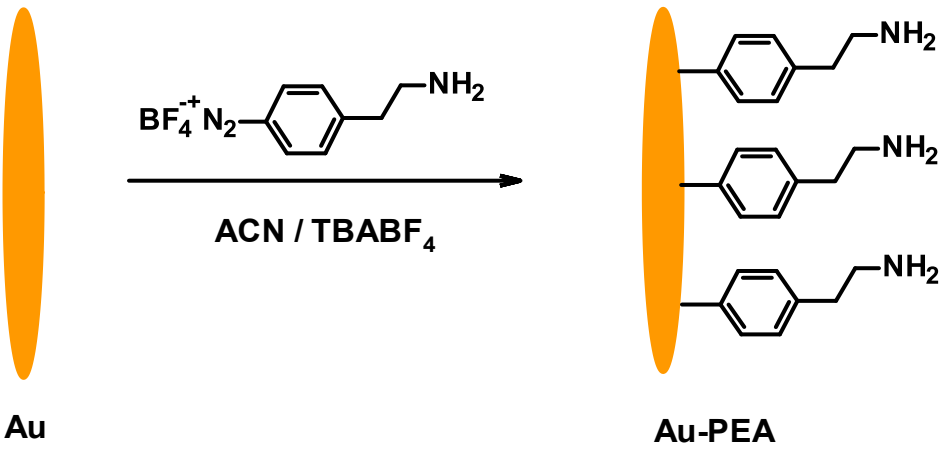


**Scheme 1.1**: Electrochemical grafting of 4-(2-aminoethyl) benzene diazonium salt (AEBD) onto gold electrode.

## 1.2 Metallophthalocyanines

Metallophthalocyanines (MPcs) have been widely studied and exhibit unique properties leading to a great diversity of technological applications including in electrochemical sensors [18–20]. The applications of MPcs in electrochemical sensors is mostly because of their excellent electrocatalytic properties and electron transfer abilities [21–23]. MPcs are 18-π electron conjugated macrocyclic molecules with metal ions at the centre. The 18-π electron system combined with an electroactive central metal ion enables MPcs to undergo fast redox processes [22]. Additionally, MPcs are also thermally and chemically stable [24] which is an added benefit in the design and fabrication of stable electrochemical sensors. Some applications of MPcs are impeded by their low solubility in common organic and aqueous solvents. This challenge led to the introduction of appropriate substituents either onto the ring system or as axial ligands on the central metal ion. The notation system and substitution positions on an MPc are shown in **Figure 1.1**. The substituents can be attached on one of the two positions, the non-peripheral (α-position) or peripheral (β-position). The non-peripheral (α) substituents are found at positions 1, 4, 8, 11, 15,18, 22 or 25, whereas the peripheral (β) substituents are found at positions 2, 3, 9, 10, 16, 17, 23 or 24.

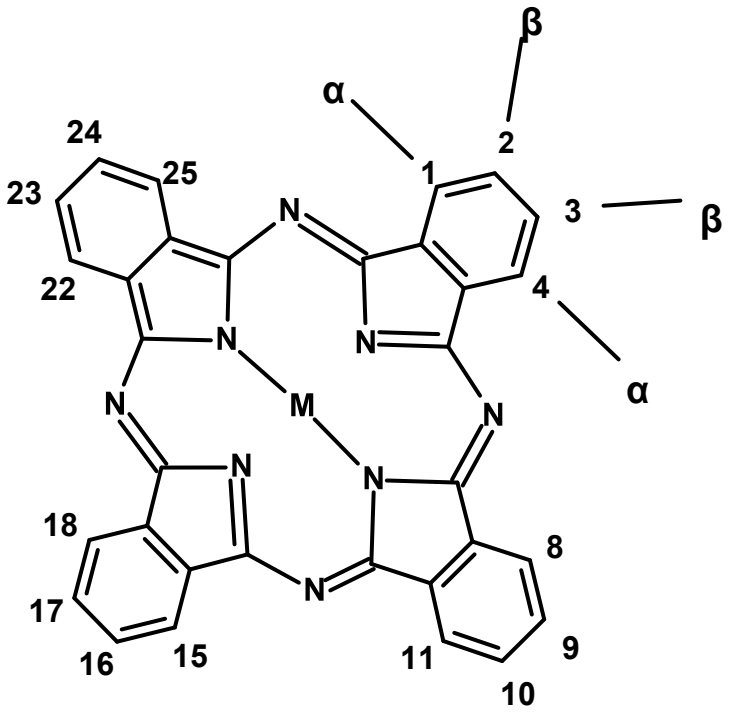


**Figure 1.1**: Molecular structure of metallophthalocyanine showing α- and β- positions and the notations.

### 1.2.1 Substituted MPcs

Substitution on MPcs improves their physical properties and solubility. Several MPcs have been synthesized with different α- and β- substituents such as alkythio, alkyloxy, nitro, amino, aminophenoxy, chloro, carboxylic acid, carboxyphenoxy, phenoxy, hydroxyl functional groups to mention but a few [**25**]. The substituents are categorized as either electron donating groups, such as alkoxy/aryloxy groups or electron withdrawing such as halogens. Electron donating and withdrawing groups affect the electrochemical properties of MPcs. The growing interest in the properties of MPcs has led to the synthesis of substituted MPcs that can be used for various possible applications. The presence of substituents on peripheral or non-peripheral positions

of the aromatic ring has the ability to increase the functionality of MPcs [26]. The synthesis of substituted MPcs in **Scheme 1.2** is achieved by cyclotetramerization of substituted phthalonitrile or pyromellitic dianhydride. MPcs that possess 4 substituents at either the peripheral or non-peripheral positions are called tetra (*t*) substituted. Whereas MPcs that have 8 substituents are called octa (*o*) substituted.

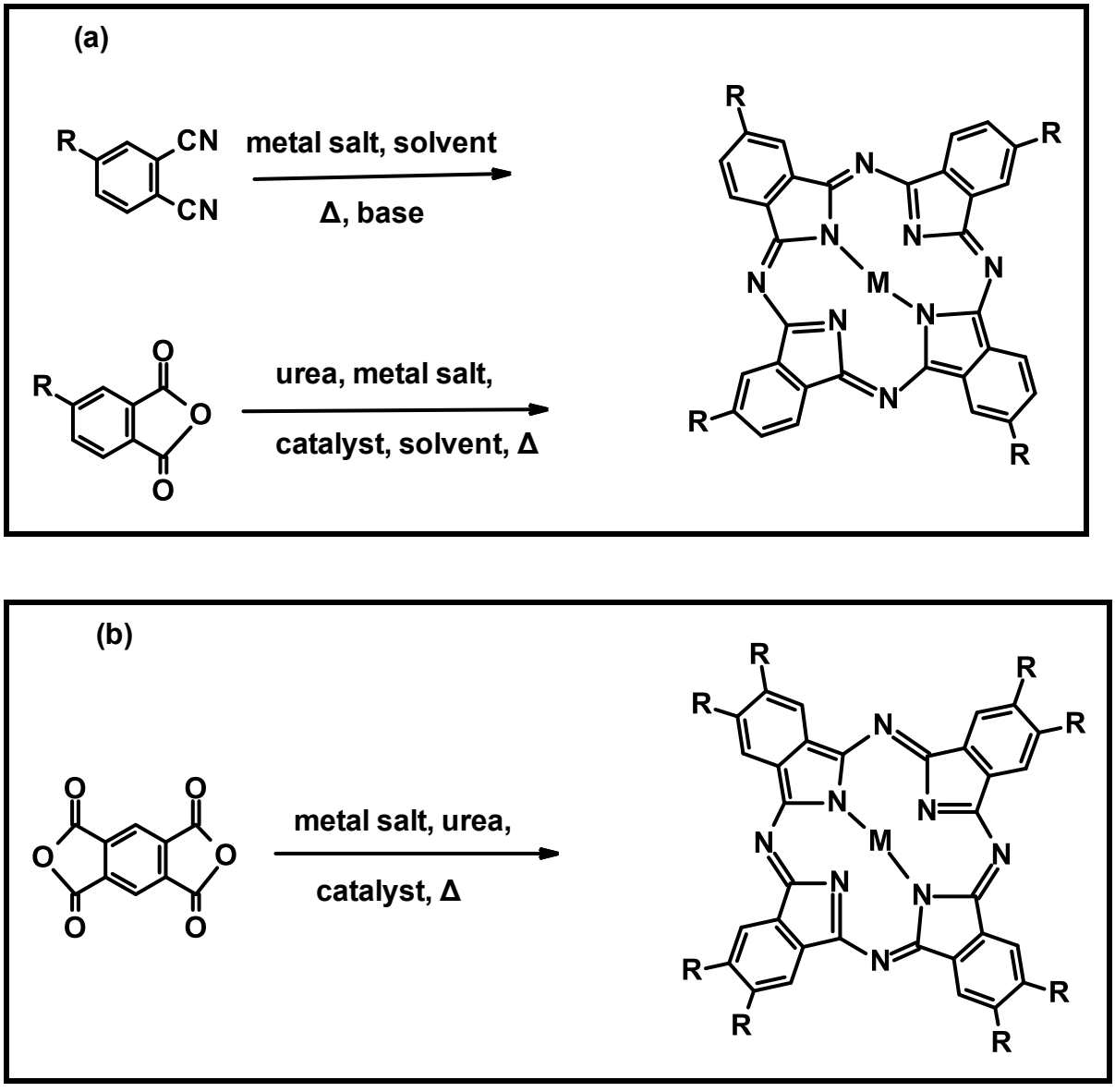


**Scheme 1.2**: Synthesis route for metallophthalocyanine, (a) tetra-substituted, (b) octa-substituted, where R = substituents.

Shirai and co-workers demonstrated the catalytic activity of di-, tetra- and octa-carboxyl metallophthalocyanines [27]. They discovered that the octa-substituted complexes of Co(II) and Fe(II) had the most extraordinary catalytic effect. Octa-substituted MPcs have been reported [26,28,29] and are synthesized with functional groups such as imide or amide or carboxylic acid at peripheral positions. Peripheral functionalization improves some properties of MPcs such as photo-sensitizer activity, electropolymerization, photo and electrochemical properties, and solubility [29,30]. The introduction of substituents has also resulted in a wide range of novel products such zinc (II) phthalocyanine fused in peripheral positions octa-substituted with alkyl linked carbazole [29], manganese tetrabenzylthio-substituted phthalocyanine [31], tetra- and octa-substituted dodecyl-mercapto tin phthalocyanine [8], cobalt (II) tetra-(3-carboxyphenoxy) phthalocyanine [15] among others.

An integral component of this study is to describe the synthesis and characterization of novel peripherally octa-substituted metallophthalocyanines, containing cobalt and iron as central metal ions.

### 1.2.2 MPcs synthesized in this study

Synthesis of MPcs is tailored for specific applications through various central metal ions and substituents. The synthesized MPcs in this study required the acyl chloride (-COCl) functional groups for immobilization of the MPc via spontaneous amidation reaction with the phenylethylamine (-$NH_2$) pre-grafted gold electrode surfaces. Tetra-substituted acyl chloride MPcs have been reported [32,33]. An increase in the acyl chloride functional groups on the MPcs in this study is achieved by octa substitution. This is done to enhance the properties such as the spontaneity of the immobilization

of the metallophthalocyanine to the pre-grafted PEA gold electrode, increase the surface area for the redox process and increase the electrocatalytic and electrostatic properties on the surface of the electrochemical sensor.

### 1.2.3 Synthesis of MOAClPc in this study

The synthesis of peripherally octa-substituted acyl chloride metallophthalocynanines (MOAClPc) was achieved using of 1, 2, 4, 5-tetracarboxylic dianhydride (pyromellitic dianhydride) as a starting reagent [18,34]. The synthesis was done in the presence of a catalyst to aid cyclotetramerization with a source of nitrogen, i.e., urea and a metal salt exposed in high temperatures. Pyromellitic dianhydride (PMDA) was used because of its bifunctional reagent that brings about the polycyclotetramerization in substituted MPc synthesis. Firstly, octa-substituted carboxylic acid metallophthalocyanines (MOCAPc) was formed and then converted to acyl chloride using thionyl chloride. **Figure 1.2** shows the chemical structure of the newly synthesized cobalt (CoOAClPc) and iron (FeOAClPc) octa acyl chloride phthalocyanines.

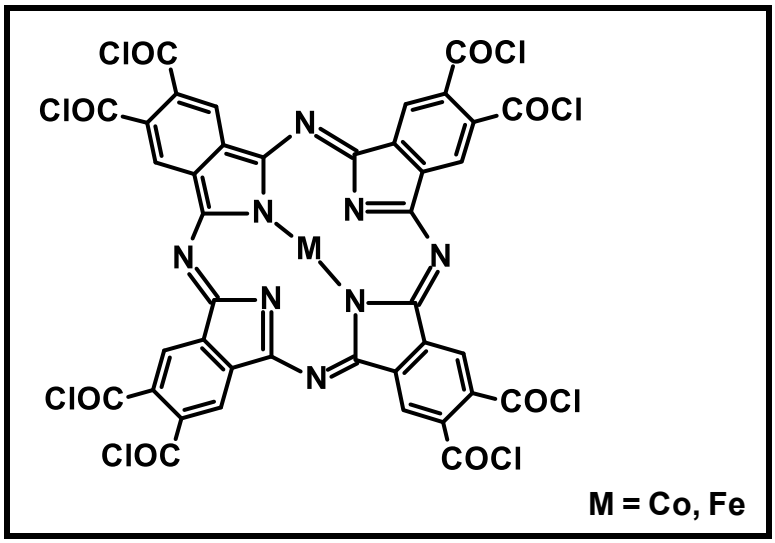


**Figure 1.2**: Chemical structure of cobalt (CoOAClPc) and iron (FeOAClPc) octa acyl chloride phthalocyanines.

### 1.2.4 Electrocatalytic properties of MPcs

Research has established transition metals to be used in MPcs as electrocatalysts [35–37]. The mostly used metals in phthalocyanine electrochemistry are Co, Fe, and Mn. These have excellent electrocatalytic properties. Generally, MPc complexes are immobilized on electrode surfaces by adsorption or otherwise attached to the electrode surface. The electrochemistry of MPc is broad with several redox processes involved that are affected by different factors. These factors include the nature of MPc itself and its substituents, axial ligands, central metal ion and solvents [38]. The electrocatalytic activity of MPcs involves redox processes that occur at the central metal ion or at the ring system [39]. It is enhanced by their π donor-acceptor functionality [40]. The electrocatalytic activity of MPcs has also been related to the redox potentials of the central metal ion [40,41]. A general mechanism involved in metal oxidation-analyte oxidation process is represented by **Equations 1.1** and **1.2**.

The first oxidation occurs at the central metal due to $M^{II}Pc|M^{III}Pc$ couple and then follows the mediated catalytic oxidation of the analytes (Analy) to its oxidized products [40,41]. A metal free Pc exist as a dianion, represented as $Pc^{-2}$ [42] when it loses $2H^+$. Metalation with $M^{2+}$ metal ion (mostly transition metal ions) results in a neutral Pc (MPc). When the metal ion is $M^{3+}$, the formed MPc contains an axial ligand, for an example, using $InCl_3$ results in In(Cl)Pc with chlorine as an axial ligand [43,44].

$$M^{II}Pc \rightarrow M^{III}Pc + e^- \quad (1.1)$$

$$M^{III}Pc + Analy \rightarrow M^{II}Pc + products \quad (1.2)$$

MPcs have not only shown remarkable results as electrocatalysts for vast redox processes but also in the development of metallophthalocyanine based electrochemical sensors for the detection of various analytes of interest [45,46]. This work will use the newly synthesized MPcs as electrocatalysts in the design of an electrochemical sensor for the detection of catecholamine neurotransmitters. The work will investigate the covalent attachment of MPc onto pre-electrografted phenylethylamine on gold electrode.

### 1.2.5 Spontaneous immobilization of MPc

The electrografted surface needs to have functional groups that can react with the substituents on the MPc. A lot of work has been done on gold electrode, centered on electrografting and coupling reactions using click chemistry (alkyne-azide reaction) [47] and Schiff reaction (aldehyde-amine reaction) [36]. Amide coupling reagents such as dicyclohexyl carbodiimide (DCC) and N-hydroxysuccinimide (NHS) have been used in immobilization of carboxylic acid functionalized MPcs onto self-assembled

monolayers (SAMs) modified gold electrodes [48] and their coupling onto amine functionalized substrates [49]. Several other studies have also used chemical reagents to activate the carboxylic acid functional groups for the fabrication of the electrochemical sensors [13,15]. A cost-effective method of immobilization of MPcs as electrocatalysts without use of the coupling reagents is desirable. In this work, the synthesized metal octa acyl chloride phthalocyanine is immobilized onto the gold electrode pre-grafted with phenylethylamine. The electrografted gold electrode bears -$NH_2$ functional groups while the metallophthalocyanines have acyl chloride functional groups on peripheral positions. Acyl chlorides (-COCl) are the most reactive among carboxylic acid derivatives and they undergo various nucleophilic acyl substitutions. The acyl chloride functional groups are investigated for their spontaneous amidation via nucleophilic addition/elimination reaction without use of amide coupling reagents such as DCC and NHS. The acyl chlorides readily and spontaneously react with amine (-$NH_2$) functional groups to form amide bonds. **Scheme 1.3** shows the mechanism for nucleophilic addition/elimination reaction between acyl chlorides and amines.

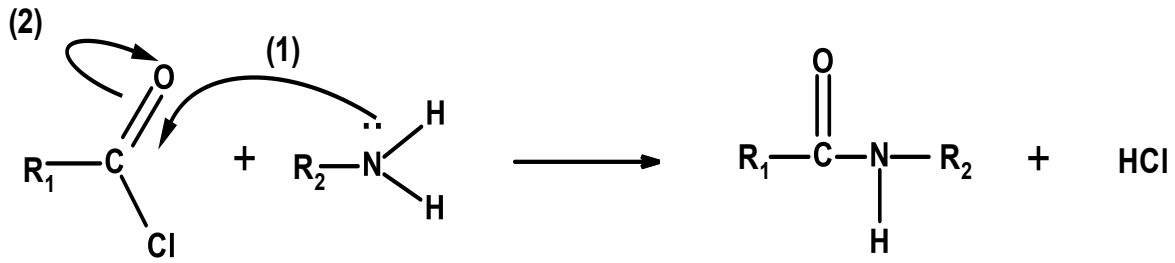


**Scheme 1.3**: Nucleophilic addition/elimination reaction between acyl chlorides and amines.

## 1.3 Catecholamine neurotransmitters detection and interferences

It has always been important to determine catecholamine neurotransmitters. The role they play in biological systems is crucial for monitoring the onset of various irreversible neurodegenerative disorders (NDDs) such as Parkinson's, Alzheimer's, Huntington's diseases. The importance of neurotransmitters arises from their fluctuating concentrations as a result of mood swings, during pleasurable activities, sleep, stress or fear. The brain is always trying to keep the balance of the neurotransmitters in response to the ongoing external and internal needs. The imbalance can either be due to excessive or insufficient neurotransmitters. Apart from being clinical biomarkers for the NDDs, the detection of neurotransmitters is also important to monitor and control drug treatment. Several different methods have been used for the detection of catecholamine neurotransmitters. Electrochemical detection of catecholamine neurotransmitters is a feasible method, cost effective, sensitive, and easy to use. The major problem researchers face with the electrochemical detection of the catecholamine neurotransmitters in real samples is the coexisting electroactive species such as ascorbic acid and uric acids [50]. The interfering species hinder precise detection and determination of the catecholamine neurotransmitters. Many electroactive interfering species oxidize at similar potentials with the catecholamine NTs on many convectional electrodes [50]. This leads to overlapped voltammetric responses and poor selectivity. Therefore, it is very difficult to simultaneously detect the catecholamine NTs in the presence of ascorbic acid and uric acid. To overcome this problem, two procedures are normally used. The first procedure involves improving the selectivity and the electrocatalytic behavior of the electrode to aid significant separation of the oxidation potentials to allow accurate discrimination of the catecholamine NTs from the interferences. The other procedure is the use of pH

sensitive functional groups to screen off the interferences. In this work, the latter method of screening NTs using pH sensitive electrochemical sensors was explored. The designed electrochemical sensor was evaluated towards the pH sensitive screening off anionic interferences such as ascorbic acid and uric acid. At physiological pH 7.4, the carboxylic acid functional groups are deprotonated resulting in a negatively charged surface of the electrochemical sensor. As a result, ascorbic acid and uric acid that exists as anions can be screened off by electrostatic repulsion that occurs due to the negatively charged $-COO^-$ functional groups on the electrode surface. While an electrostatic interaction is facilitated between the cationic and neutral catecholamine neurotransmitters and the negatively charged electrode surface.

## 1.4 Aims and objectives of this thesis

The aim of the study is to design an electrochemical sensor using a simple but stable method of modifying gold electrode using electroactive and electrocatalytic metallophthalocyanines bearing pH sensitive functional groups for the detection of catecholamine neurotransmitters (dopamine, norepinephrine, and epinephrine) and screening off ascorbic acid and uric acid as interferences.

*The objectives of this thesis include:*

(i) To synthesize and characterize metal octa acyl chloride phthalocyanine (MOAClPc), (M = Co, Fe) using Fourier Transform Infrared (FT-IR) spectroscopy, UV-vis, magnetic circular dichroism (MCD) and mass spectroscopy and elemental analysis.

(ii) To electrograft 4-(2-aminoethyl) benzene diazonium salt (AEBD) onto gold electrode to yield an amine functionalized gold electrode.

(iii) To covalently immobilize the synthesized MOAClPc onto the electrografted phenylethylamine gold electrode via spontaneous amidation.

(iv) To characterize the modified electrode surfaces using different surface sensitive techniques such as cyclic voltammetry (CV), electrochemical impedance spectroscopy and X-ray photoelectron spectroscopy (XPS).

(v) To investigate the electrocatalytic properties of MPc modified electrodes for the detection of catecholamine neurotransmitters (dopamine, norepinephrine and epinephrine).

(vi) To investigate the designed electrochemical sensor in screening off ascorbic acid and uric acid using pH sensitivity.

(vii) To investigate the performance of the electrochemical sensor in real samples including human serum and new-born calf serum.

## 1.5 Chapter layout

This thesis comprises six chapters;

- **Chapter one**: States the problem statement and the justification of the intended study. It defines the aims and objectives of the study.
- **Chapter two**: Literature review chapter which outlines the background and dwells deep into the literature of what has been done and accomplished in the determination of catecholamine neurotransmitters.
- **Chapter three**: Discuss the novel covalent immobilization strategy of cobalt (II) octa acyl chloride phthalocyanines (CoOAClPc) onto phenylethylamine (PEA)

pre-grafted gold electrode via spontaneous amidation. The chapter also sheds some light into the effect of pH on the fabricated gold electrode and the electrocatalysis of the modified electrode.

- **Chapter four**: The most catalytic metallophthalocyanine complex was investigated as possible substitute for CoOAClPc. The development of an electrochemical sensor based on stable thin film of PEA and covalent immobilization of iron (II) octa acyl chloride phthalocyanines (FeOAClPc) for the detection of catecholamine neurotransmitters and screening off ascorbic acid and uric acid was investigated in depth.
- **Chapter five**: Discussion on the major findings of the results and the comparison of the two electrodes fabricated in this work and compared to literature is described in detail.
- **Chapter six**: Summarizes the conclusions that were reached from this study and the possible future perspectives and research outlook are highlighted.

## 1.6 References


[1] Y. Shao, J. Wang, H. Wu, J. Liu, I.A. Aksay, Y. Lin, Graphene based electrochemical sensors and biosensors: A review, *Electroanal.* 22 (**2010**) 1027–1036. https://doi.org/10.1002/elan.200900571.

[2] A. Chen, S. Chatterjee, Nanomaterials based electrochemical sensors for biomedical applications, *Chem. Soc. Rev.* 42 (**2013)** 5425–5438. https://doi.org/10.1039/c3cs35518g.

[3] K. Ozoemena, T. Nyokong, Voltammetric characterization of the self-

assembled monolayer (SAM) of octabutylthiophthalocyaninatoiron(II): A potential electrochemical sensor, *Electrochim. Acta* 47 (**2002**) 4035–4043. https://doi.org/10.1016/S0013-4686(02)00362-6.

[4] Z. Tavakolian-Ardakani, O. Hosu, C. Cristea, M. Mazloum-Ardakani, G. Marrazza, Latest trends in electrochemical sensors for neurotransmitters: A review, *Sensors* 19 (**2019**) 2037. https://doi.org/10.3390/s19092037.

[5] J.A. Ribeiro, P.M.V. Fernandes, C.M. Pereira, F. Silva, Electrochemical sensors and biosensors for determination of catecholamine neurotransmitters: A review, *Talanta* 160 (**2016**) 653–679. https://doi.org/10.1016/j.talanta.2016.06.066.

[6] H. Randriamahazaka, J. Ghilane, Electrografting and controlled surface functionalization of carbon based surfaces for electroanalysis, *Electroanal.* 28 (**2016**) 13–26. https://doi.org/10.1002/elan.201500527.

[7] S. Kumar, N. Kaur, A.K. Sharma, A. Mahajan, R.K. Bedi, Improved $Cl_2$ sensing characteristics of reduced graphene oxide when decorated with copper phthalocyanine nanoflowers, *RSC Adv.* 7 (**2017**) 25229–25236. https://doi.org/10.1039/c7ra02212c.

[8] S. Khene, D.A. Geraldo, C.A. Togo, J. Limson, T. Nyokong, Synthesis, electrochemical characterization of tetra- and octa-substituted dodecyl-mercapto tin phthalocyanines in solution and as self-assembled monolayers, *Electrochim. Acta* 54 (**2008**) 183–191. https://doi.org/10.1016/j.electacta.2008.08.018.

[9] S. Kesavan, S.B. Revin, S.A. John, Fabrication, characterization and

application of a grafting based gold nanoparticles electrode for the selective determination of an important neurotransmitter, *J. Mater. Chem.* 22 (**2012**) 17560–17567. https://doi.org/10.1039/c2jm33013j.

[10] E. Delamarche, B. Michel, H. Kang, C. Gerber, Thermal stability of self-assembled monolayers, *Am. Chem. Soc.* 2775 (**1994**) 4103–4108. https://doi.org/0743-7463/94/2410-4103$04.50/0.

[11] D. Bélanger, J. Pinson, Electrografting: A powerful method for surface modification, *Chem. Soc. Rev.* 40 (**2011**) 3995–4048. https://doi.org/10.1039/c0cs00149j.

[12] S. Griveau, D. Mercier, C. Vautrin-Ul, A. Chaussé, Electrochemical grafting by reduction of 4-aminoethylbenzenediazonium salt: Application to the immobilization of (bio)molecules, *Electrochem. Commun.* 9 (**2007**) 2768–2773. https://doi.org/10.1016/j.elecom.2007.09.004.

[13] O.K. Adeniyi, P.N. Mashazi, Stable thin films of human P53 antigen on gold surface for the detection of tumour associated anti-P53 autoantibodies, *Electrochim. Acta* 331 (**2020**) 135272. https://doi.org/10.1016/j.electacta.2019.135272.

[14] G.K. Ramachandran, T.J. Hopson, A.M. Rawtett, L.A. Nagahara, A. Primak, S.M. Lindsay, A bond-fluctuation mechanism for stochastic switching in wired molecules, *Sci.* 300 (**2003**) 1413–1416. https://doi.org/10.1126/science.1083825.

[15] K. Tshenkeng, P. Mashazi, Covalent attachment of cobalt (II) tetra-(3-carboxyphenoxy) phthalocyanine onto pre-grafted gold electrode for the

determination of catecholamine neurotransmitters, *Electrochim. Acta* 360 (**2020**) 137015. https://doi.org/10.1016/j.electacta.2020.137015.

[16] D. Hetemi, V. Noël, J. Pinson, Grafting of diazonium salts on surfaces: Application to biosensors, *Biosens.* 10 (**2020**). https://doi.org/10.3390/bios10010004.

[17] J.J. Gooding, Advances in interfacial design for electrochemical biosensors and sensors: Aryl diazonium salts for modifying carbon and metal electrodes, *Electroanal.* 20 (**2008**) 573–582. https://doi.org/10.1002/elan.200704124.

[18] K. Sakamoto, E. Ohno, Synthesis and electron transfer property of phthalocyanine derivatives, *Prog. Org. Coatings* 31 (**1997**) 139–145. https://doi.org/10.1016/S0300-9440(97)00029-5.

[19] Z. Huang, J. Huang, N. Chen, J. Huang, Synthesis, characterization and properties of some metallophthalocyanine complexes substituted by N-piperidineethanol, *J. Coord. Chem.* 61 (**2008**) 2315–2324. https://doi.org/10.1080/00958970801905254.

[20] S. Hun, K. Jin, W. Namgoong, S. Bum, Y. Jeong, Y. Kim, Synthesis and characteristics of metal-phthalocyanines tetra- substituted at non-peripheral (a) or peripheral (b) positions , and their applications in LCD color filters, *J. Incl. Phenom. Macrocycl. Chem.* 82 (**2015**) 195–202. https://doi.org/10.1007/s10847-015-0514-y.

[21] K. Sakamoto, E. Ohno-Okumura, Syntheses and functional properties of phthalocyanines, *Mater. (Basel)* 2 (**2009**) 1127–1179. https://doi.org/10.3390/ma2031127.

[22] I.S. Hosu, Q. Wang, A. Vasilescu, S.F. Peteu, V. Raditoiu, S. Railian, V. Zaitsev, K. Turcheniuk, Q. Wang, M. Li, R. Boukherroub, S. Szunerits, Cobalt phthalocyanine tetracarboxylic acid modified reduced graphene oxide: A sensitive matrix for the electrocatalytic detection of peroxynitrite and hydrogen peroxide, *RSC Adv.* 5 (**2015**) 1474–1484. https://doi.org/10.1039/c4ra09781e.

[23] S. Arslan, Phthalocyanines: Structure, synthesis, purification and applications, *J. Life Sci.* 6 (**2016**) 188–197. http://www.yasambilimleridergisi.com/makale/pdf/1466373234.pdf.

[24] C. Hamann, M. Hietschold, A. Mrwa, M. Müller, M. Starke, R. Kilper, Phthalocyanine thin films for molecular electronics, *Mol. Electron.* (**1991**) 129–138. https://doi.org/10.1007/978-94-011-3392-0_14.

[25] V.N. Nemykina, E.A. Lukyanets, Synthesis of substituted phthalocyanines, *Arkivoc.* 2010 (**2010**) 136–208. https://doi.org/10.3998/ark.5550190.0011.104.

[26] E.A. Kuzmina, T. V. Dubinina, N.E. Borisova, L.G. Tomilova, Octachloro- and hexadecafluoro-substituted lanthanide (III) phthalocyaninates: Synthesis and spectral properties, *Macroheterocycles* 10 (**2017**) 520–525. https://doi.org/10.6060/mhc171253d.

[27] T.T. Tasso, T. Furuyama, N. Kobayashi, Absorption and electrochemical properties of cobalt and iron phthalocyanines and their quaternized derivatives: Aggregation equilibrium and oxygen reduction electrocatalysis, *Am. Chem. Soc.* 52 (**2013**) 9206–9215. https://doi.org/10.1021/ic4002048.

[28] K. Ozoemena, P. Westbroek, T. Nyokong, Cyclic voltammetric studies of octabutylthiophthalocyaninato-cobalt (II) and its self-assembled monolayer

(SAM) on gold electrode, *JPP.* 6 (**2002**) 98–106. https://doi.org/10.1142/S1088424602000130.

[29] R. Olgac, T. Soganci, Y. Baygu, Y. Gök, M. Ak, Zinc(II) phthalocyanine fused in peripheral positions octa-substituted with alkyl linked carbazole: Synthesis, electropolymerization and its electro-optic and biosensor applications, *Biosens. Bioelectron.* 98 (**2017**) 202–209. https://doi.org/10.1016/j.bios.2017.06.028.

[30] M. Hanack, M. Lang, Conducting stacked metallophthalocyanines and related compounds, *Adv. Mater.* 6 (**1994**) 819–833. https://doi.org/10.1002/adma.19940061103.

[31] F. Matemadombo, S. Griveau, F. Bedioui, T. Nyokong, Electrochemical characterization of self-assembled monolayer of a novel manganese tetrabenzylthio-substituted phthalocyanine and its use in nitrite oxidation, *Electroanal.* 20 (**2008**) 1863–1872. https://doi.org/10.1002/elan.200804269.

[32] H. Shirai, A. Maruyama, K. Kobayashi, N. Hojo, K. Urushido, Functional metal-porphyrazine derivatives and their polymers, 4. Synthesis of poly(styrene) bonded Fe(III)- as well as Co(II)-4,4′,4″,4‴-tetracarboxyphthalocyanine and their catalase-like activity, *Die Makromol. Chemie.* 181 (**1980**) 575–584.

[33] P.N. Mashazi, P. Westbroek, K.I. Ozoemena, T. Nyokong, Surface chemistry and electrocatalytic behaviour of tetra-carboxy substituted iron, cobalt and manganese phthalocyanine monolayers on gold electrode, *Electrochim. Acta* 53 (**2007**) 1858–1869. https://doi.org/10.1016/j.electacta.2007.08.044.

[34] D.R. Boston, J.C. Bailar, Phthalocyanine derivatives from 1, 2, 4, 5-tetracyanobenzene or pyromellitic dianhydride and metal salts, *Inorg. Chem*.

11 (**1972**) 1578–1583. https://doi.org/10.1021/ic50113a025.

[35] K. De Wael, A. Adriaens, Comparison between the electrocatalytic properties of different metal ion phthalocyanines and porphyrins towards the oxidation of hydroxide, *Talanta* 74 (**2008**) 1562–1567. https://doi.org/10.1016/j.talanta.2007.09.034.

[36] P. Mashazi, T. Nyokong, Electrocatalytic studies of covalently immobilized metal tetra-amino phthalocyanines onto derivatized screen-printed gold electrodes, *Microchim. Acta* 171 (**2010**) 321–332. https://doi.org/10.1007/s00604-010-0438-6.

[37] K. Ozoemena, P. Westbroek, T. Nyokong, Long-term stability of a gold electrode modified with a self-assembled monolayer of octabutylthiophthalocyaninato-cobalt(II) towards L-cysteine detection, *Electrochem. Commun.* 3 (**2001**) 529–534. https://doi.org/10.1016/S1388-2481(01)00213-2.

[38] B. Simic-Glavaski, A.A. Tanaka, M.E. Kenney, E. Yeager, Spectroscopic and electrochemical studies of transition-metal tetrasulfonated phthalocyanines, *J. Electroanal. Chem.* 229 (**1987**) 285–296. https://doi.org/10.1016/0022-0728(87)85146-x.

[39] J.H. Zagal, M.A. Gulppi, G. Cárdenas-Jirón, Metal-centered redox chemistry of substituted cobalt phthalocyanines adsorbed on graphite and correlations with MO calculations and Hammett parameters. Electrocatalytic reduction of a disulfide, *Polyhedron* 19 (**2000**) 2255–2260. https://doi.org/10.1016/S0277-5387(00)00486-1.

[40] S. Griveau, J. Pavez, J.H. Zagal, F. Bedioui, Electro-oxidation of 2-mercaptoethanol on adsorbed monomeric and electropolymerized cobalt tetra-aminophthalocyanine films. Effect of film thickness, *J. Electroanal. Chem.* 497 (**2001**) 75–83. https://doi.org/10.1016/S0022-0728(00)00454-X.

[41] S. Maree, T. Nyokong, Electrocatalytic behavior of substituted cobalt phthalocyanines towards the oxidation of cysteine, *J. Electroanal. Chem.* 492 (**2000**) 120–127. https://doi.org/10.1016/S0022-0728(00)00281-3.

[42] J.F. Myers, G.W.R. Canham, A.B.P. Lever, Higher oxidation level phthalocyanine complexes of chromium, iron, cobalt and zinc. Phthalocyanine radical species, *Inorg. Chem.* 14 (**1975**) 461–468. https://doi.org/10.1021/ic50145a002.

[43] S. Gorduk, Investigation of singlet oxygen production property of peripherally tetra-substituted In (III) Cl phthalocyanine for photodynamic therapy, *J. Turkish Chem. Soc.* 8 (**2021**) 279–288.

[44] Y.U. Chen, Soluble axially substituted phthalocyanines : Synthesis and nonlinear optical response, *J. Mater. Sci.* 41 (**2006**) 2169–2185. https://doi.org/10.1007/s10853-006-5552-9.

[45] J.H. Zagal, S. Griveau, J.F. Silva, T. Nyokong, F. Bedioui, Metallophthalocyanine-based molecular materials as catalysts for electrochemical reactions, *Coord. Chem. Rev.* 254 (**2010**) 2755–2791. https://doi.org/10.1016/j.ccr.2010.05.001.

[46] J.H. Zagal, Metallophthalocyanines as catalysts in electrochemical reactions, *Coord. Chem. Rev.* 119 (**1992**) 89–136. https://doi.org/10.1016/0010-

8545(92)80031-L.

[47] D. Mwanza, S. Mvango, S. Khene, T. Nyokong, P. Mashazi, Exploiting click chemistry for the covalent immobilization of tetra (4-propargyloxyphenoxy) metallophthalocyanines onto phenylazide-grafted gold surfaces, *Electrochim. Acta* 254 (**2017**) 89–100. https://doi.org/10.1016/j.electacta.2017.09.115.

[48] B.O. Agboola, K.I. Ozoemena, Efficient electrocatalytic detection of epinephrine at gold electrodes modified with self-assembled metallo-octacarboxyphthalocyanine complexes, *Electroanal.* 20 (**2008**) 1696–1707. https://doi.org/10.1002/elan.200804240.

[49] B.O. Agboola, K.I. Ozoemena, Synergistic enhancement of supercapacitance upon integration of nickel (II) octa [(3,5-biscarboxylate)-phenoxy] phthalocyanine with SWCNT-phenylamine, *J. Power Sources* 195 (**2010**) 3841–3848. https://doi.org/10.1016/j.jpowsour.2009.12.095.

[50] R.D. O'Neill, Microvoltammetric techniques and sensors for monitoring neurochemical dynamics in vivo: A review, *Analyst* 119 (**1994**) 767–779. https://doi.org/10.1039/AN9941900767.

# Chapter 2

## 2 Literature review

### 2.1 Neurotransmitters

The neuronal networks in the brain process large amounts of information received from different senses such as sight, feel and hearing. Neurons are used to transmit this information throughout the brain using electrical impulses [1]. Neurons are highly specialized cells, and their composition, metabolism and shape have been adapted to receive, modify, and transmit signals efficiently. These processes take place at specific sites called synapses. This is where the signaling output neuron and the signaling input neuron coincide. The chemical molecules that carry the messages are called the neurotransmitters (NTs). Neurotransmitters play an important role in the mammalian brain. Basically, the brain neuronal communications occur through the exocytotic secretion of neurotransmitters into the synaptic junctions and the surrounding extracellular fluids [2]. The neurotransmitters then transmit the messages from one nerve cell across a synapse to the next target nerve cell, gland cell or muscle [3]. The general action of neurotransmitters through the synaptic cleft is shown in **Figure 2.1**. The neurotransmitters are stored in synaptic vesicles in the pre-synaptic neuron. Upon activation, neurotransmitters are secreted into the synaptic cleft where they diffuse and bind to the neurotransmitter receptors of the nerve cells which can either stimulate or inhibit an electrical response in the post-synaptic neuron [4].

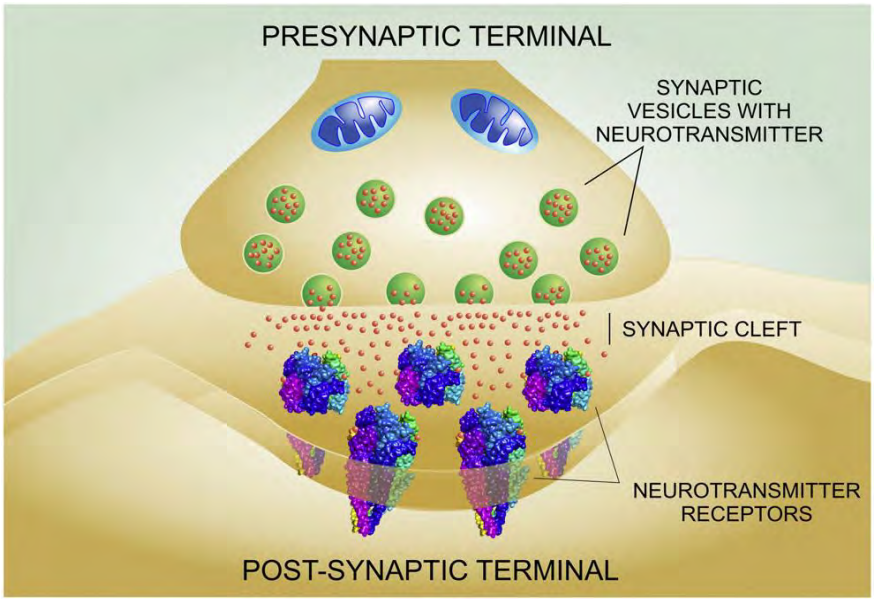


**Figure 2.1**: The general action of neurotransmitters through the synaptic cleft [4].

## 2.2 Classification of neurotransmitters

Approximately 100 different neurotransmitters are known [5] with acetylcholine being the first known neurotransmitter [6]. Neurotransmitters have been classified based on physiological functions, molecular structure or mode of action. The main classes to which the human neurotransmitters belong to are the molecular structures, and these are amino acids, biogenic amines, and soluble gases among others [6]. A class of biogenic amines of interest to the present study are catecholamine neurotransmitters.

## 2.3 Catecholamine neurotransmitters

Catecholamine NTs are found in the peripheral and in the central nervous system (CNS) [1]. The main function of catecholamine NTs is to excite, inhibit or otherwise influence the activity of cells. They contain one amino group attached to an aromatic

ring (catechol moiety) by a 2-carbon chain. The three known catecholamine NTs are dopamine (DA), norepinephrine (NOR), and epinephrine (EP). They are all derived from the same precursor L-DOPA which is itself derived from the amino acid tyrosine [7]. **Figure 2.2** shows chemical structures of the catecholamine NTs; (a) dopamine, (b) norepinephrine, and (c) epinephrine.

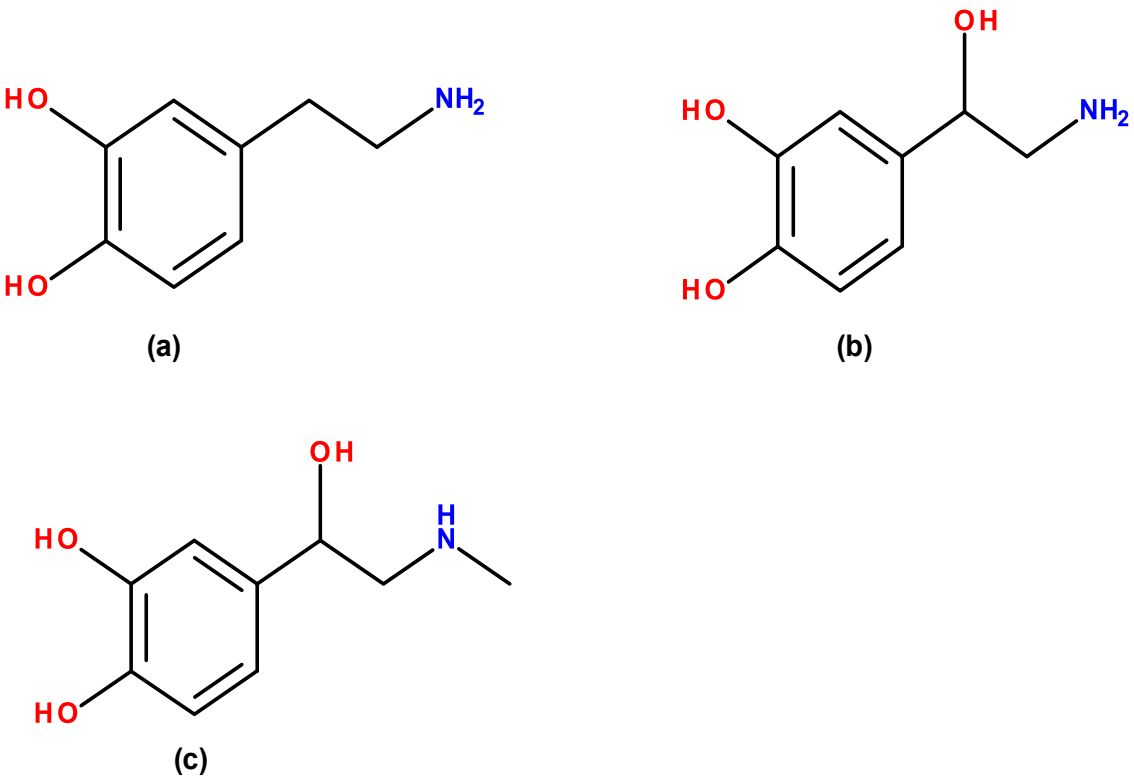


**Figure 2.2**: Chemical structure of (a) dopamine, (b) norepinephrine, and (c) epinephrine.

### 2.3.1 Dopamine

Dopamine (DA) plays an essential role in the peripheral nervous system. It regulates motor functions and motivational behaviors [7]. The two fundamental brain functions are motor activations and reward mediated learning. The reward system is the circuitry

(in the brain) responsible for motivational behaviors and emotions of feeling satisfied. This system is activated by natural rewards such as feelings of pleasure, food and drink, as well as addictive drugs. For instance, addictive drugs like cocaine act by stimulating the release of dopamine from specific brain areas [1]. DA levels measured in resting individuals have been reported to be approximately 10 – 50 ng/L [8]. The high fluctuating levels of dopamine are associated with many psychiatric disorders, including Schizophrenia, Parkinson's and Huntington's disease [7].

### 2.3.2 Norepinephrine

Norepinephrine (NOR) (also known as noradrenaline) acts as both as a hormone and a neurotransmitter in the human body. It regulates functions such as attention, stress and depression, cardiovascular system and improves the speed at which responsive actions occur [6]. Normal NOR levels range within 0.150 – 0.800 µg/L [8]. Abnormal concentrations of norepinephrine can lead to major depressive disorder (MDD), attention deficit hyperactivity disorder (ADHD), Schizophrenia and Parkinson's disease.

### 2.3.3 Epinephrine

Epinephrine (EP) (also known as adrenaline) is found in the hypothalamus and medulla in the brain. It also acts both as a hormone and neurotransmitter. EP stimulates catecholamine receptors in a variety of organs [1]. It plays a crucial role in the transmission of nerve impulse [9], in the flight-or-fight response by increasing the heart rate, vasodilation and blood sugar [7]. EP levels are approximately within 0.010 – 0.050 µg/L when measured in resting individuals [8]. Elevated concentrations of

epinephrine are associated with Schizophrenia, Huntington's and Parkinson's diseases as well as drug addiction [9].

### 2.3.4 Synthesis of catecholamine neurotransmitters

Scheme 2.1 shows the biological (enzymatic) synthesis of the catecholamine NTs [8]. The first step in the synthesis of catecholamine NTs is the catalysis of tyrosine by tyrosine hydroxylase enzyme to form L-3,4-dihydroxyphenylalanine (L-DOPA) also known as levodopa. L-DOPA undergoes decarboxylation by the enzyme L-DOPA decarboxylase to give dopamine. Norepinephrine is formed by the conversion of dopamine by activity of dopamine β-hydroxylase. The final step in the pathway is the conversion of norepinephrine by the enzyme N-methyl transferase to epinephrine.

## 2.4 Current methods for determining and detection of catecholamine NTs

In as much as catecholamine NTs play an important role in neuronal communication, they have threatening effects if not carefully monitored. Quantitative determination and detection of catecholamine NTs is essential in the biomedical fields for the diagnosis and monitoring to serve as clinical biomarkers for specific diseases. Several methods have been used for the detection of catecholamine NTs and these are Fourier-Transform Infrared (FT-IR) [10], chromatography [11], fluorescence [12], Raman [13] and capillary electrophoresis [14]. Whilst these techniques are classically with low limits of detection (LOD) and good selectivity, however they use expensive instrumentation, require complex sample pre-treatment steps leading to more time consumed before the analysis is performed.

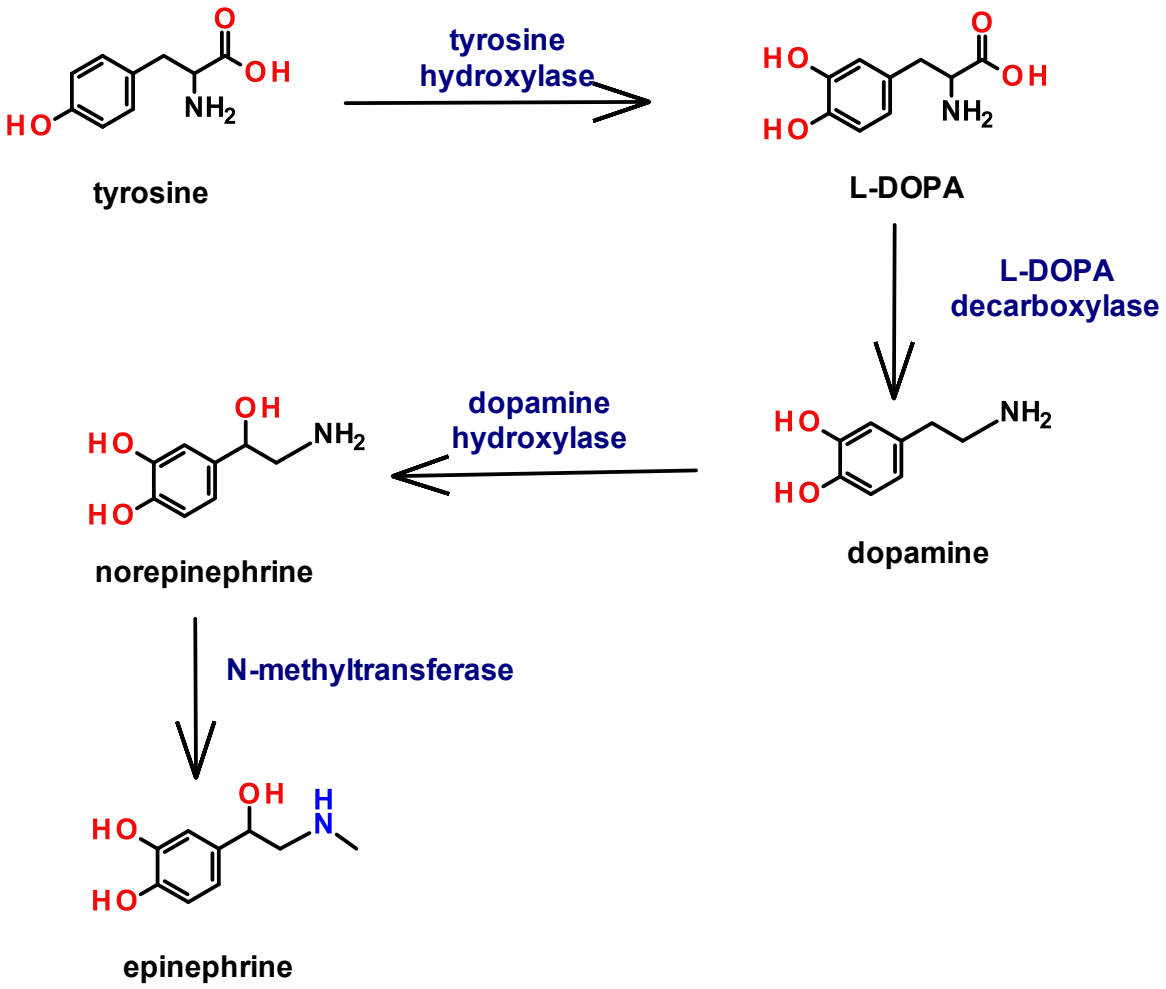


**Scheme 2.1**: Biological synthesis of the catecholamine neurotransmitters.

On the other hand, research interest has immensely grown towards electrochemical sensors for the detection of catecholamine NTs. Ralph Adams reported one of the first electrochemical studies in 1976 and since then electrochemical sensors have shown desirable features; (i) low cost, (ii) simplicity of fabrication, (iii) stability of modification, (iv) high electrocatalytic activity, (v) sensitive, selective and reproducible, (vi) based on abundant modifiers and (vii) easy and reproducible synthesis of the modifiers [15].

Catecholamine NTs can be electrochemically detected because they are electroactive [16]. In general, electrochemical sensors detect catecholamine NTs through their oxidation and reduction at a solid electrode surface. The current produced provide a quantitative measure and it is equivalent to the concentration of the specific catecholamine NT [2]. The electrocatalytic oxidation and/or reduction of the catecholamine NTs is dependent on pH. It is a two-electron process which is accompanied by a transfer of two protons, forming a corresponding ortho-o-quinone. The electrochemical oxidation and/or reduction of the catecholamine NTs is shown in **Scheme 2.2**, dopamine is used as an example. **Scheme 2.2** shows the mechanism process of the electrochemical oxidation of dopamine in physiological media pH 7.4. Electrochemistry is a powerful technique to investigate processes that involve transfer of electrons.

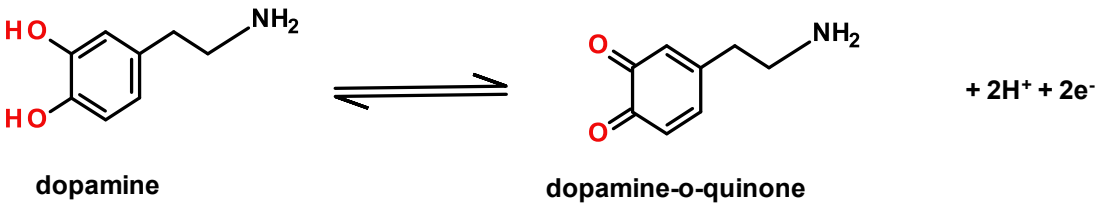


**dopamine** **dopamine-o-quinone**

**Scheme 2.2**: Electrochemical oxidation and/or reduction process of dopamine to dopamine-o-quinone.

## 2.5 Fundamentals of electrochemistry

Electrochemistry is defined as the study of chemical reactions to produce electric power such as galvanic cell [17]. Electrochemistry can otherwise be defined as the use of electricity to affect chemical processes, called electrolytic processes [17]. Electric power is produced as a result of the movement of electrons and/or ions from the solution to the metallic or semi-conductor electrodes, i.e. oxidation and vice versa,

i.e. reduction. The rate of these movements determines the potentials and currents measured in an electrochemical cell. The transfer of electrons in an electrochemical cell is controlled by mass transport mechanisms, such as migration, convection, and diffusion [17–19]. Certain conditions are controlled to have one mechanism to be involved in the cell.

Migration is the movement of ions under the influence of an electric field. To remove migration contributions, a large excess of an easily ionizable salt (e.g. NaCl) is added which will dissociate to produce inert ions [17]. Convection results from movements of the whole solution via stirring and/or solution agitation. It is not a factor in mass transport mechanism as long as the solution is quiescent and electrodes are stationary. Convection can then be driven by stirring the solution or moving the electrodes. Diffusion is the most preferable mechanism of the three because it is driven by the concentration gradient [17]. Diffusion is the movement of ions/molecules from regions of high concentrations to regions of low concentrations. In this case, homogeneity of the solution is always restored.

The most used electrochemical cell in electrochemical experiments is a three-electrode system. The three-electrode electrochemical cell, **Figure 2.3**, consists of (i) the working electrode (WE), (ii) reference electrode (RE), and (iii) the counter electrode (CE). The electrochemical reaction of interest occurs at the working electrode. The working electrode provides a high signal-to-noise characteristic and a reproducible response. The ions/electrons flow between the WE and the CE whilst the RE does not allow the passage of the electrons. The WE is selected based on the

redox behavior of the target analyte and the background current over the potential window to be investigated [18].

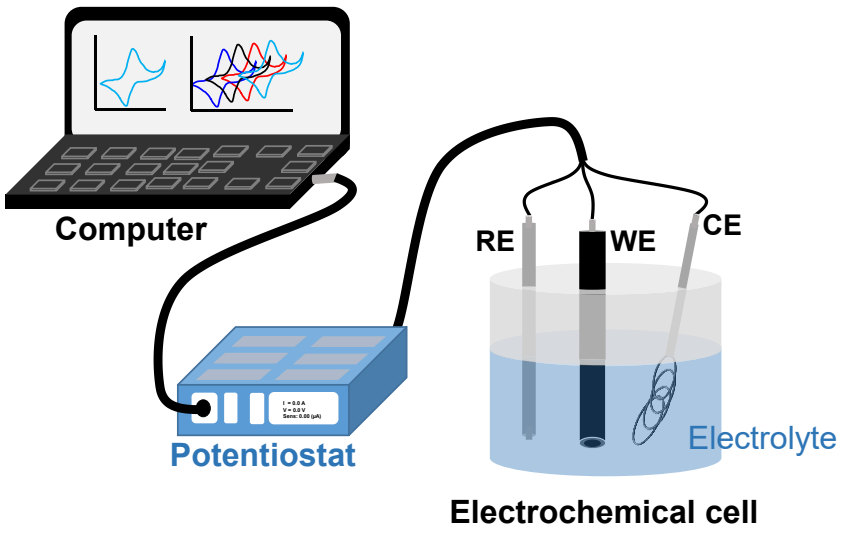


**Figure 2.3**: A diagrammatic representation of an operational electrochemistry system with computer, controller and three-electrode electrochemical cell.

Mercury, carbon, and inert materials such as gold and platinum are used as working electrodes. The RE has a characteristic constant potential which is taken as a standard/reference potential against the working electrodes in an electrochemical cell. A large surface area on the RE is required to maintain low current densities and further reduce polarization of the electrodes [17]. Several reference electrodes are used in electrochemical experiments with silver|silver chloride (Ag|AgCl) reference being the most common. The Ag|AgCl electrode comprise silver wire coated with silver chloride in a glass-tube filled with saturated solution of NaCl or KCl solution, **Figure 2.4**. A semi-permeable salt bridge at the tip of the glass-tube prevents the electrode from bulk solution [20].

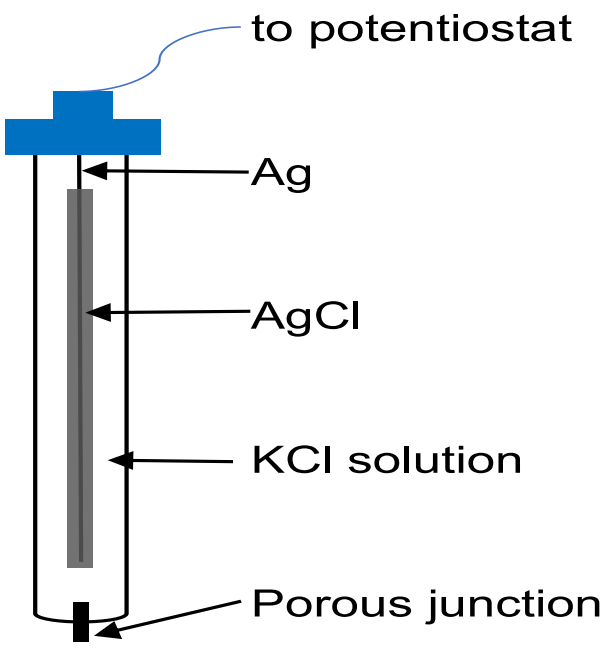


**Figure 2.4**: Schematic representation of Ag|AgCl reference electrode.

The CE completes the electrochemical circuit and is used to eliminate polarization of the reference electrode [17–19]. The CE serves as a source or sink for electrons to ensure current is passed from the external circuit through the cell. The working electrode and reference electrode maintain the potential difference (ΔE) in a potentiostat and the current (I) needed to effect this change occurs at the WE [17–19]. The commonly used CE are platinum and graphite due to their inertness and conducting nature.

The choice of the supporting electrolyte and solvent is important in the design of an electrochemical experiment. The choice of solvent depends on the solubility of the target analyte and its properties such as electrical conductivity, chemical and electrochemical inertness [17]. The solvent itself should be of high purity, inert towards analyte or product and should not readily be oxidized or reduced within the potential window of interest. The commonly used solvents are water, dimethylformamide

(DMF), dimethyl sulfoxide (DMSO), acetonitrile (ACN), dichloromethane (DCM), and methanol.

Supporting electrolytes also play an important role in an electrochemical experiment. They are responsible for (i) eliminating electron migration effect, (ii) decreasing solution resistance, and (iii) maintaining constant ionic strength. The most used supporting electrolytes in aqueous solutions include alkali chlorides, nitrates, sulphates, perchlorates, and phosphates. In organic solutions, tetra alkylammonium salts are used, for example, tetrabutylammonium perchlorate (TBAP), tetrabutylammonium tetrafluoroborate ($TBABF_4$), and tetraethylammonium perchlorate (TEAP). The supporting electrolytes are added in excess and should not be involved in the electrochemical reaction within the target potential window. The experimental solution needs to be de-aerated using inert gases before the experiment to avoid interference of oxygen [19].

## 2.6 Current methods of electrode modification and challenges faced

Various methods have been reported in the modification of electrode surfaces using metallophthalocyanines. Gold and glassy carbon are the mostly used electrodes in the fabrication of electrochemical sensors. The reported methods include drop dry method [21], electro-polymerization [22], self-assembly [23], as well as electrografting [24,25] to mention but a few.

In the drop-dry method, a metallophthalocyanine solution is directly deposited on the electrode surface through adsorption [23]. The solution is dropped and left to dry. The delocalized and conjugated metallophthalocyanine ring system forms π-π interactions

with the glassy carbon electrode [21]. The challenge with the drop-dry method is the lack of reproducibility and it is only limited to conjugated carbon-based materials to allow for the π-π interactions to occur.

Electro-polymerization involves oxidizing or reducing a monomer solution to an activated form polymerizes to form a polymer film directly onto the electrode surface [26]. Different electrode surfaces, such as platinum and carbon, can be used for the electro-polymerization. Using electro-polymerization, film growth can be prevented, and electrode passivation occurs if the polymer is not redox active [26]. The disadvantage of this method is the complex synthesis of metallophthalocyanine bearing polymer-forming functional groups [22,27,28].

Self-assembled monolayers (SAMs) are formed through chemisorption. A strong irreversible chemical film is adsorbed onto the electrode surface [26]. Gold and coinage metal electrodes are used for the self-assembly monolayer technique [29]. Substituted metallophthalocyanine complexes with functional groups such as sulphur [29,30] or amine groups [31] have strong affinity towards active electrode surface to form SAMs. The nature of SAMs formed may be affected by the central metal ion on the metallophthalocyanine or the ring substituents. While the orientation of the SAMs on the electrode surface is affected by the axial ligands or the number and nature of the substituents on the metallophthalocyanine ring. The challenge with this technique is the mobility of the SAM film on the electrode surface and environmental instability [32]. SAMs are easily oxidized in the atmosphere and are labile under high temperatures.

Research to investigate stable modification techniques continues to grow and the quest is to find reproducible methods of electrode modification. Electrochemical

grafting has received a lot of attention recently. Electrochemical grafting is a modification process that allows organic layers to bind to solid conducting substrates [33]. It involves a one electron reduction of an aryl diazonium salt and loss of nitrogen as $N_2$. The loss of $N_2$ results in an aryl radical generation which then attaches onto the surface through a metal-carbon (M-C) or carbon-carbon (C-C) covalent bond, depending on the electrode surface used [32]. Electrochemical grafting has gained great research attention due to rapid electro-reduction, formation of a strong covalent bond and it is a simple method. Diazonium electrografted layers form stable metal-carbon bond when compared to the metal-sulphur bond formed by SAMs [33,34]. For electrografting of the aryl diazonium salt, two approaches are used. The first approach involves first the ex-situ preparation of the aryl diazonium salt followed by electrografting of the diazonium salt. The second approach involves the in-situ preparation of aryl diazonium salt also followed by electrografting and attachment of the aryl radical onto the electrode surface. Reducing the aryl diazonium salt directly on the electrode surface via ex-situ approach is preferred to electrografting in-situ. Direct electrografting allows precise control of interfacial properties such as the thickness of the modifier molecule [35]. Another advantage is that electrografting can be done either in aqueous or organic solvents [36]. The thickness determines the electrode kinetics of a particular redox process. Experimental parameters such as applied potential, concentration of the diazonium salt and scan rate can be optimized to get the required layer [37]. Formation of a monolayer can be achieved when concentration of the diazonium salt is less than 1.0 mM and multilayers when above 1.0 mM [38]. In the present study, the aryl diazonium salt is directly electrografted onto a gold electrode to achieve a phenylethylamine (PEA) monolayer thin film.

## 2.7 Phthalocyanines

Phthalocyanine (Pcs) are blue-green coloured macrocyclic organic molecules which are similar to the naturally occurring porphyrins. Since their accidental discovery in the early 1900s, Pcs have been applied in many fields. They exist as either metal free molecules ($H_2$Pcs) (a) or as metallated molecules (MPcs) (b) as shown in **Figure 2.5**.

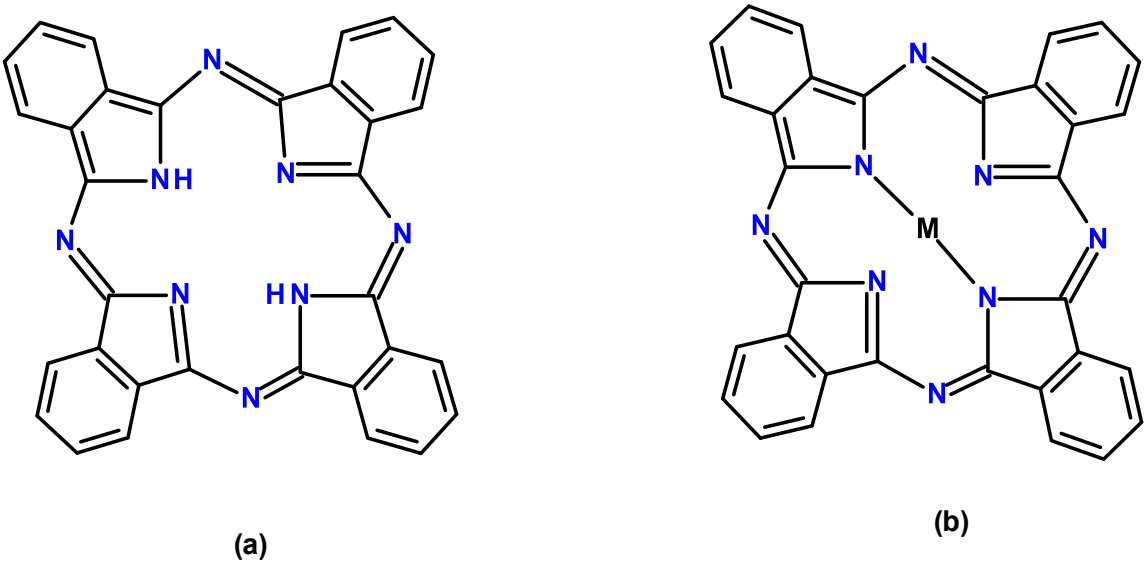


**Figure 2.5**: Chemical structures of (a) metal-free ($H_2$Pc) and (b) metallated phthalocyanines, where M represents the central metal ion.

Metalated phthalocyanines commonly called metallophthalocyanines (MPcs) have metals inserted within the central cavity of the molecule. Metallophthalocyanines exhibit interesting physicochemical and electrochemical properties that have led to their wide industrial applications. They have been used as building blocks in photosensitizers, chemical sensors, liquid crystals, non-linear optics, and electrocatalysts [**39–43**]. The application of MPcs is mostly because of their ability to

transfer electrons due to the 18 π-electron conjugated ring system around the molecule [44].

### 2.7.1 Nomenclature of phthalocyanines

The nomenclature of metallophthalocyanines is derived from the formular a-$(L)_n$ -MPc-n&p-S [45] as shown in Figure 2.6.

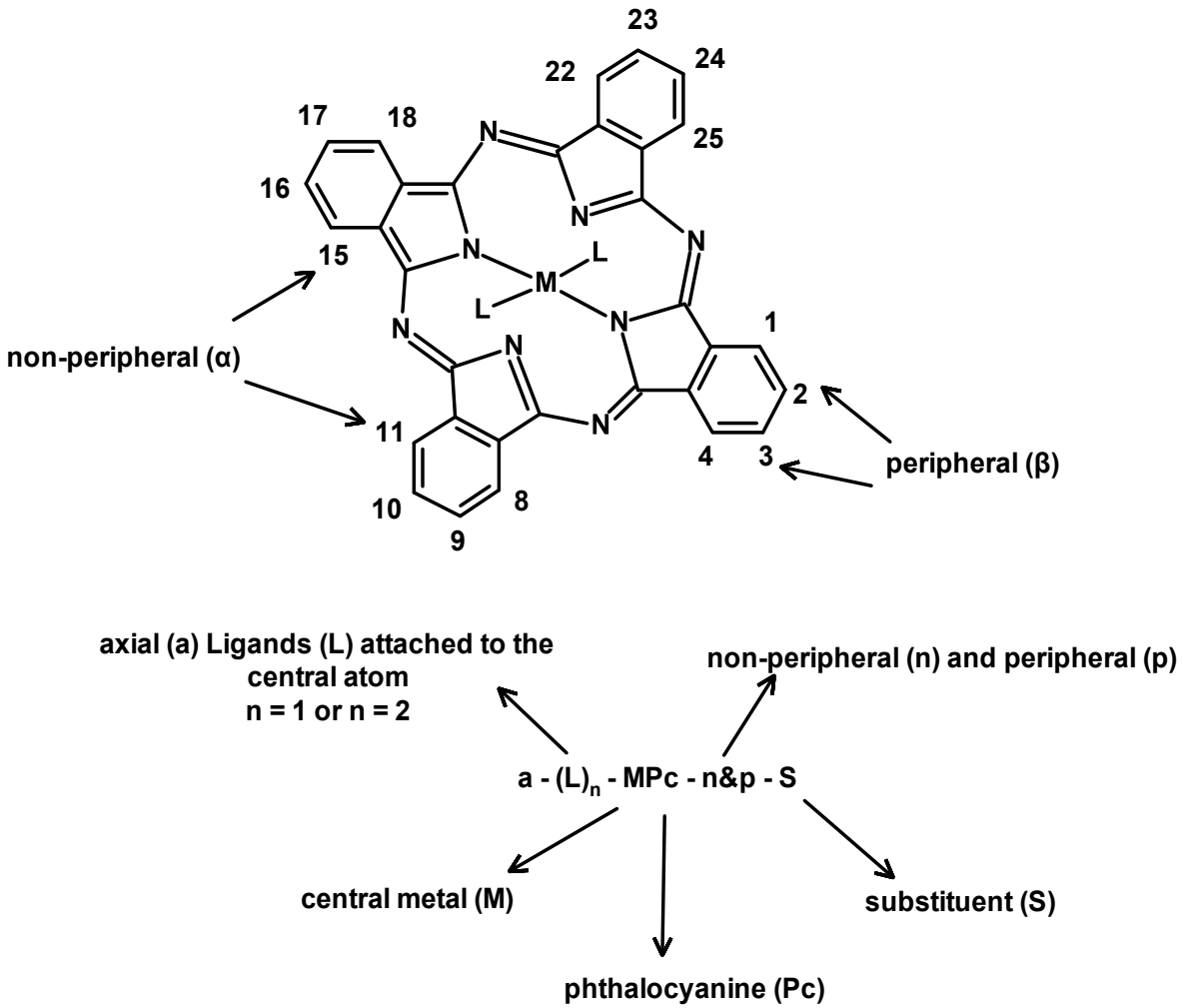


Figure 2.6: Nomenclature of metallophthalocyanine.

### 2.7.2 Synthesis of MPcs

The synthesis procedure depends on the type and application of the metallophthalocyanine [46]. Generally, MPcs are synthesized from several precursors such as phthalonitriles, phthalimides, phthalic anhydrides, phthalic acids, **Scheme 2.3** [40,47]. Cyclotetramerization of these precursors in the presence of the metal salt gives a metallophthalocyanine. Alternatively, MPcs can be prepared by replacing central hydrogens from a metal-free phthalocyanine with a metal ion.

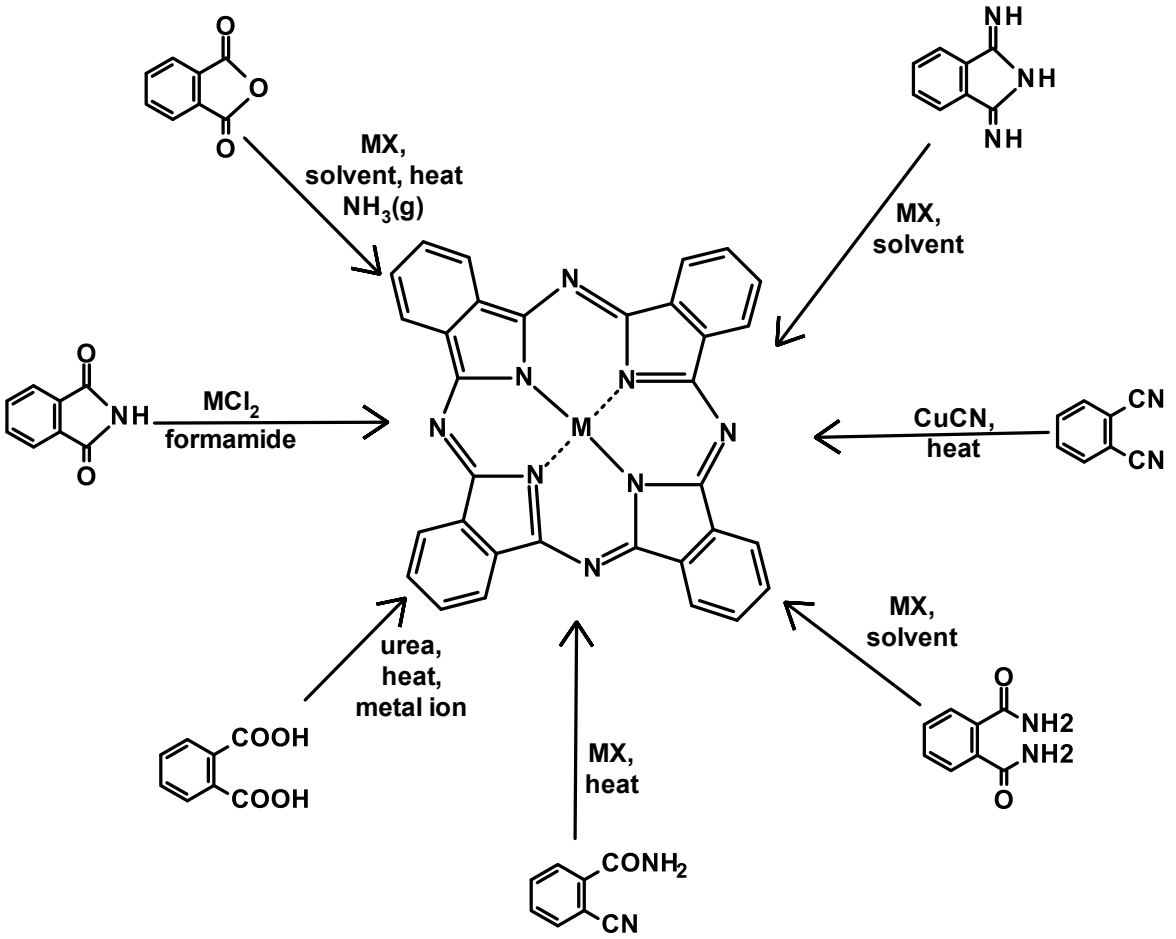


**Scheme 2.3**: General synthesis scheme for metallophthalocyanine from different precursors.

### 2.7.3 Electronic properties of MPcs

The UV-vis spectra of MPcs show 2 characteristic absorption bands called the Q and the B (Soret) bands. The Soret (or B) band is in the ultraviolet (blue) region between 300 – 500 nm. The Q band is observed in the near-IR (red) region between 600 – 800 nm. **Figure 2.7** shows the typical absorption spectrum of MPc.

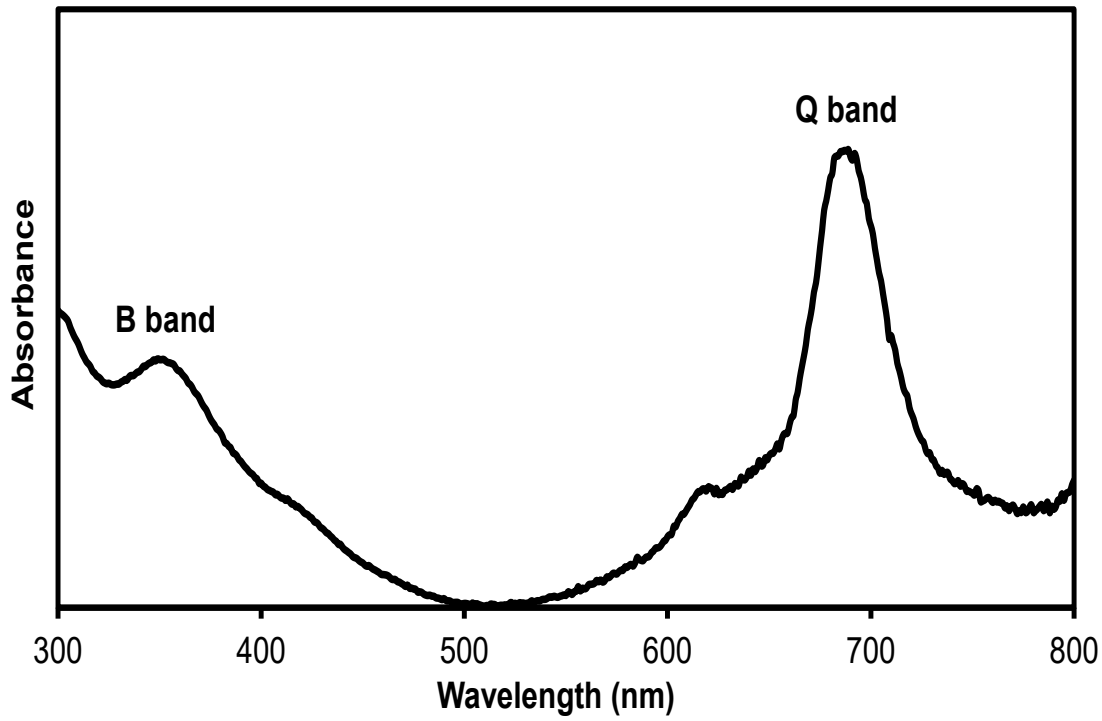


**Figure 2.7**: Typical UV-vis absorption spectrum of a metallophthalocyanine.

**Figure 2.8** shows the origins of both the B and the Q bands as explained by the Gouterman's four-orbital model. Both bands arise due to π-π* transitions. The B band result from the electron transition from $a_{2u}$ or $b_{2u}$ of the highest occupied molecular orbital (HOMO) to the $e_g$ orbital of the lowest unoccupied molecular orbital (LUMO). The model suggests that the Q band results from the transition from $a_{1u}$ of the (HOMO) to $e_g$ of the (LUMO) [48].

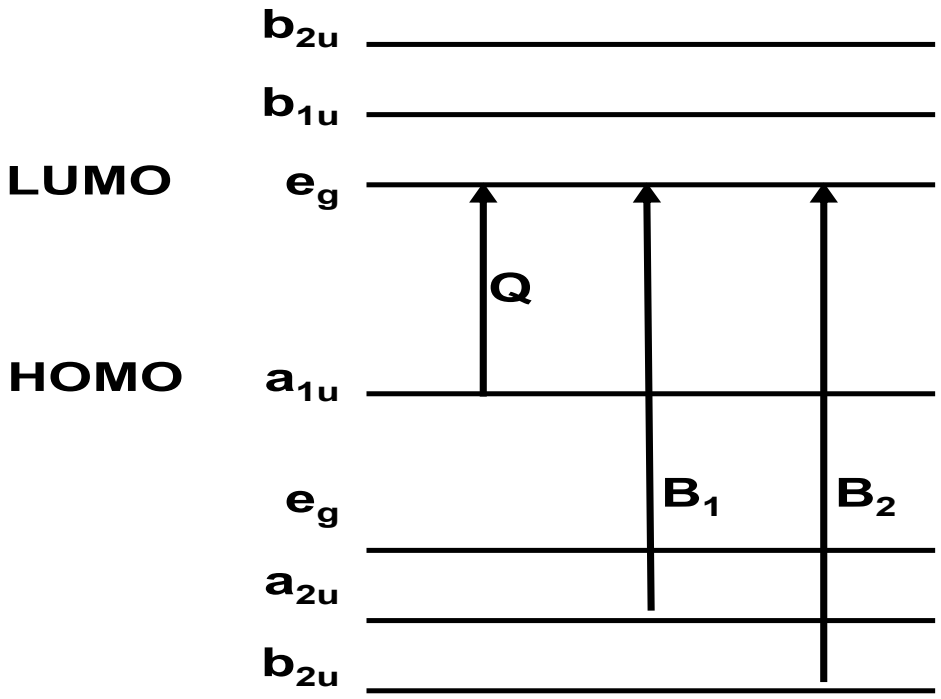


**Figure 2.8**: Gouterman's four-orbital model showing electron transitions and origins of B and Q bands.

## 2.8 Applications of MPcs

Metallophthalocyanines are the most studied class of macrocyclic organo-metallic functional materials. They remain being one type of molecule having a wide variety of applications. MPcs have remarkable physico-chemical properties that lead to several attractive potential applications in various fields. The applications of MPcs range from semi-conductors [49], to molecular electronics [50], photo-sensitizers for photodynamic therapy (PDT) of cancer [45], catalysis [51], fuel cells [41], photovoltaic cells [39] among others. Torre et al. [49] outlined the reasons why MPcs have been applied in so many scientific and technological work. MPcs are applied as electrocatalysts in the present study.

### 2.8.1 MPcs as electrocatalysts

MPc complexes are well known as catalysts for both homogeneous and heterogeneous chemical reactions. They present some advantages over metals and metal oxides not only because of the cost but also because their physical properties can be tuned to the desired catalytic properties. MPc have been used as electrocatalysts in the design of electrochemical sensors as electrode modifiers. The fabrication of electrode surfaces with metallophthalocyanine catalyzes the electron transfer processes on the electrode surface. The electrochemical behavior of the MPc is determined by the central metal ion, chemical nature of the substituents i.e. either electron donating or electron withdrawing, the position of the substituents, i.e. either peripheral or non-peripheral and as well as solvents [21,52]. MPcs exhibit interesting redox properties and stability hence their use as electrocatalysts. The planar structure of MPcs allow them to undergo redox processes without losing their stability [21]. The first-row transition metals (notably Mn, Fe and Co) phthalocyanine have proved to be excellent homogeneous and heterogeneous electrocatalyst for different inorganic and organic molecules [53].

In the design of electrochemical sensors, MPcs are immobilized as electrocatalysts onto the electrode surface. The electrode will then take the properties of the immobilized MPc and form an electroactive interface. The MPc interact with the analyte of interest and act as an electron mediator and hence allow for the redox reaction to occur. The different central metal ions with different oxidation state results in different electrochemical properties of the MPc. During the redox reaction, the MPc changes its oxidation state as it interacts with the analyte and thereafter recover its initial oxidation. Electroactive central metal ions are of interest in this study. It can be

noted that metallophthalocyanines with non-electroactive central metal ions can also undergo redox processes mediated by the conjugated ring system itself.

The redox processes in the MPc occur on the central metal ion if the metal d-orbitals/energy level lie between the HOMO and the LUMO gap of the MPc ring [**51**]. On the other hand, the oxidation of the analyte depends on the energy level occupied on the HOMO. While the reduction depends on the energy level of the LUMO. The redox processes also occur through successive one electron transfer between the working electrode and the π-conjugated ring system.

The redox processes occurring on the metal in the metallophthalocyanine are expected only to Mn, Fe and Co derivatives due to the fact that their d-orbitals are positioned between HOMO and LUMO [**51**]. M(II) | M(I) and M(III) | M(II) reversible couples are observed for Fe and Co phthalocyanine. Fe and Co metals exist with +2 oxidation state ($Fe^{2+}$, $Co^{2+}$) whilst the ring exists as a dianion $MPc^{-2}$ [**45,51**]. The dianion $MPc^{-2}$ can be reduced or oxidized to different oxidation states. The oxidation process on the ring, $MPc^{-2}$ results in the formation of $MPc^{-1}$ and $MPc^{0}$ species due to removal of 2 electrons from the HOMO ($a_{1u}$) orbitals. The reduction processes is the succession addition of 4 electrons to the LUMO ($e_g$) of an $MPc^{-2}$ resulting in the formation of $MPc^{-3}$, $MPc^{-4}$, $MPc^{-5}$ and $MPc^{-6}$ species [**54,55**].

## 2.9 References

[1] J.A. Ribeiro, P.M.V. Fernandes, C.M. Pereira, F. Silva, Electrochemical sensors and biosensors for determination of catecholamine neurotransmitters: A review, *Talanta* 160 (**2016**) 653–679.

https://doi.org/10.1016/j.talanta.2016.06.066.

[2] E.S. Bucher, R.M. Wightman, Electrochemical analysis of neurotransmitters, *Annu. Rev. Anal. Chem.* 8 (**2015**) 239–261. https://doi.org/10.1146/annurev-anchem-071114-040426.

[3] G.D. Chiara, The principles of nerve cell communication, *Alcohol Health Res. World* 21 (**1997**) 107–108.

[4] M.V. Borroni, A.S. Vallés, F.J. Barrantes, The lipid habitats of neurotransmitter receptors in brain, *Biochim. Biophys. Acta - Biomembr.* 1858 (**2016**) 2662–2670. https://doi.org/10.1016/j.bbamem.2016.07.005.

[5] G.L. Kovács, The endocrine brain: Pathophysiological role of neuropeptide-neurotransmitter interactions., *Ejifcc.* 15 (**2004**) 107–112. http://www.ncbi.nlm.nih.gov/pubmed/29988948%0Ahttp://www.pubmedcentral.nih.gov/articlerender.fcgi?artid=PMC6034195.

[6] Z. Tavakolian-Ardakani, O. Hosu, C. Cristea, M. Mazloum-Ardakani, G. Marrazza, Latest trends in electrochemical sensors for neurotransmitters: A review, *Sensors* 19 (**2019**) 2037. https://doi.org/10.3390/s19092037.

[7] S.D. Niyonambaza, P. Kumar, P. Xing, J. Mathault, P. De Koninck, E. Boisselier, M. Boukadoum, A. Miled, A Review of neurotransmitters sensing methods for neuro-engineering research, *Appl. Sci.* 9 (**2019**) 1–31. https://doi.org/10.3390/app9214719.

[8] S. Latifi, K. Lidsky, J.L. Blumer, Pharmacology of inotropic agents in infants and children, *Prog. Pediatr. Cardiol.* 12 (**2000**) 57–79. https://doi.org/10.1016/S1058-9813(00)00059-X.

[9] D.M. Fouad, W.A. El-Said, Selective electrochemical detection of epinephrine using gold nanoporous film, *J. Nanomater.* 2016 (**2016**). https://doi.org/10.1155/2016/6194230.

[10] X. Wang, J.I.N. Baokang, L.I.N. Xiangqin, In-situ FTIR spectroelectrochemical study of dopamine at a glassy carbon electrode in a neutral solution, *Anal. Sci.* 18 (**2002**) 931–933. https://doi.org/10.2116/analsci.18.931.

[11] V. Carrera, E. Sabater, E. Vilanova, M.A. Sogorb, A simple and rapid HPLC-MS method for the simultaneous determination of epinephrine, norepinephrine, dopamine and 5-hydroxytryptamine: Application to the secretion of bovine chromaffin cell cultures, *J. Chromatogr. B Anal. Technol. Biomed. Life Sci.* 847 (**2007**) 88–94. https://doi.org/10.1016/j.jchromb.2006.09.032.

[12] K.E. Secor, T.E. Glass, Selective amine recognition: Development of a chemosensor for dopamine and norepinephrine, *Org. Lett.* 6 (**2004**) 3727–3730. https://doi.org/10.1021/ol048625f.

[13] W.J. Barreto, S. Ponzoni, P. Sassi, A Raman and UV-vis study of catecholamines oxidized with Mn(III), *Spectrochim. Acta - Part A Mol. Biomol. Spectrosc.* 55 (**1998**) 65–72. https://doi.org/10.1016/S1386-1425(98)00164-4.

[14] L.A. Kartsova, A.A. Sidorova, V.A. Kazakov, E.A. Bessonova, A.Y. Yashin, Determination of catecholamines by capillary electrophoresis and reversed-phase high-performance liquid chromatography, *J. Anal. Chem.* 59 (**2004**) 737–741. https://doi.org/1061-9348/04/5908-0737.

[15] M. Sajid, N. Baig, K. Alhooshani, Chemically modified electrodes for electrochemical detection of dopamine: Challenges and opportunities, *TrAC - Trends Anal. Chem.* 118 (**2019**) 368–385.

https://doi.org/10.1016/j.trac.2019.05.042.

[16] N. Fourati, M. Seydou, C. Zerrouki, A. Singh, S. Samanta, F. Maurel, D.K. Aswal, M. Chehimi, Ultrasensitive and selective detection of dopamine using cobalt-phthalocyanine nanopillar-based surface acoustic wave sensor, *ACS Appl. Mater. Int.* 6 (**2014**) 22378–22386. https://doi.org/10.1021/am506403f.

[17] A. Kaifer, M. Gómez-Kaifer, Supramolecular electrochemistry, *Supramol. Electrochem.* (**2007**) 1–241. https://doi.org/10.1002/9783527613601.

[18] A. J. Bard, L. R.Faulkner, Electrochemical methods, fundamentals and applications, John wiley & Sons, Inc. 2 (**2019**) 1-44. https://doi.org/10.1038/s41929-019-0277-8.

[19] C.M.A. Brett, A.N.A. Maria, O. Brett, Principles, methods and applications, *Oxford Univ. Press.* (**1993**) 1–102.

[20] P.T. Kissinger, W.R. Heineman, Laboratory techniques in electroanalytical chemistry, Revised and expanded, *Marcel Dekker, Inc.* 2 (**1996**) 11–483.

[21] S. Centane, O.J. Achadu, T. Nyokong, Effects of substituents on the electrocatalytic activity of cobalt phthalocyanines when conjugated to graphene quantum dots, *Electroanal.* 29 (**2017**) 2470–2482. https://doi.org/10.1002/elan.201700252.

[22] J. Obirai, N.P. Rodrigues, F. Bedioui, T. Nyokong, Synthesis, spectral and electrochemical properties of a new family of pyrrole substituted cobalt, iron, manganese, nickel and zinc phthalocyanine complexes, *JPP.* 7 (**2003**) 508–520. https://doi.org/10.1142/S1088424603000641.

[23] N. Sehlotho, T. Nyokong, Electrocatalytic oxidation of thiocyanate, l-cysteine

and 2-mercaptoethanol by self-assembled monolayer of cobalt tetraethoxy thiophene phthalocyanine, *Electrochim. Acta* 51 (**2006**) 4463–4470. https://doi.org/10.1016/j.electacta.2005.12.024.

[24] D. Mwanza, S. Mvango, S. Khene, T. Nyokong, P. Mashazi, Exploiting click chemistry for the covalent immobilization of tetra (4-propargyloxyphenoxy) metallophthalocyanines onto phenylazide-grafted gold surfaces, *Electrochim. Acta* 254 (**2017**) 89–100. https://doi.org/10.1016/j.electacta.2017.09.115.

[25] K. Tshenkeng, P. Mashazi, Covalent attachment of cobalt (II) tetra-(3-carboxyphenoxy) phthalocyanine onto pre-grafted gold electrode for the determination of catecholamine neurotransmitters, *Electrochim. Acta* 360 (**2020**) 137015. https://doi.org/10.1016/j.electacta.2020.137015.

[26] N. Carolina, C. Hill, Chemically modified electrodes: Terminology and definitions (IUPAC Recommendations 1997), *Pure Appl. Chem.* 69 (**1997**) 1317–1323.

[27] D. Akyüz, Ü. Demirbaş, A. Koca, F. Çelik, H. Kantekin, Electrochemistry, electropolymerization and electrochromism of novel phthalocyanines bearing morpholine groups, *J. Mol. Struct.* 1206 (**2020**) 127674. https://doi.org/10.1016/j.molstruc.2019.127674.

[28] V. Çakir, F. Demir, Z. Biyiklioğlu, A. Koca, H. Kantekin, Synthesis, characterization, electrochemical and spectroelectrochemical properties of metal-free and metallophthalocyanines bearing electropolymerizable dimethylamine groups, D*ye. Pigment* 98 (**2013**) 414–421. https://doi.org/10.1016/j.dyepig.2013.03.021.

[29] S. Khene, D.A. Geraldo, C.A. Togo, J. Limson, T. Nyokong, Synthesis,

electrochemical characterization of tetra- and octa-substituted dodecyl-mercapto tin phthalocyanines in solution and as self-assembled monolayers, *Electrochim. Acta* 54 (**2008**) 183–191. https://doi.org/10.1016/j.electacta.2008.08.018.

[30] K.I. Ozoemena, T. Nyokong, P. Westbroek, Self-Assembled Monolayers of cobalt and iron phthalocyanine complexes on gold electrodes: Comparative surface electrochemistry and electrocatalytic interaction with thiols and thiocyanate, *Electroanal.* 15 **(2003**) 1762–1770. https://doi.org/10.1002/elan.200302753.

[31] M. Nemakal, S. Aralekallu, I. Mohammed, K.P. Keshavananda, L. Koodlur Sannegowda, Chemisorbed palladium phthalocyanine for simultaneous determination of biomolecules, *Microchem. J.* 143 (**2018**) 82–91. https://doi.org/10.1016/j.microc.2018.07.039.

[32] S. Kesavan, S.B. Revin, S.A. John, Fabrication, characterization and application of a grafting based gold nanoparticles electrode for the selective determination of an important neurotransmitter, *J. Mater. Chem.* 22 (**2012**) 17560–17567. https://doi.org/10.1039/c2jm33013j.

[33] D. Bélanger, J. Pinson, Electrografting: A powerful method for surface modification, *Chem. Soc. Rev.* 40 (**2011**) 3995–4048. https://doi.org/10.1039/c0cs00149j.

[34] D. Hetemi, V. Noël, J. Pinson, Grafting of diazonium salts on surfaces: Application to biosensors, *Biosens.* 10 (**2020**) 4-36. https://doi.org/10.3390/bios10010004.

[35] H. Randriamahazaka, J. Ghilane, Electrografting and controlled surface

functionalization of carbon based surfaces for electroanalysis, *Electroanal.* 28 (**2016**) 13–26. https://doi.org/10.1002/elan.201500527.

[36] S. Griveau, D. Mercier, C. Vautrin-Ul, A. Chaussé, Electrochemical grafting by reduction of 4-aminoethylbenzenediazonium salt: Application to the immobilization of (bio)molecules, *Electrochem. Commun.* 9 (**2007**) 2768–2773. https://doi.org/10.1016/j.elecom.2007.09.004.

[37] J. Pinson, Attachment of organic layers to materials surfaces by reduction of diazonium salts, Aryl diazonium salts new coupling agents, *Polym. Surf. Sci.* (**2012**) 1–35. https://doi.org/10.1002/9783527650446.ch1.

[38] P.S. Adarakatti, S.K. Kempahanumakkagari, Modified electrodes for sensing, *Electrochem.* 15 (**2019**) 58-95. https://doi.org/10.1039/9781788013895-00058.

[39] L. Tahershamsi, Y. Gerasymchuk, A. Wedzynska, M. Ptak, I. Tretyakova, A. Lukowiak, Synthesis, spectroscopic characterization and photoactivity of Zr(IV) phthalocyanines functionalized with aminobenzoic acids and their GO-based composites, *C - J. Carbon Res.* 6 (**2019**) 1-13. https://doi.org/10.3390/c6010001.

[40] A.Y. D. Wohrle, M. Eskes, K. Shigehara, A simple synthesis of 4,5 disubstituted 1,2 dicyanobenzenez and 2,3,9,10,16,17,23,24 octasubstituted phthalocyanines, *Synthesis* (**1993**) 194–196.

[41] A.B.P. Lever, M.R. Hempstead, C.C. Leznoff, W. Liu, M. Melnik, W.A. Nevin, P. Seymour, Recent studies in phthalocyanine chemistry, *Pure Appl. Chem.* 58 (**1986**) 1467–1476. https://doi.org/10.1351/pac198658111467.

[42] P.N. Mashazi, P. Westbroek, K.I. Ozoemena, T. Nyokong, Surface chemistry

and electrocatalytic behaviour of tetra-carboxy substituted iron, cobalt and manganese phthalocyanine monolayers on gold electrode, *Electrochim. Acta* 53 (**2007**) 1858–1869. https://doi.org/10.1016/j.electacta.2007.08.044.

[43] J. Oni, T. Nyokong, Simultaneous voltammetric determination of dopamine and serotonin on carbon paste electrodes modified with iron(II) phthalocyanine complexes, *Anal. Chim. Acta* 434 (**2001**) 9–21. https://doi.org/10.1016/S0003-2670(01)00822-4.

[44] I.S. Hosu, Q. Wang, A. Vasilescu, S.F. Peteu, V. Raditoiu, S. Railian, V. Zaitsev, K. Turcheniuk, Q. Wang, M. Li, R. Boukherroub, S. Szunerits, Cobalt phthalocyanine tetracarboxylic acid modified reduced graphene oxide: A sensitive matrix for the electrocatalytic detection of peroxynitrite and hydrogen peroxide, *RSC Adv.* 5 (**2015**) 1474–1484. https://doi.org/10.1039/c4ra09781e.

[45] S. Arslan, Phthalocyanines: Structure, synthesis, purification and applications, *Batman Univ. J. Life Sci.* 6 (**2016**) 188–197. http://www.yasambilimleridergisi.com/makale/pdf/1466373234.pdf.

[46] M.S. RodríGuez-Morgade, G. De La Torre, T. Torres, Design and synthesis of low-symmetry phthalocyanines and related systems, *Porphyr. Handb.* 15 (**2003**) 125-160. https://doi.org/10.1016/B978-0-08-092389-5.50009-2.

[47] V.N. Nemykina, E.A. Lukyanets, Synthesis of substituted phthalocyanines, *Arkivoc.* 2010 (**2010**) 136–208. https://doi.org/10.3998/ark.5550190.0011.104.

[48] C. Weiss, H. Kobayashi, M. Gouterman, Spectra of porphyrins. Part III. Self-consistent molecular orbital calculations of porphyrin and related ring systems, *J. Mol. Spectrosc.* 16 (**1965**) 415–450. https://doi.org/10.1016/0022-2852(65)90132-3.

[49] G. De La Torre, C.G. Claessens, T. Torres, Phthalocyanines: Old dyes, new materials. Putting color in nanotechnology, *Chem. Commun.* (**2007**) 2000–2015. https://doi.org/10.1039/b614234f.

[50] C. Hamann, M. Hietschold, A. Mrwa, M. Müller, M. Starke, R. Kilper, Phthalocyanine thin films for molecular electronics, *Mol. Electron.* (**1991**) 129–138. https://doi.org/10.1007/978-94-011-3392-0_14.

[51] J.H. Zagal, Metallophthalocyanines as catalysts in electrochemical reactions, *Coord. Chem. Rev.* 119 (**1992**) 89–136. https://doi.org/10.1016/0010-8545(92)80031-L.

[52] B. Simic-Glavaski, A.A. Tanaka, M.E. Kenney, E. Yeager, Spectroscopic and electrochemical studies of transition-metal tetrasulfonated phthalocyanines, *J. Electroanal. Chem. Interfacial Electrochem.* 229 (**1987**) 285–296. https://doi.org/10.1016/0022-0728(87)85146-x.

[53] B.O. Agboola, K.I. Ozoemena, Self-assembly and heterogeneous electron transfer properties of metallo-octacarboxyphthalocyanine complexes on gold electrode, *Phys. Chem. Chem. Phys.* 10 (**2008**) 2399–2408. https://doi.org/10.1039/b800611c.

[54] J. Nackiewicz, M. Kliber, Synthesis and selected properties of metallo and metal-free 2,3,9,10,16,17,23,24-octacarboxyphthalocyanines, *Arkivoc.* 2015 (**2015**) 269–299. https://doi.org/10.3998/ark.5550190.p008.923.

[55] J. Mack, N. Kobayashi, Low symmetry phthalocyanines and their analogues, *J. Am. Chem. Soc.* 111 (**2011**) 281–321. https://doi.org/https://doi.org/10.1021/cr9003049.

# Chapter 3

## 3 Novel covalent immobilization of cobalt (II) octa acyl chloride phthalocyanines onto phenylethylamine pre-grafted gold via spontaneous amidation


### Abstract

In this work, a gold electrode surface was pre-grafted with phenylethylamine (PEA) thin film for spontaneous covalent immobilization of cobalt (II) octa acyl chloride (CoOAClPc) via the nucleophilic addition reaction. Pre-grafting of PEA thin film was achieved by electrochemical reduction of 4-(2-aminoethyl) benzene diazonium (AEBD) salt. Cobalt (II) octa acyl chloride phthalocyanine (CoOAClPc) was successfully synthesized and covalently immobilized onto the pre-grafted gold electrode surface to form a thin monolayer of Au-PEA-CoOAClPc. Upon hydrolysis of the thin monolayer, the -COCl terminal functional groups were converted to -COOH to form Au-PEA-CoOCAPc. The presence of PEA and PEA-CoOCAPc was confirmed by electrochemical X-ray photoelectron spectroscopy surface characterization. The pH sensitivity of -COOH terminal groups was studied using a negatively charged $[Fe(CN)_6]^{3-/4-}$ and a positively charged $[Ru(NH_3)_6]^{2+/3+}$ redox probes. The Au-PEA-CoOCAPc was investigated for electrocatalytic and electroanalytical properties towards the detection of catecholamine neurotransmitters (dopamine, epinephrine, and norepinephrine). The electrocatalytic oxidation of the catecholamine neurotransmitters in PBS solution (pH 7.4) was studied using differential pulse voltammetry (DPV) in a linear range up to 50 µM. The LOD was determined to be 64 nM, 0.22 µM and 0.17 µM for dopamine (DA), epinephrine (EP) and norepinephrine

(NOR) respectively. The limit of quantification (LOQ) was determined to be 0.21 µM, 0.73 µM and 0.56 µM for DA, EP and NOR respectively. Stable and reproducible novel method of electrode fabrication to form Au-PEA-CoOCAPc was achieved. Excellent analytical properties (sensitivity, low detection limits and limit of quantification) were obtained by using the fabricated electrochemical sensors, Au-PEA-CoOCAPc, for the determination of catecholamine neurotransmitters and screening of ascorbic acid (AA).

## 3.1 Introduction

Dopamine (DA), epinephrine (EP) and norepinephrine (NOR) are catecholamine neurotransmitters that play an important role in the brain neuronal communication, processing extensive information in the synaptic junctions and the surrounding extra-cellular fluid throughout the body [1–3]. The slightest change in the concentrations of catecholamine neurotransmitters is associated with Alzheimer's, Parkinson's and Huntington's diseases [4]. Therefore, quantitative detection and determination of these neurotransmitters is of great importance. Several techniques that have been used to detect neurotransmitters include fluorimetry, chromatography and capillary [5]. However, these techniques are expensive, time consuming and not suitable for onsite monitoring. Since catecholamine neurotransmitters are electroactive, they can be detected by electrochemical sensors [2,6] in a cost effective, sensitive and easy-to-use manner [1,5]. Poor electrochemical properties of catecholamine neurotransmitters have been displayed on bare electrodes [6,7] due to required high oxidation overpotentials and strong interference in sample media. To improve on the challenges, electrodes can be modified with materials to: (a) lower the oxidation

overpotentials, (b) increase sensitivity of the electrode, and (c) improve selectivity towards catecholamines.

Metallophthalocyanines (MPc) modified electrodes have been used as electrochemical sensors to quantify catecholamines [2,8–10]. MPcs are 18 π-electron highly conjugated macrocyclic molecules with similar core-structure to the naturally occurring porphyrins containing a central metal ion. Cobalt phthalocyanine and its derivatives are the most widely studied metal phthalocyanines as electrode modifiers [11] because of their biocompatibility, chemical inertness and good catalytic activity [12]. They have proved to be excellent catalysts for many reactions. Most of the applications as electrocatalysts involve exchange of electrons between them and the electron donors or acceptors [12]. The interaction of cobalt phthalocyanine with an oxidation substrate involves the Co(III) | Co(II) redox process. Cobalt phthalocyanines have been applied in electrochemical sensor fabrication because of their excellent electron transfer abilities allowing them to undergo redox reactions [13–15]. The high electron transfer ability leads to the excellent electrocatalytic property of the electrochemical sensors [16–18]. The major challenge encountered in the electrochemical detection of catecholamine neurotransmitters in real samples is the coexisting interferences such as ascorbic acid (AA) [19] which hinder precise detection and determination of neurotransmitters. Ascorbic acid has an overlapping oxidation potential as the catecholamine neurotransmitters [19] due to their similar structure. MPc modified electrochemical sensors bearing pH sensitive functional groups can be used to overcome this challenge by screening off the AA [20–22]. The electrocatalytic process of MPcs is not only affected by the central metal ion but also the peripheral substituents [23–25]. However, development of MPc modified electrochemical sensors require several steps of fabrication. Tshenkeng and Mashazi, 2020 [22]

modified a phenylethylamine pre-grafted gold electrode with cobalt (II) tetra-(3-carboxyphenoxy) phthalocyanine and used amide coupling reagents such as dicyclohexyl carbodiimide (DCC) and N-hydroxysuccinimide (NHS). Several studies have also used the amide coupling reagents for the immobilization of carboxylic acid functionalized MPcs onto self-assembled monolayer (SAMs) modified gold electrodes [21] and for their coupling onto amine functionalized substrates [26].

A cost-effective method of immobilizing metallophthalocyanine as an electrocatalyst whilst requiring fewer chemical reagents is desirable. In this study, the acyl chloride (-COCl) functional groups were formed on the peripheral positions of MPc and investigated for their spontaneous amidation via the nucleophilic addition/elimination reaction without amide coupling reagents such as DCC and NHS. Acyl chloride functional groups readily and spontaneously react with amine ($–NH_2$) functional groups to form amide bonds. The amine functional groups were accomplished using stable electrografted phenylethylamine (PEA) onto gold to form Au-PEA surface. The Au-PEA surface was further used to immobilize cobalt (II) octa acyl chloride phthalocyanine (CoOAClPc) forming an Au-PEA-CoOAClPc electrode surface. The unreacted peripheral acyl chloride functional groups were converted to carboxylic acid via nucleophilic acyl substitution reaction in hygroscopic environment. An increase in carboxylic acid functional groups resulted compared to our previous work [22]. This was done to improve the pH sensitivity of the MPc thin films and thus affording the screening of anionic interference like ascorbic acid. Novelty of this work is in the facile immobilization of CoOAClPc onto Au-PEA surface using acyl chloride amidation reaction to form stable thin monolayer films of Au-PEA-CoOCAPc. The electrocatalysis and electroanalysis of Au-PEA-CoOCAPc was evaluated towards the

detection of catecholamine neurotransmitters and pH sensitive screening of anionic interference like ascorbic acid.

### 3.1.1 Aims

(i) Synthesis and characterization of cobalt octa acyl chloride phthalocyanine (CoOAClPc).

(ii) Immobilize the CoOAClPc onto a pre-grafted phenylethylamine gold electrode.

(iii) Investigate the electrochemical properties of Au-PEA-CoOAClPc and pH sensitive screening off ascorbic acid.

## 3.2 Experimental

### 3.2.1 Chemicals and reagents

Potassium ferrocyanide $K_4[Fe(CN)_6]$, potassium ferricyanide $K_3[Fe(CN)_6]$, dopamine (DA), DL-norepinephrine (NOR), (-)-epinephrine (EP), L-ascorbic acid (AA), tetrabutylammonium tetrafluoroborate ($TBABF_4$), tetrafluoroboric acid ($HBF_4$), sodium chloride (NaCl), potassium chloride (KCl), pyromellitic dianhydride (PMDA), urea, thionyl chloride, toluene and pyridine were purchased from Sigma-Aldrich. Potassium hydroxide pellets (KOH), absolute ethanol (EtOH), acetonitrile (ACN), ammonium molybdate, potassium dihydrogen phosphate ($KH_2PO_4$) and disodium hydrogen phosphate ($Na_2HPO_4$) were purchased from SAARCHEM. Sodium Nitrite ($NaNO_2$), 98% sulfuric acid ($H_2SO_4$), dimethylformamide (DMF), 30% Hydrogen peroxide ($H_2O_2$) were purchased from Associated Chemical Enterprises (ACE). 4-(2-Aminoethyl)aniline was purchased from Sigma-Aldrich and used for the synthesis of

4-(2-aminoethyl) benzene diazonium (AEBD) salt using previously reported method [27]. AEBD was stored at 4ºC before use. All aqueous solutions were prepared using ultra-pure water with the resistivity of 18 MΩ.cm (at 25 °C) obtained from a Milli-Q Water Purification System purchased from Millipore Corporation. Phosphate buffer solution (PBS, 0.010 M) was prepared following a previous method [28]. Sodium hydroxide (NaOH, 0.10 M) and hydrochloric acid (HCl, 0.10 M) were used to adjust the pH of the PBS solution to the appropriate values.

### 3.2.2 Apparatus and instrumentations

Fourier transform infrared (FT-IR) spectra were obtained from a Perkin-Elmer Universal ATR Sampling accessory spectrum 100 FT-IR spectrometer. A Thermo Scientific Multiskan Sky Microplate spectrophotometer was used to obtain the ultraviolet-visible (UV-vis) absorption spectrum. Magnetic circular dichroism (MCD) spectra were measured using a Chirascan Plus spectropolarimeter. Mass spectra were acquired on a Bruker Autoflex II MALDI-TOF mass spectrometer using α-cyano-4-hydroxycinnamic as the matrix.

Cyclic voltammetry (CV), electrochemical impedance spectroscopy (EIS) and differential pulse voltammetry (DPV) were recorded using an AUTOLAB PGSTAT302N potentiostat/galvanostat workstation interfaced to a Proline desktop computer equipped with a 1.10 version NOVA software. All electrochemical measurements were measured in an electrochemical cell containing three electrodes, a working electrode (WE), either a bare gold surface or a modified gold surface,

platinum wire as a counter electrode (CE) and silver-silver chloride (Ag|AgCl) as the reference electrode (RE).

### 3.2.3 Synthesis of cobalt (II) octa carboxylic acid phthalocyanine (CoOCAPc, 3)

The cobalt (II) octa carboxylic acid phthalocyanine complex was synthesized from pyromellitic dianhydride (**1**), cobalt (II) chloride salt and urea following an established method [29]. Briefly, pyromellitic dianhydride (2.5 g, 11.5 mmol), urea (13.0 g, 0.22 mol), cobalt (II) chloride salt (23.5 mmol) and ammonium molybdate (0.10 g) were placed in a round bottom flask and heated until the reaction was fused without bubbles observed. The resultant product was washed with water, acetone and 6N HCl and left to dry over night at 50°C to yield an amide phthalocyanine (**2**). Amide phthalocyanine (**2**, 0.50 g) of the dried product was hydrolyzed with 50% KOH at 100°C for 8 hours. The mixture was cooled to room temperature, diluted with water and filtered. The filtered compound was acidified with concentrated HCl and left to stand and precipitate to form the required cobalt (II) octa carboxylic acid phthalocyanine (**3**), which was filtered, washed with 1N HCl and acetone and dried at 50°C in the oven.

CoOCAPc:

- Yield (48.7%), FT-IR ($\bar{\upsilon}$, $cm^{-1}$): 2915, 2843, 2330, 2114, 1694 (C=O), 1516, 1453, 1307, 1059, 723, 623.
- UV-vis ($\lambda_{max}$, nm) (log ε): 688 (3.33), 346 (3.30).
- MS (MALDI-TOF) (m/z): Calculated: 925.02, Found: 926.45 $[M + H]^+$.

### 3.2.4 Synthesis of cobalt (II) octa acyl chloride phthalocyanine (CoOAClPc, 4)

Cobalt (II) octa acyl chloride phthalocyanine (CoOAClPc, **4**) was synthesized from its cobalt (II) octa carboxylic acid phthalocyanine (CoOCAPc, **3**) derivative following the reported method [**15**]. Cobalt (II) octa carboxylic acid phthalocyanine (0.10 g, 0.11 mmol) was refluxed with 2 ml thionyl chloride, 2 ml dry toluene in the presence of a few drops of pyridine for 10 hours. The resultant green solid was washed with toluene and collected by centrifugation and left to dry overnight at 50 °C in the oven to obtain the cobalt (II) octa acyl chloride phthalocyanine.

CoOCAClPc:

- Yield (94.1%) FT-IR ($\bar{\upsilon}$, $cm^{-1}$): 2911, 2841, 2325, 2114, 1950, 1704 (C=O), 1518, 1482, 1312, 1060, 728, 675 (C-Cl), 635.
- UV-vis ($\lambda_{max}$, nm) (log ε): 690 (4.78), 354 (4.70).
- MS (MALDI-TOF) (m/z): Calculated: 1032.81, Found: 1033.03 $[M\text{-}Cl]^+$.

### 3.2.5 Electrode pre-modification and immobilization of CoOAClPc, 4

A gold electrode was cleaned following an established procedure [**30**] by polishing to mirror finish on a Beuhler felt pad using an aqueous slurry of alumina (1.0 µm, 0.30 µm and 0.050 µm). The mechanically polished electrode was then ultrasonicated for 5 min each in ethanol and subsequently in deionized water. The electrode was etched for 2 minutes in a freshly prepared “Piranha” solution of 3:1 (v/v) 98% $H_2SO_4$:30% $H_2O_2$. The gold electrode was then rinsed in copious amounts of deionized water and dried in a stream of nitrogen. The cleanliness of the gold electrode was confirmed by electrochemical cycling in 0.10 M $H_2SO_4$ by cycling the electrode between - 0.20 V

and +1.5 V (vs Ag|AgCl in 3.0 M KCl) at a scan rate of 100 $mV.s^{-1}$, until reproducible voltammograms were obtained.

Pre-modification was achieved by electrografting the Au electrode with phenylethylamine (PEA). This was achieved following a previous method [**18,20,25**]. The cleaned electrode was immersed into a solution of 5 ml acetonitrile (ACN) containing 1.0 mM 4-(2-aminoethyl)benzene diazonium (AEBD) salt and 0.10 M $TBABF_4$ and the electrografting was conducted between +0.40 V and -0.40 V, at a scan rate of 50 $mV.s^{-1}$. An aryl radical was produced that attached onto the Au surface to form a thin film of Au-PEA. The Au-PEA electrode was immersed in a 1.0 ml dry DMF solution of CoOAClPc (1.0 mg, 0.97 µmol) for 4 hours, to give a thin monolayer of Au-PEA-CoOAClPc surface. CoOAClPc was immobilized by reacting amino functional groups of Au-PEA with -COCl to form amide bond. Dry DMF was used to prevent the hydrolysis of acyl chloride functional groups and forming carboxylic acid before amide reaction. The use of primary amine ($-NH_2$) reacts readily and spontaneously with acyl chloride (-COCl) to form amide bond (-CONH-) and loss of HCl. The Au-PEA-CoOAClPc surface was rinsed with dry DMF to remove any physically adsorbed CoOAClPc. Finally, the Au-PEA-CoOAClPc was rinsed with water which hydrolyzed the terminal acyl chloride groups to form carboxylic acid groups, Au-PEA-CoOCAPc.

## 3.3 Results and discussion

### 3.3.1 Synthesis of cobalt (II) octa acyl chloride phthalocyanine (CoOAClPc, 4)

The synthesis of CoOAClPc (**4**) was achieved by refluxing CoOCAPc (**3**) as shown in **Scheme 3.1**. Pyromellitic dianhydride (**1**) was used because it is a bifunctional reagent. It brings about poly-cyclotetramerization in the synthesis of phthalocyanines [29]. The synthesized CoOCAPc (**3**) and CoOAClPc (**4**) were successfully characterized by FT-IR, UV-vis spectroscopy, MCD, and mass spectroscopy. Octa-substituted metal Pcs synthesized from pyromellitic dianhydride have been reported to have functional groups such as carboxylic acid, imide, or amide at the peripheral positions. In this study the acid chloride was synthesized successfully. The immobilization of the acid chloride cobalt phthalocyanine onto the phenylethylamine pre-grafted gold electrode was simplified and no need for additional reagents and an amide bond forms.

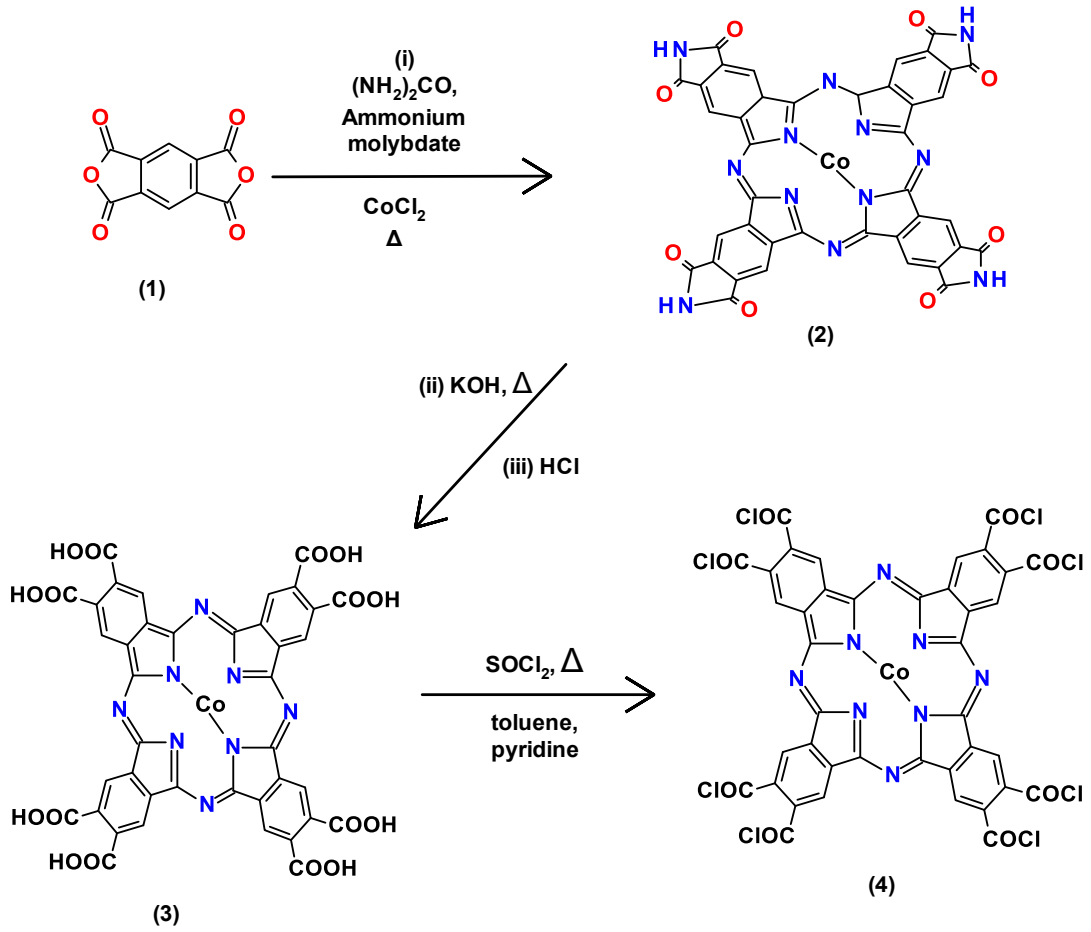


**Scheme 3.1**: Synthesis of cobalt (II) octa acyl chloride phthalocyanine (CoOAClPc, **4**).

### 3.3.2 Characterization of CoOCAPc (3) and CoOAClPc (4)

**Figure 3.1** shows FT-IR spectra of (i) PMDA, (ii) CoOCAPc and (iii) CoOAClPc. Vibrational bands (at 900 – 1000 $cm^{-1}$) were observed for the metal phthalocyanines. A broad stretch was observed at wavenumbers above 2100 $cm^{-1}$ due to O-H. A shift of the carbonyl (C=O) vibrational bands was observed from 1697 $cm^{-1}$ for CoOCAPc to 1709 $cm^{-1}$ for CoOAClPc. Chlorine is a highly electronegative halogen element and an electron acceptor, therefore weakens the C=O leading to shift in vibrational band

to higher values. A vibrational band was observed at 676 $cm^{-1}$ for C-Cl confirming the formation of the CoOAClPc.

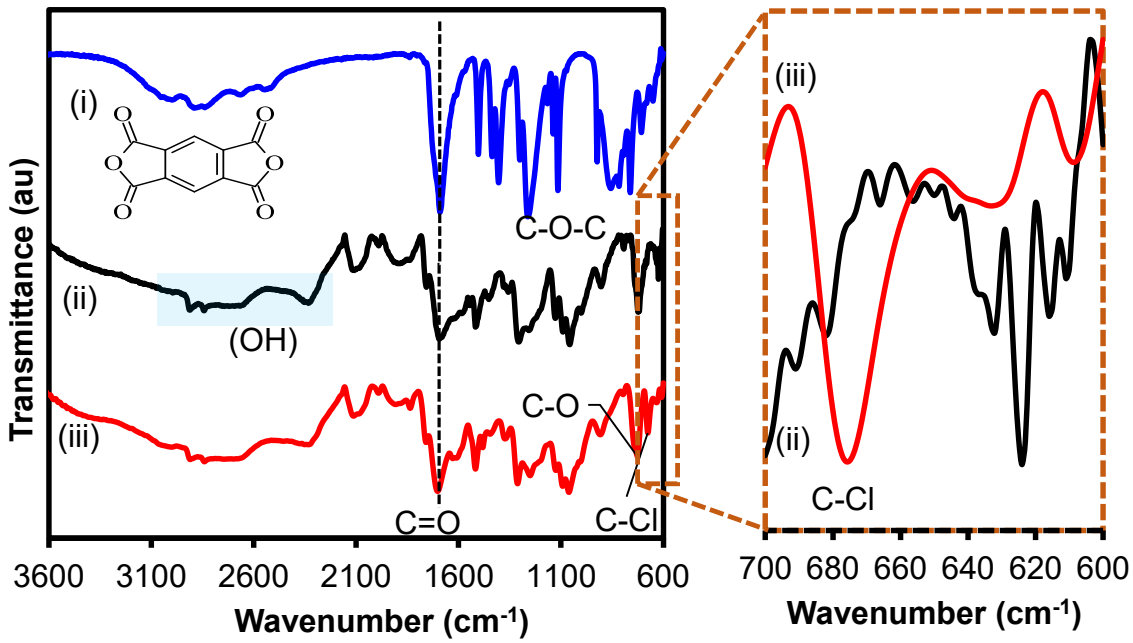


**Figure 3.1**: FT-IR spectra of (i) pyromellitic dianhydride (PMDA, **1**), (ii) cobalt (II) octa carboxylic acid phthalocyanine (CoOCAPc, **3**) and (iii) cobalt (II) octa acyl chloride phthalocyanine (CoOAClPc, **4**).

The UV-vis and MCD spectra of the synthesized MPcs in dry DMF are shown in **Figure 3.2** for (a) CoOCAPc and (b) CoOAClPc. The MPcs showed the typical electronic spectra with two absorption bands, the Q band between 600 – 700 nm and the B band in the near UV region between 300 – 350 nm, both corresponding to π-π* transitions [**31,32**]. The MCD spectrum showed the Faraday A1 terms based on Gouterman's 4-orbital model. The B band for CoOCAPc in the UV-vis spectrum has an inflection point in the MCD spectrum at 346 nm while CoOAClPc showed the B band at 354 nm. The Q band for CoOAClPc on the UV-vis spectrum shifted at 690 nm as compared to CoOCAPc whose absorption maxima was at 688 nm and both were Faraday A term

under MCD. The shift in Q band from 688 nm for CoOCAPc to 690 nm for CoOAClPc was due to electronegative Cl at the peripheral functional group. For CoOAClPc, the Q-band shows a splitting probably due to the asymmetry because of incomplete chlorination [33].

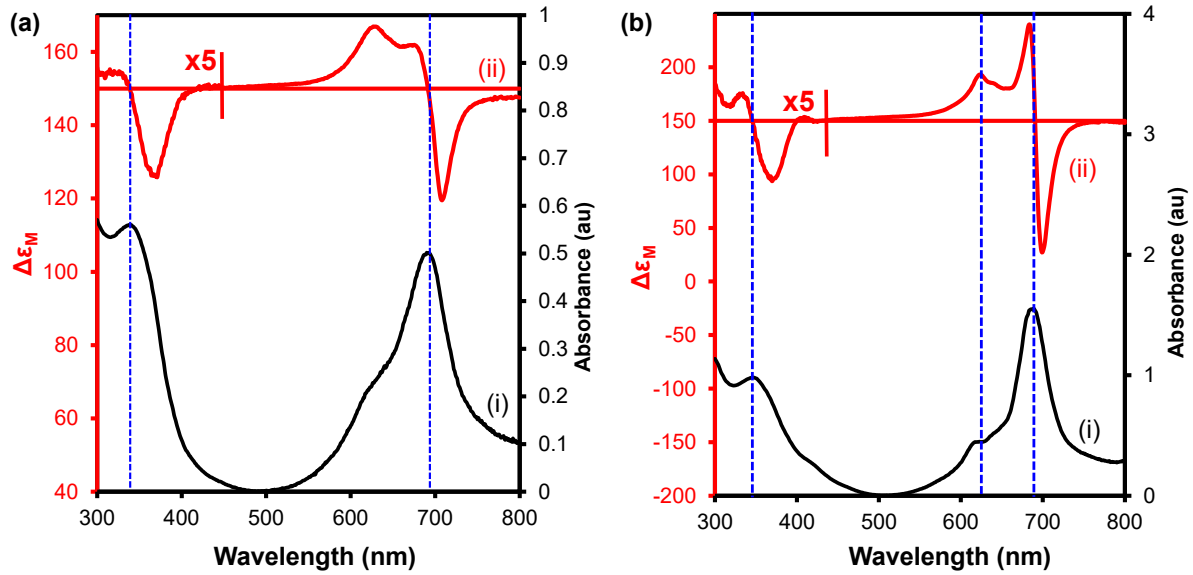


**Figure 3.2**: (i) UV-vis and (ii) MCD spectra of (a) cobalt (II) octa carboxylic acid phthalocyanine (CoOCAPc) and (b) cobalt (II) octa acyl chloride phthalocyanine (CoOAClPc) in dry DMF.

CoOCAPc (**3**) and CoOAClPc (**4**) were further characterized using mass spectroscopy, which gives information on the ratio of their mass-to-charge (m/z). The intensity of the peak shows the abundance of the ionic species with respective m/z ratio [34]. **Figure 3.3** (a) and (b) show the mass spectra of CoOCAPc and CoOAClPc respectively. MPcs degrade with molecular ion peaks corresponding to $[M]^+$, $[M \pm nH]^+$ where n = 1 – 3 [8]. The mass spectroscopy showed the presence of characteristic peaks confirming CoOCAPc and CoOAClPc with peaks corresponding to the molecular ion, m/z = 926.45 and m/z = 1033.03 respectively while the calculated masses are 925.55 and 1032.81, respectively. The obtained mass-to-charge ratio

corresponds to $[M + H]^+$ ions for the CoOCAPc and $[M\text{-}Cl]^+$ ion for the CoAClPc. The m/z value for CoAClPc was less Cl, hence the $[M\text{-}Cl]^+$. The formation of CoOAClPc resulted in higher mass-to-charge ratio much higher due to C-Cl functional groups confirming the successful synthesis of CoOAClPc complex.

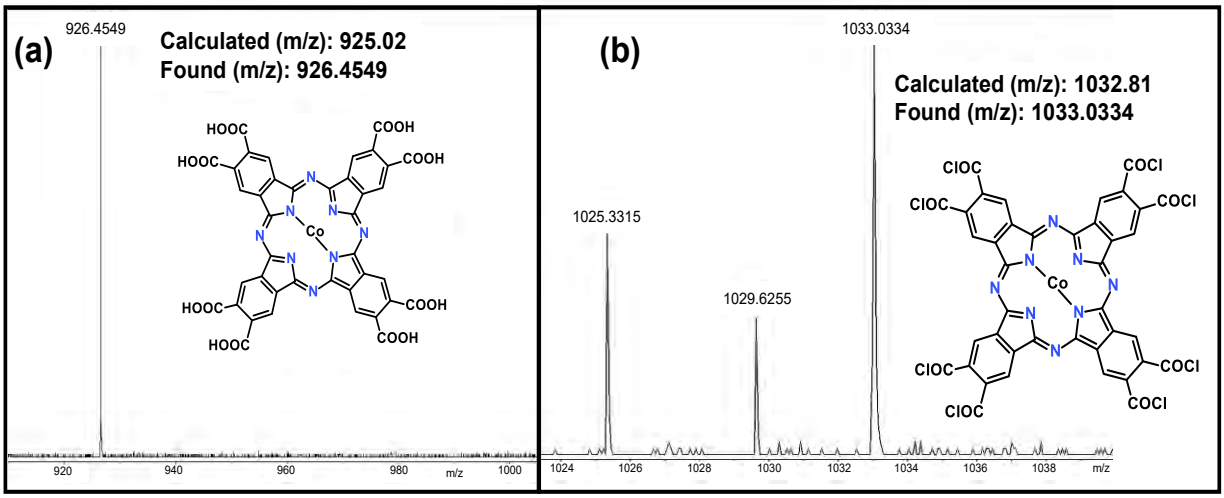


**Figure 3.3**: Mass-spectra and the corresponding chemical structure of (a) CoOCAPc and (b) CoOAClPc.

### 3.3.3 Electrografting of AEBD onto Au electrode and immobilization of CoOAClPc (4) to form Au-PEA-CoOCAPc, Scheme 3.2.

**Figure 3.4** shows cyclic voltammograms (CVs) obtained for the electrografting of the Au electrode by electroreduction of AEBD salt. The electroreduction of the diazonium salt was confirmed by a reduction peak. A broad reduction peak was observed at around 0.18 V on the first scan. This was due to the generation of the radical and scanning reductively resulting in grafting of the radical to form Au-C bond. Upon repetitive scanning, the reduction current drastically decreased, and the reduction peak disappeared. This was because an insulating organic thin film was formed onto the surface passivating the Au and giving an Au-PEA surface. The resulting

modification is very stable due to formation of a covalent bond between the Au surface and the aryl group [35]. Gold electrode modified with aryl diazonium salt have been characterized with lower capacitance and high rate of electron transfer [36]. The surface coverage ($\Gamma_{PEA}$, mol.cm$^{-2}$) of the grafted PEA film was determined by measuring the total charge (Q, 2.29 x 10$^{-9}$ C) under the reduction peak and using the following **Equation 3.1**,

$$\Gamma_{PEA} = \frac{Q}{nFA} \qquad (\mathbf{3.1})$$

where n (= 1) is the number of electrons for the reduction of AEBD, F (96485 C.mol$^{-1}$) is the faradays constant and A (= 0.0201 cm$^{-2}$) is the geometric area of the gold electrode (r = 0.80 mm). The surface coverage ($\Gamma_{PEA}$) was calculated to be 1.18 x 10$^{-12}$ mol.cm$^{-2}$. The surface coverage confirms the formation of PEA thin film which blocked gold surface from further reducing of AEBD (second scan showed no AEBD reduction peak).

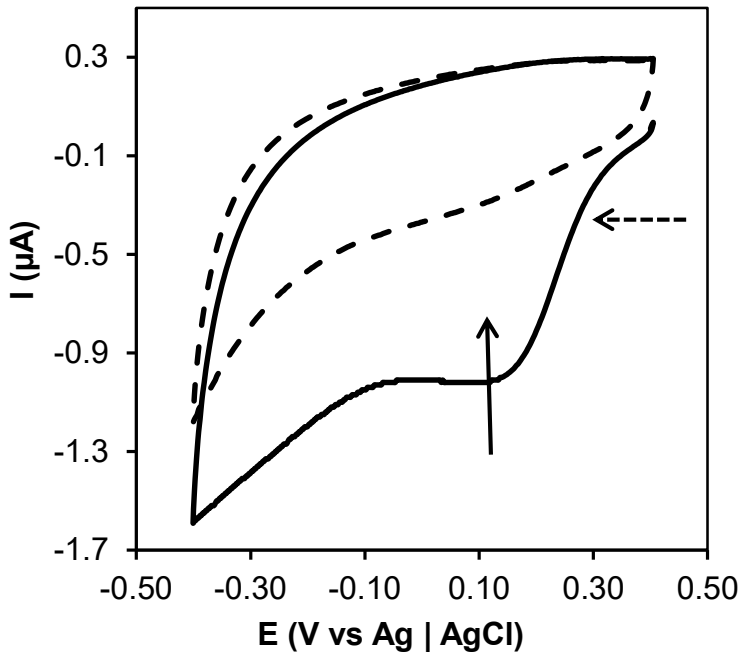


**Figure 3.4**: CVs for the electrografting of ACN containing 1.0 mM AEBD salt and 0.10 M $TBABF_4$ on Au electrode. Scan rate = 50 mV.s$^{-1}$.

CVs in **Figure 3.4** confirmed electrografting of PEA thin films to form Au-PEA. The CoOAClPc was covalently immobilized following spontaneous amidation reaction. The details are described in **Section 3.2.5** and after rinsing with dry DMF and water, Au-PEA-CoOCAPc formed, **Scheme 3.2**.

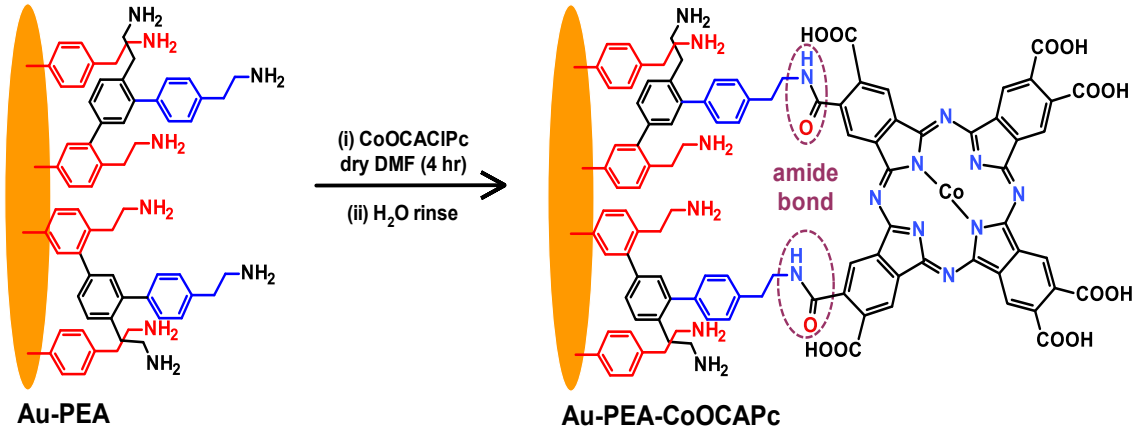


**Scheme 3.2**: Electrografting of AEBD to form Au-PEA [**20,22,27**] and immobilization of CoOAClPc thin monolayer film onto Au-PEA electrode to form Au-PEA-CoOCAPc.

### 3.3.4 Electrochemical characterization of the bare Au, Au-PEA and Au-PEA-CoOCAPc surfaces

Electrochemical characterization of electrode modification was accomplished using cyclic voltammetry (CV) and electrochemical impedance spectroscopy (EIS). The redox probing species used were a negatively charged, $[Fe(CN)_6]^{3-/4-}$ and a positively charged, $[Ru(NH_3)_6]^{2+/3+}$. **Figure 3.5** shows CVs and their corresponding EIS of (i) bare Au, (ii) Au-PEA and (iii) Au-PEA-CoOCAPc measured in 2.0 mM (a) $[Fe(CN)_6]^{3-/4-}$ and (b) $[Ru(NH_3)_6]^{2+/3+}$ containing 0.10 M KCl at a scan rate of 50 mV $s^{-1}$. The CV measured for bare Au in **Figure 3.5(a)(i)** shows a peak-to-peak separation (ΔE) of 73 ± 4.5 mV. This value depicts the expected excellent reversibility of $[Fe(CN)_6]^{3-/4-}$ redox couple on Au surfaces. Theoretically, the peak-to-peak separation should be 59.2 mV from

Nernst equation, however ohmic drop variations results in high value of ΔE [22]. The CV for Au-PEA surface in **Figure 3.5(a)(ii)** was almost the same as the bare Au, with a peak-to-peak separation of 73 ± 4.5 mV. Both Au and Au-PEA exhibited a one-electron transfer kinetics [37].

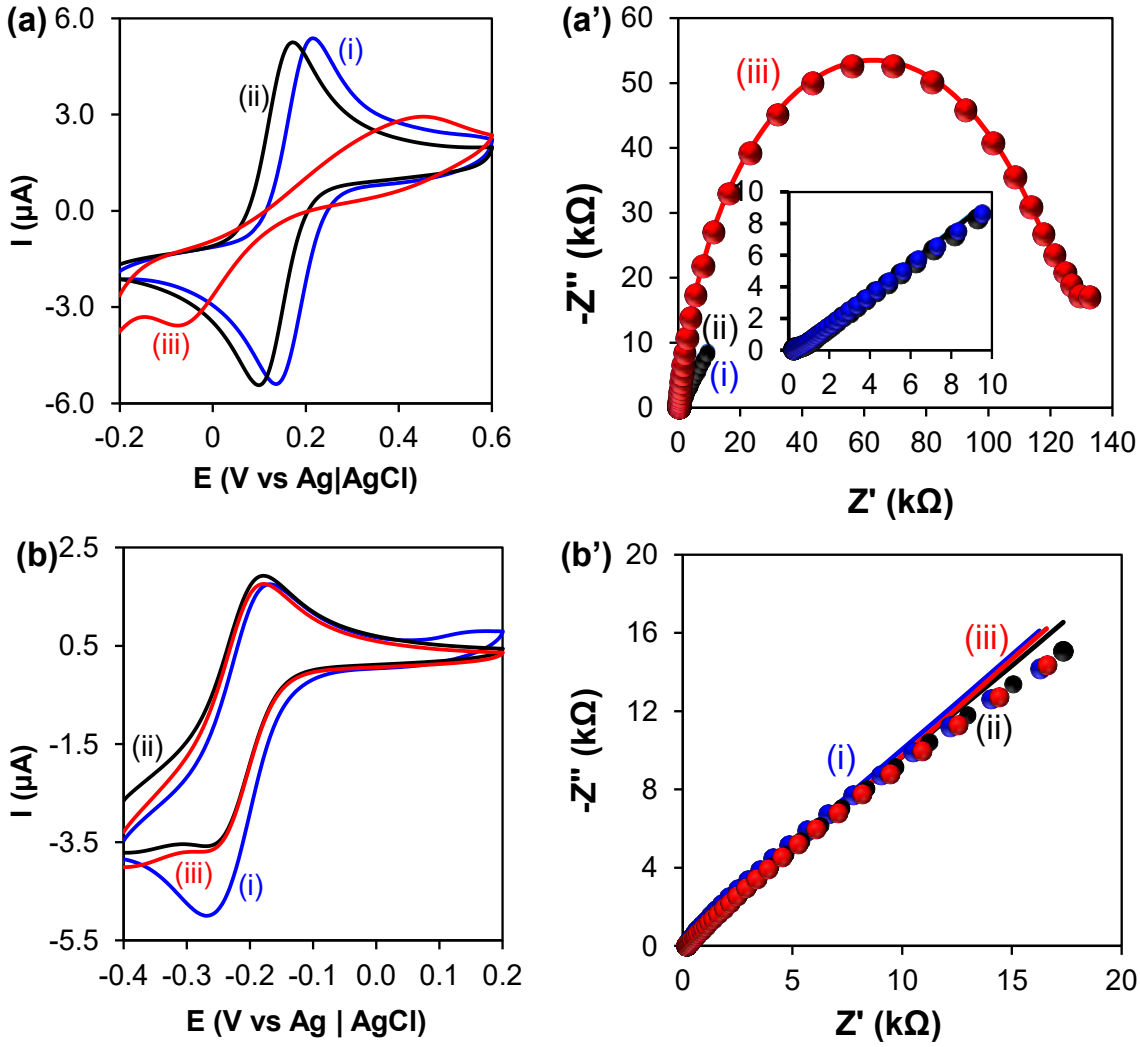


**Figure 3.5**: CVs and Nyquist plots of (i) bare Au, (ii) Au-PEA and (iii) Au-PEA-CoOCAPc measured in 2.0 mM (a) $[Fe(CN)_6]^{3-/4-}$ and (b) $[Ru(NH_3)_6]^{2+/3+}$ containing 0.10 M KCl. Scan rate = 50 $mV.s^{-1}$.

The oxidation and reduction peaks at Au-PEA-CoOCAPc shifted to high positive and negative potential values, resulting in an increase in ΔE from 73 ± 4.5 mV for Au and

Au-PEA to 432 ± 3.8 mV. The peak currents decreased as shown confirming the blocking property of the CoOCAPc. This was attributed to the terminal negatively charged carboxylic groups ($-COO^-$) at pH 7.4. The carboxylic acid groups have a pKa value less than 5 and hence at pH 7.4 the -COOH groups are deprotonated ($-COO^-$). The negatively charged carboxylic acid groups, $-COO^-$ on the Au-PEA-CoOCAPc surface repels the $[Fe(CN)_6]^{3-/4-}$, hence, blocking the redox reaction. The blocking behaviour also confirms the successful immobilization of CoOAClPc onto Au-PEA surface. **Figure 3.5(b)** shows the CVs of (i) Au, (ii) Au-PEA and (iii) Au-PEA-CoOCAPc electrodes in the $[Ru(NH_3)_6]^{2+/3+}$ and they exhibited a redox process. On the bare Au, **Figure 3.5(b)(i)**, a redox peak with ΔE of 78 ± 2.8 mV was observed. The Au-PEA, **Figure 3.5(b)(ii)** showed a smaller ΔE = 59 ± 2.4 mV, compared to bare Au, due to the thin PEA film. The Au-PEA-CoOCAPc, **Figure 3.5(b)(iii)** exhibited a slightly higher ΔE of 68 ± 1.4 mV. The ΔE were all < 78 ± 2.8 mV for a bare Au and this was attributed to terminal $-NH_2$ for Au-PEA and $-COO^-$ of the Au-PEA-CoOCAPc being neutral and negatively charged and not blocking the $[Ru(NH_3)_6]^{2+/3+}$ redox probe. The two redox probes were studied at pH 7.4 and the terminal -COOH functional groups are negatively charged ($-COO^-$). The negatively charged $[Fe(CN)_6]^{3-/4-}$ was repelled by the negatively charged terminal $-COO^-$ functional group. The positively charged probe, $[Ru(NH_3)_6]^{2+/3+}$ was attracted onto the negatively charged electrode surface. Hence the ΔE decreased from 432 ± 3.8 mV for $[Fe(CN)_6]^{3-/4-}$ to 68 ± 1.4 mV for $[Ru(NH_3)_6]^{2+/3+}$.

Electrochemical impedance spectroscopy (EIS) was also used to study the electron transfer behaviour of the bare and modified electrode surfaces. The EIS data was represented by the Nyquist plots in **Figure 3.5** for (i) bare Au, (ii) Au-PEA and (iii) Au-

PEA-CoOCAPc in 2.0 mM (a') $[Fe(CN)_6]^{3-/4-}$ and (b') $[Ru(NH_3)_6]^{2+/3+}$ both containing 0.10 M KCl. The EIS data in $[Fe(CN)_6]^{3-/4-}$, **Figure 3.5(a')**, was measured at equilibrium potential ($E_{1/2}$ = 148 mV) for the bare electrode. The Randles equivalent circuit, $R_S(Q[R_{CT}Z_W])$, where $R_S$ is the resistance of the solution or electrolyte, $R_{CT}$ is the charge-transfer resistance, Q is the capacitance either constant phase element (CPE) or double-layer capacitance ($C_{dl}$), and $Z_W$ is the Warburg impedance, was used to fit the data as described before [**38**]. The Au-PEA-CoOCAPc in $[Fe(CN)_6]^{3-/4-}$ impedance data was fitted without $Z_W$. The components combinations were such that the $R_S$ is in series with a parallel connection of CPE/$C_{dl}$ and $R_{CT}$ which is in series with $Z_W$. The raw and fitted data was analysed and represented as the Nyquist plot (-Z'' vs Z'). The semi-circle on the plot signifies a charge transfer process and the extent of the charge transfer resistance is represented by the size of the semi-circle [**15**]. It was observed that both bare Au and Au-PEA exhibited a small semi-circle diameter indicating a rapid electron transfer process. The semi-circle increased in the diameter confirming the modification of the Au-PEA surface with CoOCAPc to form Au-PEA-CoOCAPc. Electrode modification resulted in the increase of charge transfer resistance ($R_{CT}$). The CoOCAPc blocks the surface, hindering electron transfer and hence the bigger $R_{CT}$ for Au-PEA-CoOCAPc surface. In this study, a slight increase in $R_{CT}$ was observed from bare Au (0.43 kΩ) to Au-PEA (0.50 kΩ) due to the thin PEA film. A significant increase was observed from Au-PEA (0.50 kΩ) to Au-PEA-CoOCAPc (121.2 kΩ). A marked increased in $R_{CT}$ for Au-PEA-CoOCAPc surface was due to electrostatic repulsion of negatively charged $-COO^-$ group repelling the negatively charged $[Fe(CN)_6]^{3-/4-}$ redox probe as seen on the CV studies. In $[Ru(NH_3)_6]^{2+/3+}$, **Figure 3.5(b')**, the applied potential was at $E_{1/2}$ = -218 mV. The $R_{CT}$ increased from 10.7 Ω to 113 Ω from the bare Au (i) to Au-PEA (ii) respectively. The increase in $R_{CT}$ value was a

characteristic of a formation of PEA thin film. On Au-PEA-CoOCAPc, **Figure 3.5(b')(iii)**, the $R_{CT}$ decreased to 76.5 Ω. The decrease in RCT for Au-PEA-CoOCAPc to 76.5 Ω from 113 Ω for Au-PEA was due to very thin film of Au-PEA with positive charge ($-NH_3^+$) at pH 7.4 resulting in electrostatic repulsion with $[Ru(NH_3)_6]^{2+/3+}$. Au-PEA-CoOCAPc was negatively charged and thus resulting electrostatic attraction with $[Ru(NH_3)_6]^{2+/3+}$. EIS is an excellent technique to determine the kinetic parameters and surface coverage.

The surface coverage, Θ of the modified electrode was calculated using **Equation 3.2**,

$$\theta = 1 - \frac{R_{CT}(bare)}{R_{CT}(thin\ layer)} \qquad (\mathbf{3.2})$$

where $R_{CT}$ (bare) is the charge transfer resistance of the bare Au and $R_{CT}$ (thin layer) is the charge transfer resistance of the modified Au electrode. The surface coverage for Au-PEA was found to be 0.146. The value increased to 0.996 for Au-PEA-CoOCAPc. A surface coverage, Θ close to 1 (Θ > 0.9) shows that a completely close-packed stable thin film was formed [**39**]. This was due to the modification of the electrode by the CoOAClPc.

The EIS data was also used to calculate the apparent electron transfer rate constant, $K_{app}$ using **Equation 3.3** [**39**],

$$K_{app} = \frac{RT}{n^2F^2AR_{CT}C} \qquad (\mathbf{3.3})$$

where A is the geometric area of the gold electrode surface (0.0201 $cm^2$), $R_{CT}$ is the charge-transfer resistance, C is the concentration (2.0 mM) of the $[Fe(CN)_6]^{3-/4-}$ and R is the universal gas constant, T is the temperature, and F is Faraday's constant. The $K_{app}$ values for Au and Au-PEA were found to be 3.06 x $10^{-5}$ $cm.s^{-1}$ and 2.62 x $10^{-5}$

cm.s$^{-1}$ respectively. The $K_{app}$ decreased from bare Au to Au-PEA. The $K_{app}$ then drastically decreased to 1.08 x $10^{-7}$ cm.s$^{-1}$ for Au-PEA-CoOCAPc. These results suggested that the PEA-CoOCAPc layer blocked the surface and decreased the electron transfer rate.

Further characterization of the surfaces was investigated in 0.010 M KOH and 1.0 mM $CuSO_4$ in 0.50 M $H_2SO_4$ solutions. **Figure 3.6** shows the CVs of (i) Au, (ii) Au-PEA (iii) Au-PEA-CoOCAPc in (a) 0.010 M KOH and (b) 1.0 mM $CuSO_4$ in 0.50 M $H_2SO_4$. **Figure 3.6(a)** shows that bare Au in **Figure 3.6(a)(i)** gave both redox peaks and these decreased on Au-PEA surface in **Figure 3.6(a)(ii)**. Upon immobilizing with CoOCAPc, **Figure 3.6(a)(iii)**, the reduction and oxidation peaks further decreased demonstrating the modification of the gold electrode by PEA and CoOCAPc.

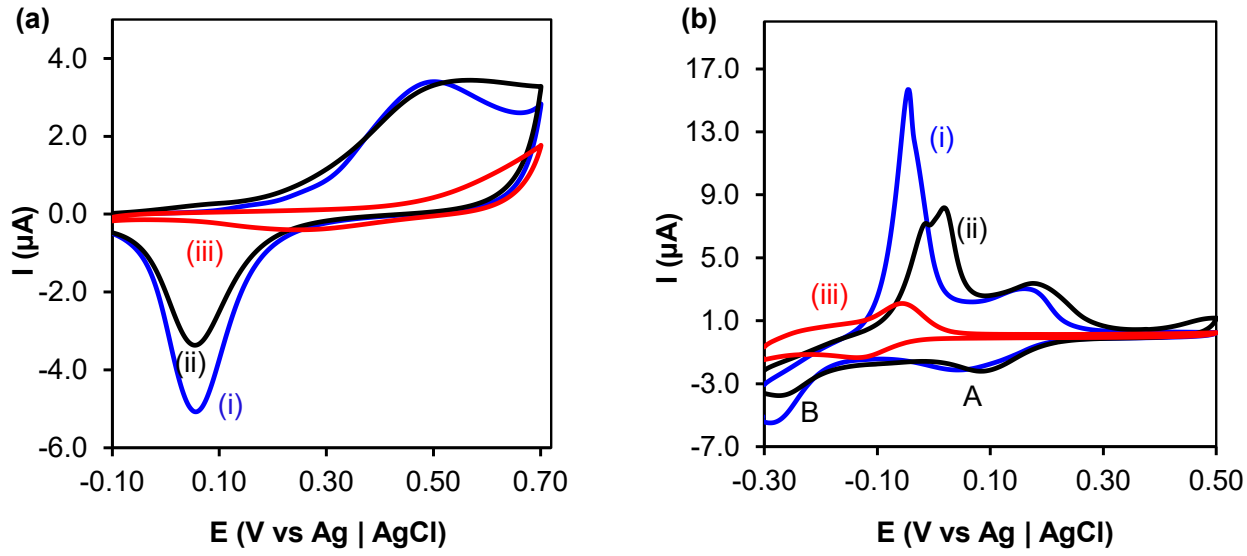


**Figure 3.6**: CVs of (i) bare Au, (ii) Au-PEA and (iii) Au-PEA-CoOCAPc measured in (a) 0.010 M KOH and (b) 1.0 mM $CuSO_4$ in 0.50 M $H_2SO_4$ solution. Scan rate = 50 mV.s$^{-1}$

An ion barrier factor, $\Gamma_{ibf}$, was calculated using **Equation 3.4** [40],

$$\Gamma_{ibf} = 1 - \frac{Q_{thin\ layer}}{Q_{bare}} \qquad (\mathbf{3.4})$$

where $Q_{thin\ layer}$ is the total charge under the reduction peak of Au-PEA or Au-PEA-CoOCAPc and $Q_{bare}$ is the total charge under the reduction peak of the bare gold electrode. The ion barrier factor gives an indication of ions or solution permeability of thin film. A $\Gamma_{ibf}$ of 1 indicates the ability of the thin layer to block the ions. The ion barrier factor was calculated to be 0.34 for PEA thin layer and 0.83 for PEA-CoOCAPc. The ion barrier factor could also be attributed to charge transfer process. The lower $\Gamma_{ibf}$ of PEA thin layer indicates that electrons could easily be transferred from the solution to the underlying gold electrode. The increased $\Gamma_{ibf}$ value for PEA-CoOCAPc layer indicates a slowed down charge transfer process. Immobilizing the CoOAClPc onto Au-PEA layer resulted in an insulated surface, hence hindering the charge transfer process which led to a high $\Gamma_{ibf}$ value. **Figure 3.6(b)** shows CVs of (i) Au, (ii) Au-PEA and (iii) Au-PEA-CoOCAPc in 1.0 mM $CuSO_4$ in 0.50 M $H_2SO_4$ solution. The underpotential deposition (UPD) of copper onto gold surface was studied to further verify the modification [8,25]. On the bare Au surface, **Figure 3.6(b)(i)**, a redox process was observed with a broad peak **(A)**, at $E_p$ = 54 mV due to metal reduction from $Cu^{II}$ to $Cu^{I}$. Further reduction from $Cu^{I}$ to $Cu^{0}$ was seen at the second reduction peak (**B**) at $E_p$ = -290 mV. The $Cu^{0}$ was deposited on the Au surface as a metallic copper layer of Au(Cu) ad-atom. A large oxidation peak at $E_p$ = -46 mV from $Cu^{0}$ to $Cu^{I}$ corresponding to the stripping of the adsorbed Cu metallic layer from the Au surface and dissolving back into solution. The gold surface on Au-PEA was accessible to Cu on the Au-PEA as was observed with the reduction peaks, the Au-PEA layer was very thin and permeable to solution ions. The results verified the surface modification of CoOCAPc with a decrease in currents due to the $Cu^{II}$ redox process

on Au-PEA-CoOCAPc, **Figure 3.6(b)(iii)**, but the redox process was not completely blocked.

### 3.3.5 XPS characterization of modified electrodes

The X-ray photoelectron spectroscopy (XPS) was also used for the characterization of Au-PEA-CoOCAPc surface. **Figure 3.7** and **3.8** shows the survey spectrum and the high resolution core-level spectra of C 1s, N 1s and O 1s. The gold coated quartz crystal (AuCQC), connected as a working electrode was modified via electrochemical grafting same as in **Figure 3.4**. The XPS survey spectra in **Figure 3.7(a)** showed the presence of the organic thin film with the presence of C 1s (54.5%), O 1s (2.7%), and N 1s (3.1%). The grafted organic thin film was attributed to the grafted PEA thin film. The persistent presence of Au 4f and Ag 3d is from the abundant AuCQC underlying gold surface used for the electrochemical grafting of PEA. The C 1s in **Figure 3.7(b)** was deconvoluted and three components at 384.9 eV due to C-C, C=C, 285.6 eV due to C-N and 288.3 eV due to C-O. The component at higher binding energies were attributed to aliphatic C-N from PEA and the C-O from ethanol used to rinse the surface. The N 1s peak in **Figure 3.8(b)** was also deconvoluted and three components were observed due to N-H at 398.2 eV, C-N at 400.2 eV and $NH_3^+$ at 402.7 eV.

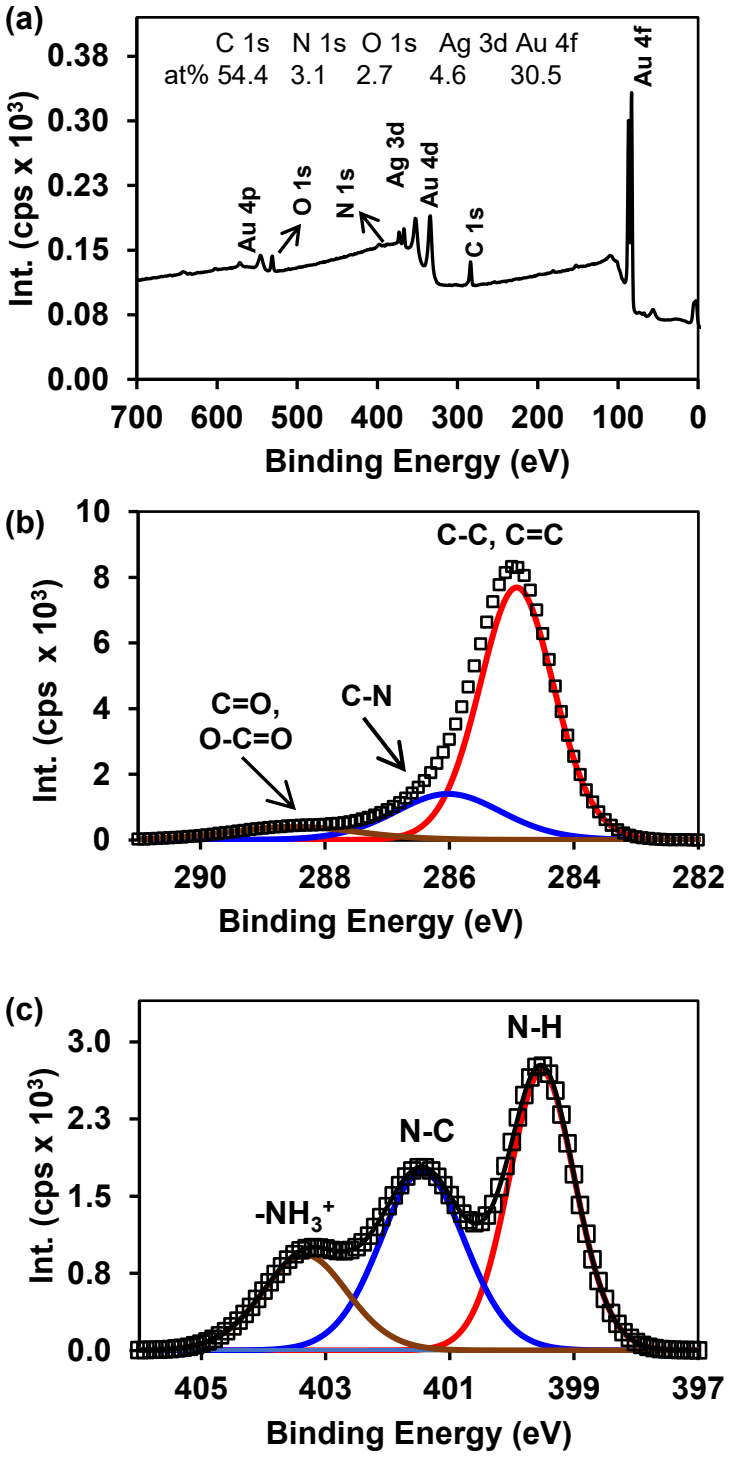


**Figure 3.7**: XPS spectra of Au-PEA, (a) survey spectrum and high-resolution core-level spectra of (b) C 1s and (c) N 1s.

The survey spectrum in **Figure 3.8(a)** showed the presence of carbon, nitrogen and oxygen which are from the PEA-CoOCAPc with the relative atomic concentrations (%at). The high-resolution core-level spectrum of C 1s was deconvoluted and five components at different positions were assigned to various species confirming the carboxylic acid at 288.9 eV in **Figure 3.8(b)**. The other components due to C-N and C=N were from CoOCAPc. The high-resolution core-level spectrum of N 1s was also deconvoluted and three peaks were due to C-N, C=N (due to CoOCAPc) and -$NH_3^+$ (due to unreacted Au-PEA) in **Figure 3.8(c)**. The oxygen high resolution core-level spectrum showed two components for carboxylic acid functional group of the CoOCAPc, **Figure 3.8(d)**. The observed XPS results confirmed the immobilization of CoOCAPc onto Au-PEA to form Au-PEA-COOCAPc.

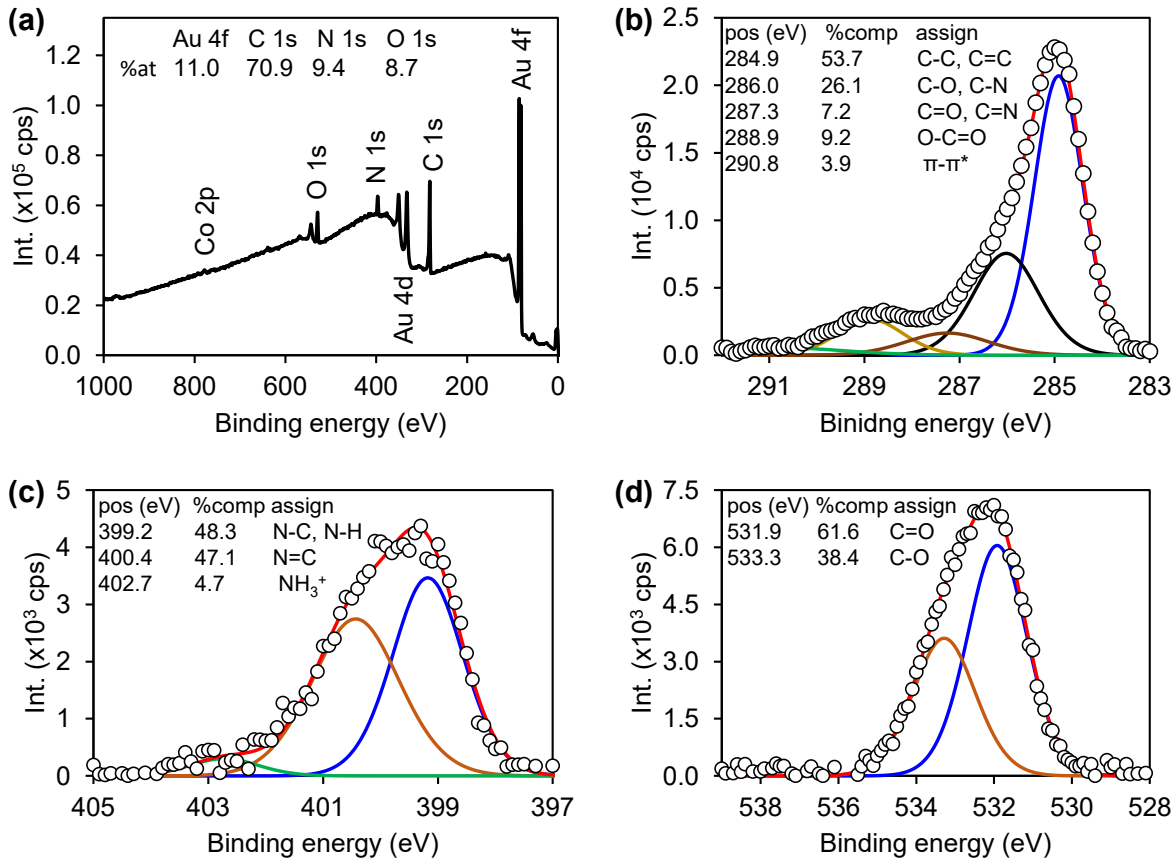


**Figure 3.8**: (a) Survey spectrum and the high resolution core-level spectra of (b) C 1s, (c) N 1s and (d) O 1s.

### 3.3.6 Effect of pH on the negatively or positively charged redox probes

A negatively and positively charged probes were investigated at pH values ranging from 3.0 to 10. This was done to determine the effect of pH on the rate of electron transfer process on the Au-PEA-CoOCAPc surface. **Figure 3.9** shows (a) and (b) CVs, corresponding (a') and (b') Nyquist plots and (c) correlation of ΔE and $R_{CT}$ vs pH of Au-PEA-CoOCAPc measured in 2.0 mM (a) $[Fe(CN)_6]^{3-/4-}$ and (b) $[Ru(NH_3)_6]^{2+/3+}$ containing 0.10 M KCl. The CVs measured for Au-PEA-CoOCAPc in 2.0 mM $[Fe(CN)_6]^{3-/4-}$, **Figure 3.9(a)** showed a decrease in peak currents with increasing in pH values. At pH values less than 5, the -COOH terminal groups are protonated and neutral and can allow $[Fe(CN)_6]^{3-/4-}$ redox process to occur, hence the higher peak currents. As the pH values of solution increased the peak-to-peak separation increased. The oxidation peak shifted from 250 mV to 480 mV as the pH increased from pH 3.0 to pH 10.0 respectively. In the same manner, the reduction peak shifted from 170 mV to -210 mV, resulting in increasing ΔE. At higher pH, above the pKa value of carboxylic acid groups, the -COOH terminal groups of the Au-PEA-CoOCAPc are deprotonated ($-COO^-$) and become negatively charged repelling a negatively charged $[Fe(CN)_6]^{3-/4-}$ redox probe. The shape of the voltammograms from pH 6.0 to 10.0 clearly showed this effect.

In the presence of the positively charged redox probe, $[Ru(NH_3)_6]^{2+/3+}$, **Figure 3.9(b)** there was no significant changes observed in the CVs with respect to peak currents. There were small changes in the decrease of the peak-to-peak separation as the pH increased from 3.0 to 10. The neutral and negatively charged thin film of Au-PEA-CoOCAPc had no effect on the redox process of a positively charged $[Ru(NH_3)_6]^{2+/3+}$ redox probe. This is a preliminary investigation of how the detection of the neurotransmitters will occur and screening of negatively charged ascorbic acid.

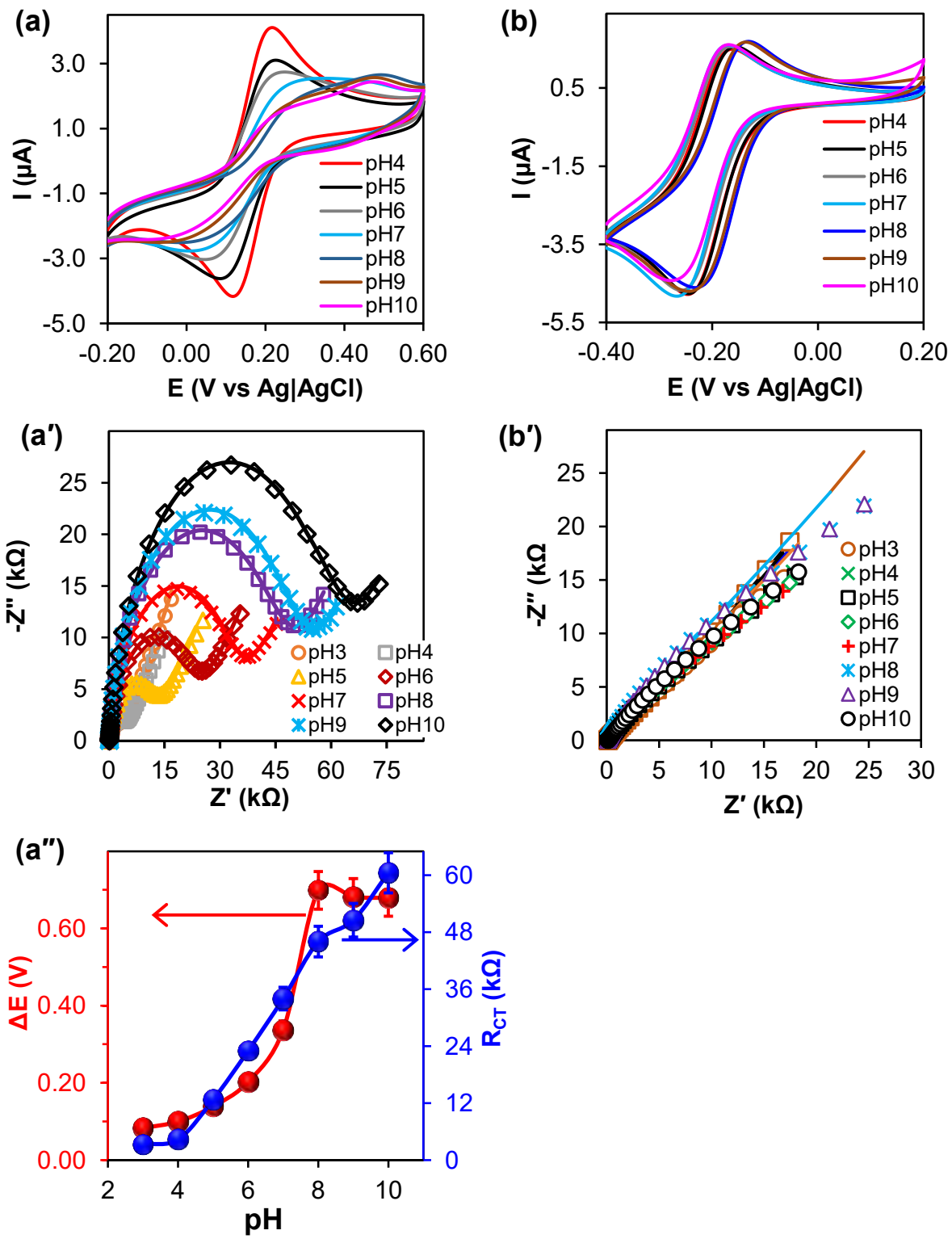


**Figure 3.9**: (a) and (b) CVs, (a') and (b') Nyquist plots and (c) correlation of ΔE and RCT vs pH of Au-PEA-CoOCAPc measured in 2.0 mM (a) $[Fe(CN)_6]^{3-/4-}$ and (b) $[Ru(NH_3)_6]^{2+/3+}$ containing 0.10 M KCl in different pH solutions ranging from (i) pH 3.0 to (viii) pH 10. Scan rate = 50 mV.s$^{-1}$ for (n = 3).

The effect of pH on Au-PEA-CoOCAPc was also studied using EIS. Typical Nyquist plots are shown in **Figure 3.9(a')** for $[Fe(CN)_6]^{3-/4-}$ and there was no significant changes observed in $R_{CT}$ for $[Ru(NH_3)_6]^{2+/3+}$, **Figure 3.9(b')**. A modified Randles circuit, $R_s$(CPE,$R_{CT}$) was used to fit the raw data and for analysis. An increase in $R_{CT}$ was observed with an increase in pH. This was shown by an increase of the semi-circle from pH 3.0 to 10.0. Peak-to-peak separation (ΔE) and $R_{CT}$ were plotted against pH in **Figure 3.9(a")**. The curves clearly showed an increase in peak-to-peak separation and charge transfer resistance due to repulsive force between $[Fe(CN)_6]^{3-/4-}$ and $-COO^-$ of Au-PEA-CoOCAPc. **Figure 3.9(b')** showed the Nyquist plot of Au-PEA-CoOCAPc in different pH conditions ranging from pH 3 to pH 10. There was no change in the Nyquist plots as the pH increased. **Table 3.1** shows a summary of the different parameters obtained for pH studies on Au-PEA-CoOCAPc.

**Table 3.1**: Summary of CV and EIS parameters of Au-PEA-CoOCAPc in 2.0 mM $[Fe(CN)_6]^{3-/4-}$ and $[Ru(NH_3)_6]^{2+/3+}$ both containing 0.10 M KCl at pH 3.0 to pH 10.

| pH | **$[Fe(CN)_6]^{3-/4-}$** | | **$[Ru(NH_3)_6]^{2+/3+}$** | |
|---|---|---|---|---|
| | **ΔE (mV)** | **$R_{CT}$ (kΩ)** | **ΔE (mV)** | **$R_{CT}$ (Ω)** |
| **3.0** | 83 | 3.10 | 78 | 35.5 |
| **4.0** | 100 | 4.30 | 85 | 44.2 |
| **5.0** | 139 | 12.7 | 88 | 43.4 |
| **6.0** | 203 | 23.0 | 93 | 442 |
| **7.0** | 334 | 34.0 | 95 | -8.25 |
| **8.0** | 698 | 46.0 | 100 | 69.2 |
| **9.0** | 681 | 50.5 | 107 | 73.6 |
| **10.0** | 679 | 60.5 | 110 | 70.7 |

ΔE: peak-to-peak separation, i.e., the difference between oxidation and reduction potentials. $R_{CT}$: charge-transfer resistance.

### 3.3.7 Electrocatalysis of the catecholamine NTs at Au, Au-PEA and Au-PEA-CoOCAPc

The electrocatalysis of Au-PEA-CoOCAPc was investigated towards the detection of catecholamine neurotransmitters. **Figure 3.10** shows CVs of Au-PEA-CoOCAPc in the (i) absence and (ii) presence of 1.0 mM (a) DA, (b) NOR, (c) EP and (d) 0.10 mM AA in 0.010 M PBS (pH 7.4).

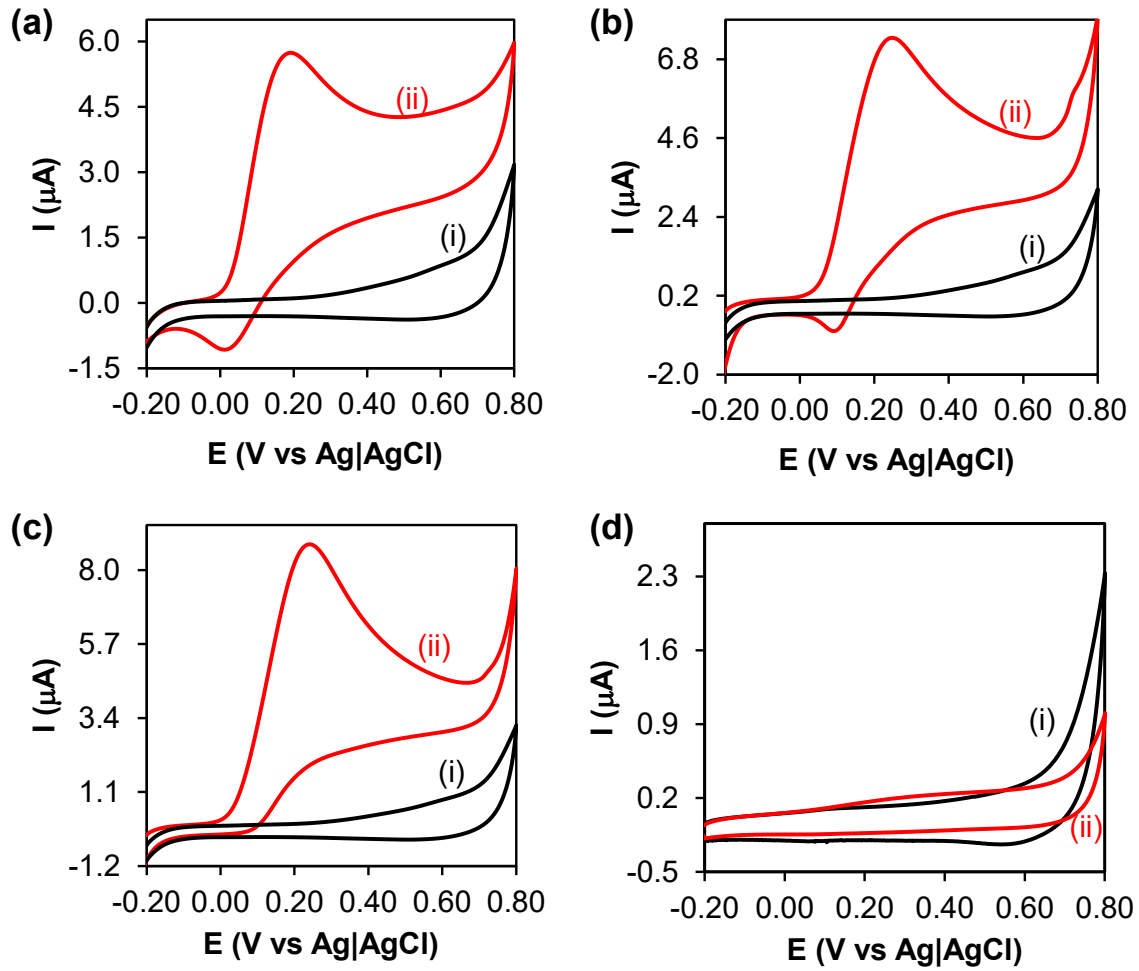


**Figure 3.10**: CVs of Au-PEA-CoOCAPC in (i) absence (ii) presence of 1.0 mM (a) DA, (b) NOR, (c) EP and (d) 0.10 mM AA in 0.010 M PBS (pH 7.4). Scan rate = 50 $mV.s^{-1}$

No electrochemical response was observed in PBS without neurotransmitters, **Figure 3.10(i)**. In the presence of dopamine, **Figure 3.10(a)(ii)**, an intense oxidation peak was observed at 193 mV and a reduction peak at 12.4 mV. In the presence of norepinephrine, an oxidation and reduction peaks were observed at 246 mV and 90.5 mV respectively, **Figure 3.10(b)(ii)**. However, in the presence of epinephrine, only an oxidation peak at 241 mV was observed with no reduction peak, **Figure 3.10(c)(ii)**. The CV scans for all the neurotransmitters are observed with enhanced oxidation peak currents, small reduction peak and a well-defined steady redox wave indicating high electrocatalytic activity of CoOCAPc immobilized on pre-grafted gold surface (Au-PEA-CoOCAPc). No electrocatalytic peak was observed for ascorbic acid, **Figure 3.10(d)(ii)**, and this was attributed to deprotonated -$COO^-$ functional groups of the Au-PEA-CoOCAPc surface at pH 7.4 which could screen off AA that exists as an ascorbate anion at pH 7.4. Henceforth, repelled by the -$COO^-$ at pH 7.4 and no electrocatalysis occurring.

The electrochemical detection of DA, NOR, EP and AA was also investigated on (i) bare Au, (ii) Au-PEA and (iii) Au-PEA-CoOCAPc in **Figure 3.11** using the third CV scan of each electrode surface. The oxidation peak of bare Au and Au-PEA was observed at higher potentials as compared to Au-PEA-CoOCAPc. The bare Au and Au-PEA electrodes showed oxidation potentials between 278 mV - 313 mV for all the neurotransmitters. The Au-PEA showed oxidation of catecholamine neurotransmitters and ascorbic acid. This was attributed to very thin layer of PEA that allows for long range electron transfer. We observed the similar effect on the $[Fe(CN)_6]^{3-/4-}$ and $[Ru(NH_3)_6]^{2+/3+}$. The oxidation potentials for Au-PEA-CoOCAPc shifted to less energy values, observed at between 195 mV – 246 mV. The oxidation peak currents

increased at the Au-PEA-CoOCAPc for all the catecholamine neurotransmitters. Higher current peaks observed on Au-PEA-CoOCAPc indicated excellent electrocatalytic property of the CoOCAPc. In addition, the detection of neurotransmitters at Au-PEA-CoOCAPc showed lower onset potentials confirming excellent electrocatalysis. Ascorbic acid was detected at bare Au and Au-PEA but not at Au-PEA-CoOCAPc. This was expected, at pH 7.4, and due to the terminal -COOH groups of the Au-PEA-CoOCAPc that are deprotonated and repel the ascorbic acid which is also negatively charged at pH 7.4.

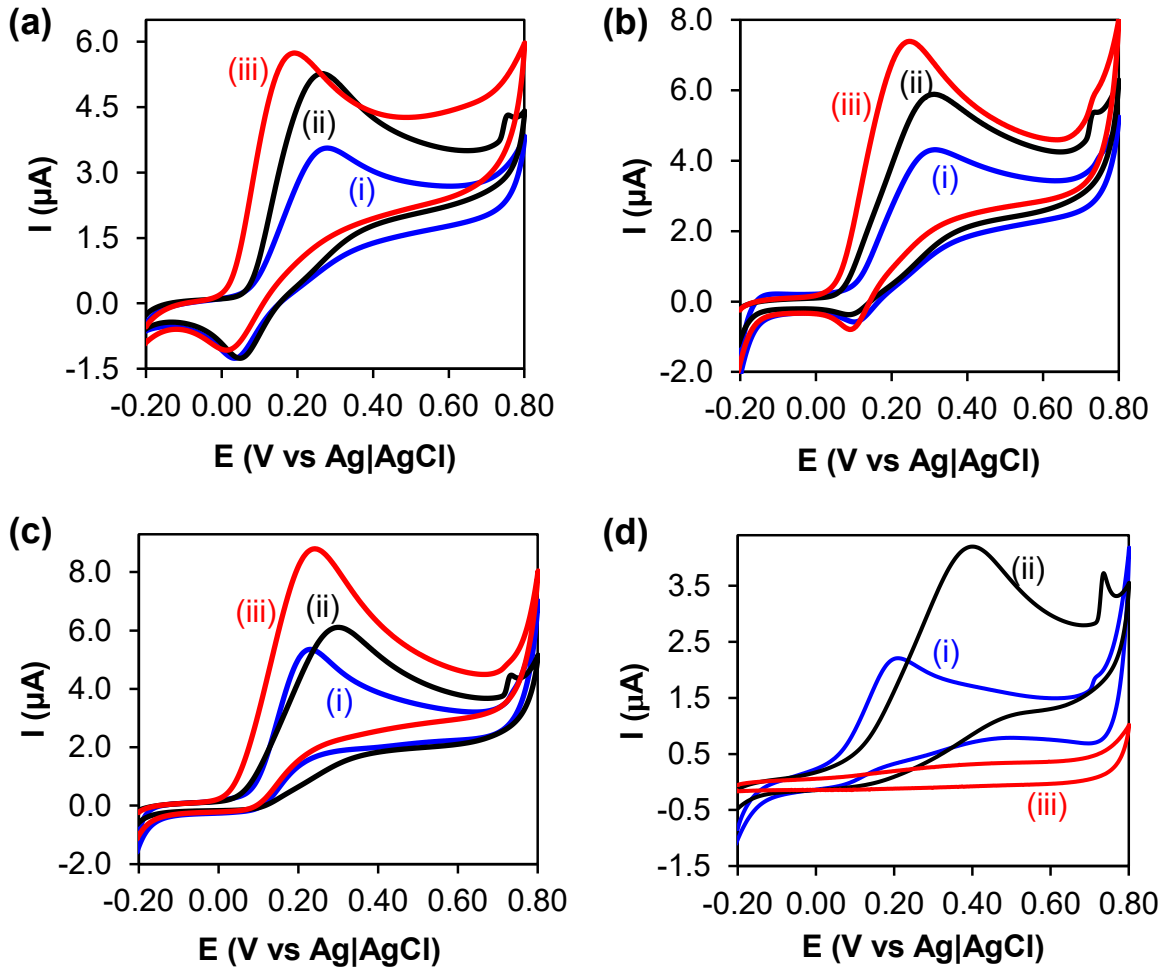


**Figure 3.11**: CVs for electrochemical oxidation of 1.0 mM (a) DA, (b) NOR, (c) EP and (d) 0.10 mM AA in 0.010 M PBS (pH 7.4) at (i) bare Au, (ii) Au-PEA and (iii) Au-PEA-CoOCAPc. Scan rate = 50 $mV.s^{-1}$.

### 3.3.8 Effect of scan rate on catecholamine NT

**Figure 3.12** shows CVs for Au-PEA-CoOCAPc in (a) 0.10 mM DA, (b) 0.10 mM NOR and (c) 0.10 mM EP in 0.010 M PBS (pH 7.4) measured at scan rates ranging from (i) 25 – (v) 125 $mV.s^{-1}$. The oxidation potential remained relatively the same, but the peak current increased with an increase in the scan rate from 25 – 125 $mV.s^{-1}$. A good linearity was seen between anodic peak currents and square roots of the scan rates. The results suggest that the nature of the redox process on the Au-PEA-CoOCAPc is a diffusion-controlled process that is, the analyte diffuses towards the electrocatalytic surface and get oxidized.

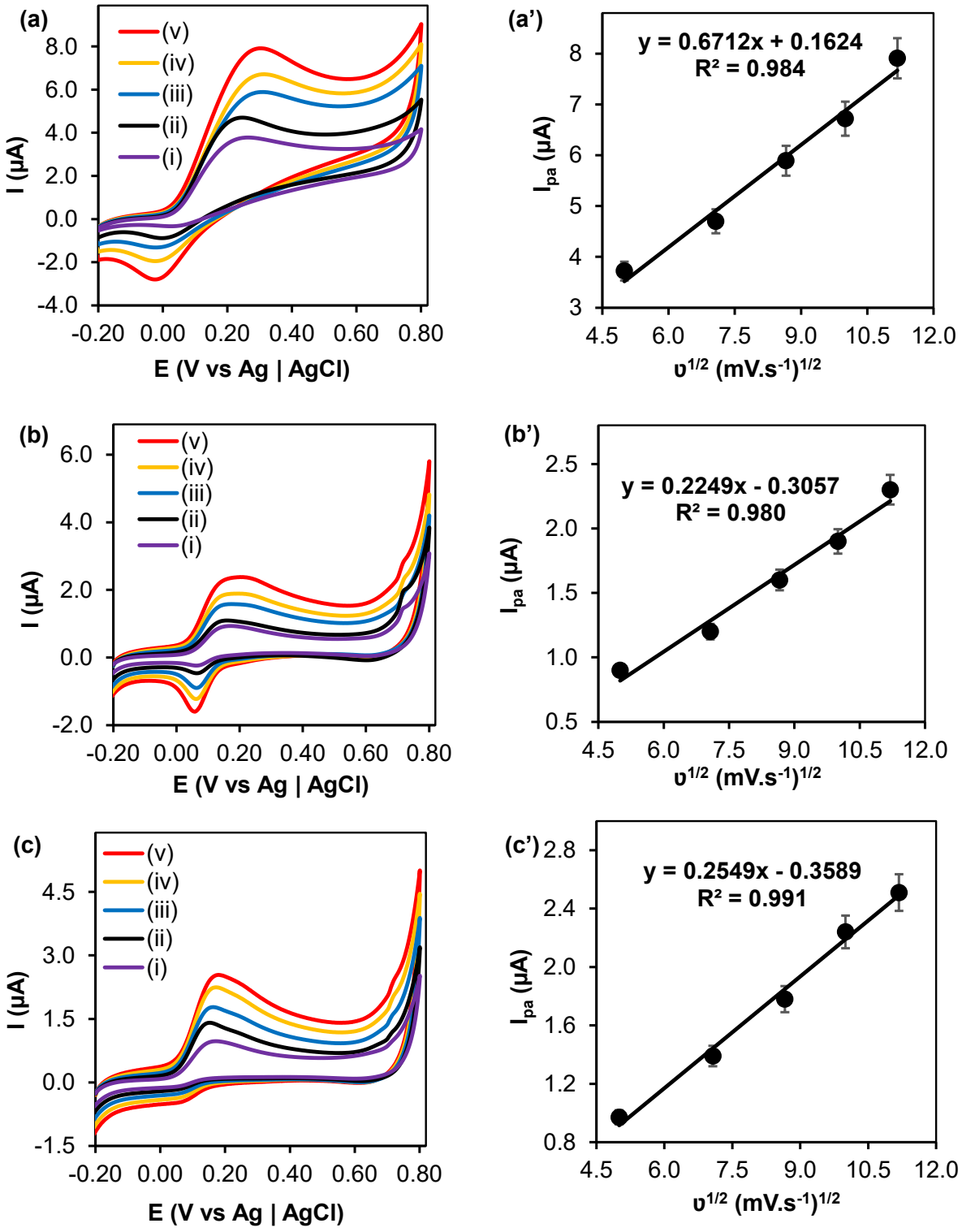


**Figure 3.12**: CVs of Au-PEA-CoOCAPc measured in PBS (pH 7.4) containing 0.10 mM (a) DA, (b) NOR and (c) EP at different scan rates (i) 25 – (v) 125 $mV.s^{-1}$ and their corresponding calibrations curves. The electrolyte solution was 0.010 M PBS (pH 7.4).

### 3.3.9 Interference studies

The selectivity of the electrochemical detection of the catecholamine neurotransmitters was investigated simultaneously in the presence ascorbic acid (AA) and guanine (GA) used as interferences. DPVs of Au-PEA-CoOCAPc in PBS (pH 7.4) containing 0.25 mM DA, 0.50 mM GA and 0.10 mM AA are shown in **Figure 3.13**. The Au-PEA-CoOCAPc selectively detected DA with GA and AA showing no peak. Ascorbic acid was repelled by the negatively charged -$COO^-$ functional groups of Au-PEA-CoOCAPc surface at pH 7.4. A broad peak was observed and shifted to slightly more positive potentials when all the analytes were mixed. The final concentration of DA was 0.25 mM in all the solutions. There was a slight oxidation peak shift from 37 mV to 72 mV. At pH 7.4, physiological condition, guanine was practically insoluble [**41,42**] and this resulted in no electrochemical signal observed even though guanine was in neutral form between pH 5 and 7.5. In **Figure 3.13b(ii)** there was no oxidation peak due to GA.

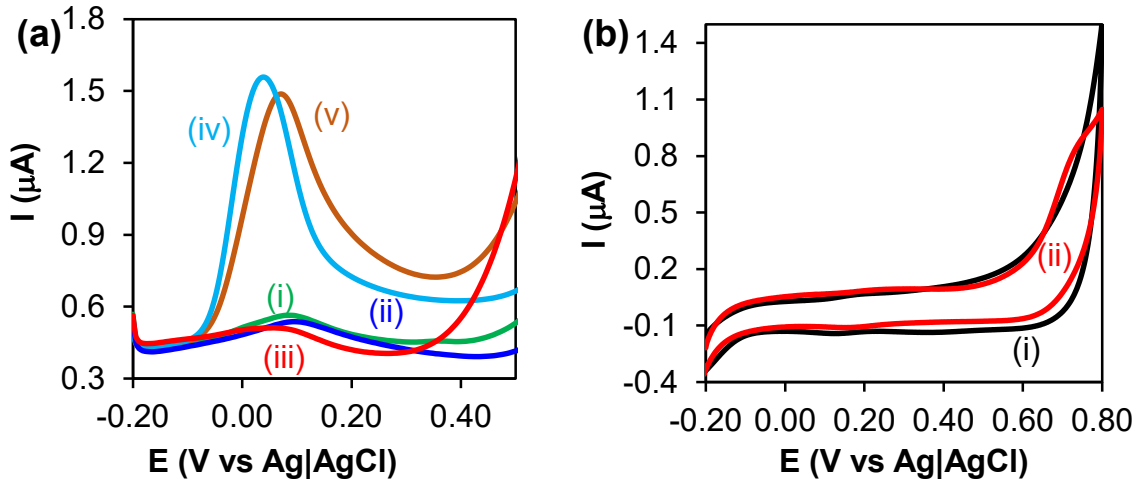


**Figure 3.13**: (a) DPVs of Au-PEA-CoOCAPc in (i) 0.010 M PBS (pH 7.4), (ii) 0.10 mM AA, (iii) 0.50 mM GA, (iv) 0.25 mM DA and (v) mixture (0.25 mM DA + 0.50 mM GA + 0.10 mM AA) all in 0.010 M PBS (pH 7.4). (b) CVs in the (i) absence and (ii) presence of 0.50 mM GA in 0.010 M PBS (pH 7.4). Scan rate = 50 $mV.s^{-1}$.h

### 3.3.10 Analytical studies of neurotransmitters at Au-PEA-CoOCAPc

Differential pulse voltammetry (DPV) was used to evaluate the effect of different concentrations of the catecholamine neurotransmitters (DA, EP and NOR). **Figure 3.14** shows DPVs and the corresponding calibration curves of Au-PEA-CoOCAPc in the presence of 1.0 µM - 50 µM for (a) DA, (b) NOR and (c) EP in PBS solution (pH 7.4). DPV showed an increase in the oxidation peak currents with increasing concentrations of catecholamine neurotransmitters (DA, EP, NOR). The oxidation potentials were observed at 37 mV for DA, 88 mV for NOR and 77 mV for EP. The DPV showed a linear increase with an increase in the concentration of DA, NOR, and EP. The regression coefficient ($R^2$) of DA was found to be 0.989, for NOR, $R^2$ = 0.99 and for EP, $R^2$ = 0.989. The Au-PEA-CoOCAPc surface exhibited a good linear plot for the concentration range from 0.10 µM – 50 µM for DA and 0.50 µM – 50 µM for NOR. The limit of detection (LOD) for DA and NOR was found to be 64 nM and 0.17 µM, and the sensitivity was 1.960 $\mu A.\mu M^{-1}.cm^{-2}$ and 0.786 $\mu A.\mu M^{-1}.cm^{-2}$ respectively. Au-PEA-CoOCAPc was linear in the [EP] range from 5.0 µM – 50 µM with a limit of detection found to be 0.22 µM, and a sensitivity of 0.552 $\mu A.\mu M^{-1}.cm^{-2}$. The pKa values for the studied catecholamine neurotransmitters are higher than 8.0. At pH 7.4, the catecholamine neurotransmitters are neutral or positively charged. At pH 7.4, the physiological condition, there is an electrostatic attraction between the positively charged catecholamine neurotransmitters and negatively charged $-COO^-$ terminal functional groups on the Au-PEA-CoOCAPc surface.

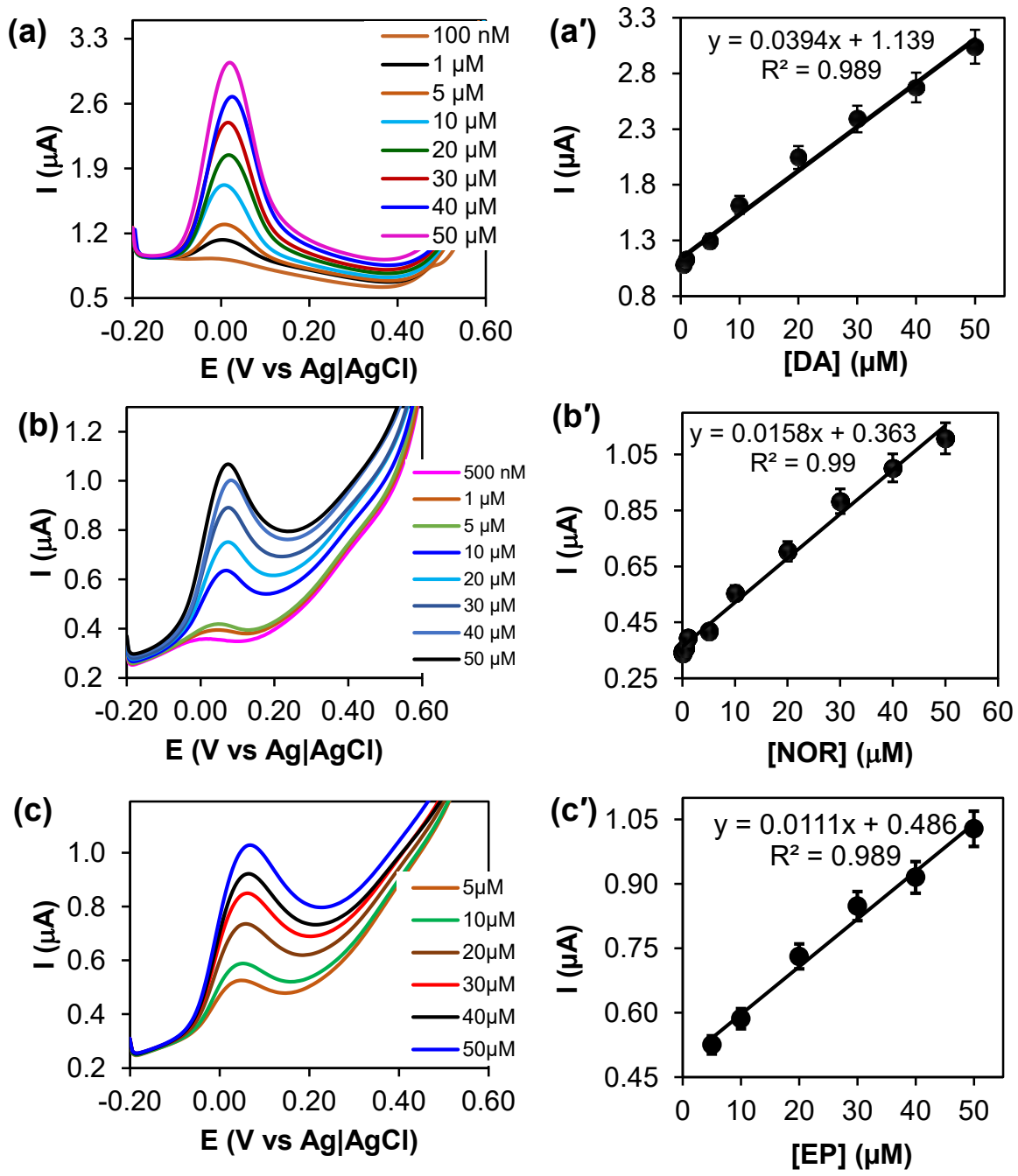


**Figure 3.14**: DPVs and calibration curves of Au-PEA-CoOCAPc from 0.10 µM – 50 µM of (a) DA, (b) NOR and (c) EP in 0.010 M PBS (pH 7.4). Scan rate = 50 mV.s$^{-1}$.

The oxidation of DA, EP and NOR is in the region for metal oxidation and hence the mechanism is a metal-based process. Phthalocyanine ring oxidation are usually at high oxidation potentials (> 600 mV vs Ag|AgCl). The electroanalytical parameters of

Au-PEA-CoOCAPc are summarized in **Table 3.2** and compared with the recently reported MPc modified gold electrochemical sensors for the detection of neurotransmitters. The electrocatalytic potentials were much lower when compared to the reported values further confirming excellent electrocatalysis. The electrocatalytic detection of the neurotransmitters was observed to exhibit comparable or even greater sensitivity with lowest detection limits when compared to other cobalt and nanomaterial conjugates reported in literature [**16,17,22,43,44**]. Sudhakara *et al* [**16**] reported selective electrochemical detection of DA on GCE modified electrode. The GCE was fabricated by drop casting the nano-material composite which is an unstable method of electrode fabrication. The limit of quantification (LOQ) was much lower for Au-PEA-CoOCAPc than for the reported electrochemical sensors in **Table 3.2**. Au-PEA-CoOCAPc also exhibited comparable to high sensitivity values when compared to the reported electrodes. The Au-PEA-CoOCAPc does not discriminate between the neurotransmitters. Further work in this regard is ongoing. Amongst the various methods currently explored, is the use of polymers and/or molecular-imprinted polymers. Their incorporation and effect on the electrocatalytic signal when integrated with phthalocyanine complexes.

**Table 3.2**: Comparison of analytical parameters of electrochemical sensors reported for detection of DA, EP and NOR.

| Analytes | $E_P$ (mV) | Detection method | LCR (µM) | LOD (µM) | LOQ (µM) | Sensitivity ($\mu A.cm^{-2}.mM^{-1}$) | Ref. |
|---|---|---|---|---|---|---|---|
| **DA** | 37 | DPV | 0.10 – 50 | 64 nM | 0.21 | 1.960 | [**TW**] |
| | [a] | CV | 20 – 200 | 64 nM | - | 1.212 | [16] |
| | [b]175 | SWV | 10 – 60 | 5.65 | 20.19 | 0.403 | [17] |
| | [c]264 | CV | 5 – 100 | 1.30 | 4.4 | $0.490_{Oxi}$ | [22] |
| | [c]110 | | | 0.95 | 3.17 | $0.440_{Red}$ | |
| | [d] | DPV | 2 – 30 | 0.43 | | 1.220 | [43] |
| **EP** | 77 | DPV | 5 - 50 | 0.22 | 0.73 | 0.552 | [**TW**] |
| | [b]205 | SWV | 10 – 60 | 4.55 | 15.16 | 0.787 | [17] |
| | [c]271 | CV | 5 – 100 | 3.08 | 10.3 | 0.220 | [22] |
| | - | DPV | 1.33 – 550 | 15.6 nM | | - | [44] |
| **NOR** | 88 | DPV | 0.50 – 50 | 0.17 | 0.56 | 0.786 | [**TW**] |
| | [b]190 | SWV | 10 – 60 | 4.56 | 15.20 | 0.350 | [17] |
| | [c]269 | CV | 5 – 100 | 2.11 | 7.02 | $0.310_{Oxi}$ | [22] |
| | [c]130 | | | 1.78 | 5.93 | $0.240_{Red}$ | |

TW = this work; [a]TACoPc/PANI = tetra-amino cobalt (II) phthalocyanine/poly aniline nanofibers; [b]SAMs/AuNPs = self-assembled monolayers /gold nanoparticles; [c]PEA-CoTCPhOPc = phenylethylamine - cobalt (II) tetra-(3-carboxylic acid phenoxy) phthalocyanine; [d]CoP-Tyr = cobalt (II) porphyrin - tyrosinase; Paraffin/MWCNT/CoPc – cobalt (II) phthalocyanine.

## 3.4 Conclusions

Cobalt (II) octa acyl chloride phthalocyanine (CoOAClPc) was successfully synthesized and characterized using FTIR, UV, MCD and mass spectroscopy. CoOAClPc was covalently immobilized onto the pre-grafted gold electrode to form a thin monolayer film of Au-PEA-CoOAClPc that hydrolyzed to for Au-PEA-CoOCAPc. The presence of PEA and PEA-CoOCAPc was confirmed by electrochemical surface characterization using cyclic voltammetry and electrochemical impedance spectroscopy. The pH sensitivity of -COOH terminal groups was observed on the negatively charged, $[Fe(CN)_6]^{3-/4-}$ and a positively charged, $[Ru(NH_3)_6]^{2+/3+}$ redox probes. The Au-PEA-CoOCAPc was investigated for electrocatalytic and electroanalytical properties toward catecholamine neurotransmitters (dopamine, epinephrine, and norepinephrine). The electrocatalytic oxidation of the catecholamine neurotransmitters in PBS solution (pH 7.4) was studied using differential pulse voltammetry (DPV) in a linear range up to 50 µM. The LOD was determined to be 64 nM, 0.22 µM and 0.17 µM for dopamine, epinephrine, and norepinephrine respectively. The limit of quantification (LOQ) was determined to be 0.21 µM, 0.73 µM and 0.56 µM for DA, EP and NOR respectively. These results confirmed a good sensitivity of Au-PEA-CoOCAPc towards catecholamine neurotransmitters and the electrode blocked the signal due to GA and AA as strong interfering species.

## 3.5 References


[1] J.A. Ribeiro, P.M.V. Fernandes, C.M. Pereira, F. Silva, Electrochemical sensors and biosensors for determination of catecholamine neurotransmitters: A review, *Talanta* 160 (**2016**) 653–679. https://doi.org/10.1016/j.talanta.2016.06.066.

[2] E.S. Bucher, R.M. Wightman, Electrochemical analysis of neurotransmitters, *Annu. Rev. Anal. Chem.* 8 (**2015**) 239–261. https://doi.org/10.1146/annurev-anchem-071114-040426.

[3] M. Sajid, N. Baig, K. Alhooshani, Chemically modified electrodes for electrochemical detection of dopamine: Challenges and opportunities, *TrAC - Trends Anal. Chem.* 118 (**2019**) 368–385. https://doi.org/10.1016/j.trac.2019.05.042.

[4] J.K. Shashikumara, B.E.K. Swamy, Electrochemical investigation of dopamine in presence of uric acid and ascorbic acid at poly (Reactive Blue) modified carbon paste electrode: A voltammetric study, *Sens. Int*. 1 (**2020**) 100008. https://doi.org/10.1016/j.sintl.2020.100008.

[5] Z. Tavakolian-Ardakani, O. Hosu, C. Cristea, M. Mazloum-Ardakani, G. Marrazza, Latest trends in electrochemical sensors for neurotransmitters: A review, *Sensors* 19 (**2019**) 2037. https://doi.org/10.3390/s19092037.

[6] S.M. Chen, K.T. Peng, The electrochemical properties of dopamine, epinephrine, norepinephrine, and their electrocatalytic reactions on cobalt(II) hexacyanoferrate films, *J. Electroanal. Chem.* 547 (**2003**) 179–189. https://doi.org/10.1016/S0022-0728(03)00220-1.

[7] S.H. Kim, J.W. Lee, I.H. Yeo, Spectroelectrochemical and electrochemical behavior of epinephrine at a gold electrode, *Electrochim. Acta* 45 (**2000**) 2889–

2895. https://doi.org/10.1016/S0013-4686(00)00364-9.

[8] P. Mashazi, E. Antunes, T. Nyokong, Probing electrochemical and electrocatalytic properties of cobalt(II) and manganese(III) octakis(hexylthio)phthalocyanine as self-assembled monolayers, *J. Porphyr. Phthalocyanines* 14 (**2010**) 932–947. https://doi.org/10.1142/S108842461000277X.

[9] E. Demir, H. Silah, B. Uslu, Phthalocyanine modified electrodes in electrochemical Analysis, *Crit. Rev. Anal. Chem.* 52 (**2020**) 1–37. https://doi.org/10.1080/10408347.2020.1806702.

[10] K.I. Ozoemena, T. Nyokong, Comparative electrochemistry and electrocatalytic activities of cobalt , iron and manganese phthalocyanine complexes axially co-ordinated to mercaptopyridine self-assembled monolayer at gold electrodes, *Electrochim. Acta* 51 (**2006**) 2669–2677. https://doi.org/10.1016/j.electacta.2005.08.007.

[11] V. Mani, S.T. Huang, R. Devasenathipathy, T.C.K. Yang, Electropolymerization of cobalt tetraamino-phthalocyanine at reduced graphene oxide for electrochemical determination of cysteine and hydrazine, *RSC Adv.* 6 (**2016**) 38463–38469. https://doi.org/10.1039/c6ra01851c.

[12] Mounesh, P. Malathesh, N.Y. Praveen Kumara, B.S. Jilani, C.D. Mruthyunjayachari, K.R. Venugopala Reddy, Synthesis and characterization of tetra-ganciclovir cobalt (II) phthalocyanine for electroanalytical applications of AA/DA/UA, *Heliyon* 5 (**2019**) e01946. https://doi.org/10.1016/j.heliyon.2019.e01946.

[13] S. Hun, K. Jin, W. Namgoong, S. Bum, Y. Jeong, Y. Kim, Synthesis and characteristics of metal-phthalocyanines tetra- substituted at non-peripheral (a)

or peripheral (b) positions , and their applications in LCD color filters, *J. Incl. Phenom. Macrocycl. Chem.* 82 (**2015**) 195–202. https://doi.org/10.1007/s10847-015-0514-y.

[14] I. Özçeşmeci, A. Koca, A. Gül, Synthesis and electrochemical and in situ spectroelectrochemical characterization of manganese, vanadyl, and cobalt phthalocyanines with 2-naphthoxy substituents, *Electrochim. Acta* 56 (**2011**) 5102–5114. https://doi.org/10.1016/j.electacta.2011.03.069.

[15] P.N. Mashazi, P. Westbroek, K.I. Ozoemena, T. Nyokong, Surface chemistry and electrocatalytic behaviour of tetra-carboxy substituted iron, cobalt and manganese phthalocyanine monolayers on gold electrode, *Electrochim. Acta* 53 (**2007**) 1858–1869. https://doi.org/10.1016/j.electacta.2007.08.044.

[16] S.M. Sudhakara, H.M.N. Kotresh, M.C. Devendrachari, F. Khan, Synthesis and electrochemical investigation of tetra amino cobalt (II) phthalocyanine functionalized polyaniline nanofiber for the selective detection of dopamine, *Electroanal*. 32 (2020) 1807–1817. https://doi.org/10.1002/elan.202000067.

[17] S. Ramirez, N. Silva, M.P. Oyarzun, J. Pavez, J.F. Silva, Gold nanostructures on self-assembled monolayers activity for epinephrine, noradrenaline and dopamine, *J. Electroanal. Chem.* 799 (**2017**) 349–357. https://doi.org/10.1016/j.jelechem.2017.06.040.

[18] N. Fourati, M. Seydou, C. Zerrouki, A. Singh, S. Samanta, F. Maurel, D.K. Aswal, M. Chehimi, Ultrasensitive and selective detection of dopamine using cobalt-phthalocyanine nanopillar-based surface acoustic wave sensor, *ACS Appl. Mater. Int.* 6 (**2014**) 22378–22386. https://doi.org/10.1021/am506403f.

[19] Y. Wei, Y. Liu, Z. Xu, S. Wang, B. Chen, D. Zhang, Y. Fang, Simultaneous detection of ascorbic acid, dopamine, and uric acid using a novel

electrochemical sensor based on palladium nanoparticles/reduced graphene oxide nanocomposite, *Int. J. Anal. Chem.* 2020 (**2020**). https://doi.org/10.1155/2020/8812443.

[20] O.K. Adeniyi, P.N. Mashazi, Stable thin films of human P53 antigen on gold surface for the detection of tumour associated anti-P53 autoantibodies, *Electrochim. Acta* 331 (**2020**) 135272. https://doi.org/10.1016/j.electacta.2019.135272.

[21] B.O. Agboola, K.I. Ozoemena, Efficient electrocatalytic detection of epinephrine at gold electrodes modified with self-assembled metallo-octacarboxyphthalocyanine complexes, *Electroanal.* 20 (**2008**) 1696–1707. https://doi.org/10.1002/elan.200804240.

[22] K. Tshenkeng, P. Mashazi, Covalent attachment of cobalt (II) tetra-(3-carboxyphenoxy) phthalocyanine onto pre-grafted gold electrode for the determination of catecholamine neurotransmitters, *Electrochim. Acta* 360 (**2020**) 137015. https://doi.org/10.1016/j.electacta.2020.137015.

[23] B.O. Agboola, K.I. Ozoemena, Self-assembly and heterogeneous electron transfer properties of metallo-octacarboxyphthalocyanine complexes on gold electrode, *Phys. Chem. Chem. Phys.* 10 (**2008**) 2399–2408. https://doi.org/10.1039/b800611c.

[24] K. Ozoemena, P. Westbroek, T. Nyokong, Cyclic voltammetric studies of octabutylthiophthalocyaninato-cobalt (II) and its self-assembled monolayer (SAM) on gold electrode, *JPP.* 6 (**2002**) 98–106. https://doi.org/10.1142/S1088424602000130.

[25] K.I. Ozoemena, T. Nyokong, P. Westbroek, Self-assembled monolayers of cobalt and iron phthalocyanine complexes on gold electrodes: comparative

surface electrochemistry and electrocatalytic interaction with thiols and thiocyanate, *Electroanal.* 15 (**2003**) 1762–1770. https://doi.org/10.1002/elan.200302753.

[26] B.O. Agboola, K.I. Ozoemena, Synergistic enhancement of supercapacitance upon integration of nickel (II) octa [(3,5-biscarboxylate)-phenoxy] phthalocyanine with SWCNT-phenylamine, *J. Power Sources* 195 (**2010**) 3841–3848. https://doi.org/10.1016/j.jpowsour.2009.12.095.

[27] S. Griveau, D. Mercier, C. Vautrin-Ul, A. Chaussé, Electrochemical grafting by reduction of 4-aminoethylbenzenediazonium salt: Application to the immobilization of (bio)molecules, *Electrochem. Commun.* 9 (**2007**) 2768–2773. https://doi.org/10.1016/j.elecom.2007.09.004.

[28] D. Song, Y. Mu, X. Liu, L. Zhao, H. Zhang, Q. Jin, An optical immunosensor based on surface plasmon resonance for determination of bFGF, *Microchem. J.* 74 (*2003*) 93–97. https://doi.org/10.1016/S0026-265X(02)00176-5.

[29] K. Sakamoto, E. Ohno, Synthesis and electron transfer property of phthalocyanine derivatives, *Prog. Org. Coatings* 31 (**1997**) 139–145. https://doi.org/10.1016/S0300-9440(97)00029-5.

[30] W. Ma, Y.L. Ying, L.X. Qin, Z. Gu, H. Zhou, D.W. Li, T.C. Sutherland, H.Y. Chen, Y.T. Long, Investigating electron-transfer processes using a biomimetic hybrid bilayer membrane system, *Nat. Protoc.* 8 (**2013**) 439–450. https://doi.org/10.1038/nprot.2013.007.

[31] A. Kalkan, Z.A. Bayir, Phthalocyanines with rigid carboxylic acid containing pendant arms, *Polyhedron* 25 (**2006**) 39–42. https://doi.org/10.1016/j.poly.2005.06.056.

[32] S. Gorduk, A. Altindal, Non-peripherally tetra substituted phthalocyanines

bearing carboxylic acid anchoring groups as photosensitizer for high efficient dye-sensitized solar cells, *J. Mol. Struct.* 1204 (**2020**) 127636. https://doi.org/10.1016/j.molstruc.2019.127636.

[33] T. Mugadza, T. Nyokong, Covalent linking of ethylene amine functionalized single-walled carbon nanotubes to cobalt (II) tetracarboxyl-phthalocyanines for use in electrocatalysis, *Synth. Met.* 160 (**2010**) 2089–2098. https://doi.org/10.1016/j.synthmet.2010.07.036.

[34] T.O. Nicolescu, Interpretation of Mass Spectra (Fourth Edition), (**2018**) 350. https://doi.org/http://dx.doi.org/10.5772/intechopen.68595.

[35] D. Bélanger, J. Pinson, Electrografting: A powerful method for surface modification, *Chem. Soc. Rev.* 40 (**2011**) 3995–4048. https://doi.org/10.1039/c0cs00149j.

[36] J.J. Gooding, Advances in interfacial design for electrochemical biosensors and sensors: Aryl diazonium salts for modifying carbon and metal electrodes, *Electroanal.* 20 (**2008**) 573–582. https://doi.org/10.1002/elan.200704124.

[37] P. Mashazi, P. Tetyana, S. Vilakazi, T. Nyokong, Electrochemical impedimetric immunosensor for the detection of measles-specific IgG antibodies after measles infections, *Biosens. Bioelectron.* 49 (**2013**) 32–38. https://doi.org/10.1016/j.bios.2013.04.028.

[38] P. Mashazi, T. Nyokong, Electrocatalytic studies of covalently immobilized metal tetra-amino phthalocyanines onto derivatized screen-printed gold electrodes, *Microchim. Acta* 171 (**2010**) 321–332. https://doi.org/10.1007/s00604-010-0438-6.

[39] S. Khene, D.A. Geraldo, C.A. Togo, J. Limson, T. Nyokong, Synthesis, electrochemical characterization of tetra- and octa-substituted dodecyl-

mercapto tin phthalocyanines in solution and as self-assembled monolayers, *Electrochim. Acta* 54 (**2008**) 183–191. https://doi.org/10.1016/j.electacta.2008.08.018.

[40] F. Matemadombo, S. Griveau, F. Bedioui, T. Nyokonga, Electrochemical characterization of self-assembled monolayer of a novel manganese tetrabenzylthio-substituted phthalocyanine and its use in nitrite oxidation, *Electroanal.* 20 (**2008**) 1863–1872. https://doi.org/10.1002/elan.200804269.

[41] T. Darvishzad, T. Lubera, S.S. Kurek, Puzzling aqueous solubility of guanine obscured by the formation of nanoparticles, *J. Phys. Chem. B.* 122 (**2018**) 7497–7502. https://doi.org/10.1021/acs.jpcb.8b04327.

[42] G. Näher, Adenine and Guanine, *Methods Enzym. Anal.* (**1974**) 1909–1915. https://doi.org/10.1016/b978-0-12-091304-6.50048-3.

[43] M. Florescu, M. David, Tyrosinase-based biosensors for selective dopamine detection, *Sensors* 17 (**2017**) 1314. https://doi.org/10.3390/s17061314.

[44] F.C. Moraes, D.L.C. Golinelli, L.H. Mascaro, S.A.S. MacHado, Determination of epinephrine in urine using multi-walled carbon nanotube modified with cobalt phthalocyanine in a paraffin composite electrode, *Sensors Actuators, B Chem.* 148 (**2010**) 492–497. https://doi.org/10.1016/j.snb.2010.05.005.

# Chapter 4

## 4 pH sensitive thin films of iron phthalocyanines as electrocatalysts for screening of ascorbic and uric acids and selective detection of neurotransmitters


### Abstract

Iron octa acyl chloride phthalocyanine (FeOAClPc) was successfully synthesized and characterized. FeOAClPc monolayer thin film was covalently immobilized onto gold electrode pre-modified using electrografting with phenylethylamine. Phenylethylamine (PEA) thin film was achieved by electroreduction of the diazonium salt to yield an amino functional gold surface, Au-PEA. Immobilization of FeOAClPc was via spontaneous acyl amidation to yield a thin monolayer of Au-PEA-FeOAClPc. The hydrolysis of unreacted -COCl resulted in the formation of the -COOH terminal functional groups on the electrode surface to yield Au-PEA-FeOCAPc. The presence of PEA and PEA-FeOCAPc was confirmed by electrochemical surface characterization using cyclic voltammetry (CV) and electrochemical impedance spectroscopy (EIS). The pH sensitivity of -COOH terminal groups was observed on the negatively charged $[Fe(CN)_6]^{3-/4-}$ and a positively charged $[Ru(NH_3)_6]^{2+/3+}$ redox probes. The Au-PEA-FeOCAPc was investigated for electrocatalytic and electroanalytical properties toward catecholamine neurotransmitters (NTs), dopamine (DA), epinephrine (EP), and norepinephrine (NOR). The electrocatalytic oxidation potentials were 153 mV, 193 mV and 249 mV respectively using cyclic voltammetry. Ascorbic acid and uric acid are strong interferents and could not be detected thus confirming excellent selectivity of Au-PEA-FeOCAPc towards catecholamine

neurotransmitters. The limit of detection (LOD) values and limit of quantification (LOQ) values (in brackets) for NTs were 0.24 µM (0.81 µM) for dopamine, 0.34 µM (1.1 µM) for norepinephrine and 0.45 µM (1.5 µM) for epinephrine. New-born calf serum samples also showed excellent selectivity towards catecholamine neurotransmitters. The electrode could be used several times due to the stability of the method employed, i.e. electrografting of PEA and covalent attachment of FeOCAPc.

## 4.1 Introduction

Metallophthalocyanines (MPcs) have been widely studied and they have shown favorable properties allowing them to be used in technological devices such as molecular electronics, photovoltaic devices, and electrochemical sensors [1–4]. MPcs are 18-π electrons conjugated structure with exceptional electron transfer abilities and can undergo fast redox reactions [5–7]. MPcs are organic compounds which are structurally comparable to the naturally occurring porphyrins having a central metal ion. Over the years, the catalytic properties of MPcs and especially those containing paramagnetic central metal ion (Fe, Co, Mn) have been evaluated their application as electrochemical sensors [8]. When MPcs are immobilized onto pre-grafted electrode surfaces, they can be used for electroanalysis as an ultrasensitive sensors for the detection of neurotransmitters [9–11].

Neurotransmitters are chemical signaling molecules that play an important role in the brain neuronal communication. They process extensive information by transmitting signals from nerve cells to target cells [11–13]. Neurotransmitters are classified as amino acids, soluble gases and biogenic amines. Of interest in this study are catecholamines, a class of biogenic amines. Catecholamines are composed of

dopamine (DA), epinephrine (EP) and norepinephrine (NOR). Abnormally high and low concentrations of catecholamine NTs are correlated with neurodegenerative disorders and diseases such as Alzheimer's, Parkinson's and Huntington's [14]. Hence, there is need for quantitative detection and monitoring of catecholamine NTs. A wide range of analytical techniques that have been reported for the detection of catecholamine NTs; are FT-IR [15], Raman [16], chromatography [17], fluorescence [18], capillary electrophoresis [19] among others. These techniques require complex sample pre-treatment and bulk instrumentation, thus making the analysis not amenable for online and field applications. On the other hand, electrochemical sensors are the most cost effective devices, can be miniaturized for portability, are easy to operate and compatible with microfabrication technologies [9,12]. Electrochemical sensors are also rapid, sensitive, and selective in the determination of catecholamine NTs. The major problem encountered in the electrochemical detection of catecholamine NTs is the interference by ascorbic acid (AA) and uric acid (UA), which co-exist in the body fluids. Ascorbic acid has an overlapping oxidation potential with the catecholamine NTs [20]. MPc modified electrochemical sensors bearing pH sensitive functional groups can be used to overcome this challenge by screening off AA and UA [10,21,22]. Various other negatively charged electrode surfaces have been designed to selectively detect catecholamine NTs in the presence of these interferents [23–25]. The electrocatalytic process of MPcs is not only affected by the central metal ion but also the peripheral substituents [26–28]. However, the development of MPc modified electrochemical sensors require several steps of fabrication or use of various additional chemicals as coupling reagents. A novel method of modifying gold electrode with phenylethylamine (PEA) for the attachment of cobalt(II) tetra-(3-carboxyphenoxy) phthalocyanine [10] was recently reported. This method used dicyclohexyl

carbodiimide (DCC) and N-hydroxysuccinimide (NHS) as carbodiimide chemistry reagents to activate the carboxylic acid functional groups and for amide bond formation. **Chapter 3** discusses the use of cobalt (II) octa carboxy acyl chloride phthalocyanine with an increased number of the carboxylic acid functional groups. This chapter investigates the immobilization of metallophthalocyanine containing iron as the central metal ion. Iron phthalocyanines are excellent electrocatalysts. Ozoemena's group [29] demonstrated that the rate of heterogeneous electron transfer is fastest for iron phthalocyanine complexes and slowest for cobalt phthalocyanine complexes. This is due to the reorganization energies associated with $Co^{III}|Co^{II}$ couple oxidation state which is sluggish compared to the $Fe^{III}|Fe^{II}$ oxidation [29]. An initial rate of decomposition of hydrogen peroxide was shown to be 30 times faster with iron octa carboxylic phthalocyanine than cobalt phthalocyanine [30]. We investigated a simpler and quicker method of immobilizing iron octa acyl chloride phthalocyanine (FeOAClPc). This method does not need for extra chemicals such as DCC and NHS. Acyl chloride functional groups on FeOAClPc allow for the ease and spontaneous amidation reaction with amine functional groups following similar procedure reported in **Chapter 3**. This method will result in improved stability of iron phthalocyanine thin films with excellent electrocatalytic reactions due to the perpendicular orientation [31]. The unreacted peripheral acyl chloride functional groups are converted to carboxylic acid via hydrolysis in aqueous solution resulting in the pH sensitive carboxylic acid functional groups which improves the solubility of the MPcs [2,5]. Iron octa carboxylic acid phthalocyanine (FeOCAPc) modified gold electrode was used for the electrocatalysis of catecholamine neurotransmitters. Facile immobilization of FeOAClPc on Au-PEA to form Au-PEA-FeOCAPc is reported and used as an electrochemical sensor for the detection of catecholamine neurotransmitters. The

carboxylic acid functional groups are water soluble and hence allow for pH sensitivity and deprotonation to screen off ascorbic acid and uric acid using analyte pH solution.

### 4.1.1 Aims

(i) To covalently immobilize iron octa acyl chloride phthalocyanine as thin monolayer film on Au grafted with phenylethylamine for the detection of catecholamine neurotransmitters.

(ii) To investigate the performance of the electrochemical sensor in real samples

## 4.2 Experimental

### 4.2.1 Chemical and reagents

Iron (II) chloride, uric acid (UA) and benzene were purchased from Sigma-Aldrich. Similar chemicals, reagents, apparatus and instrumentation were used as reported in **Section 3.2.**

### 4.2.2 Synthesis of iron (II) octa carboxylic acid phthalocyanine (FeOCAPc, 1)

A previously reported method [32] was followed and iron (II) octa carboxylic acid phthalocyanine (FeOCAPc) was achieved the same way cobalt (II) octa carboxylic acid phthalocyanine (CoOCAPc) was synthesized, **Section 3.2.3**. Iron (II) chloride (23.5 mmol) was used for the metal salt.

FeOCAPc: Yield (17.4%)

- FT-IR ($\bar{\upsilon}$, $cm^{-1}$): 2919, 2831, 2316, 2114, 1989, 1756, 1694 (C=O), 1505, 1433, 1353, 1294, 1129, 1057, 994, 896, 725, 622.
- UV-vis ($\lambda_{max}$, nm) log ε: 333 (4.41), 677 (4.20).
- MS (MALDI-TOF) (m/z): Calculated: 922.02, Found: 923.89 $[M + H]^+$

### 4.2.3 Synthesis of iron (II) octa acyl chloride phthalocyanine (FeOAClPc, 2)

Iron (II) octa acyl chloride phthalocyanine (FeOAClPc) was synthesized by hydrolysis of iron (II) octa carboxylic acid phthalocyanine (FeOCAPc) as shown in **Scheme 4.1** [**1**]. Briefly, iron (II) octa carboxylic acid phthalocyanine (0.10 g, 0.11 mmol) was refluxed with 2 ml thionyl chloride, 2 ml dry benzene in the presence of a few drops of pyridine for 10 hours. The resultant green solid was washed with benzene and collected by centrifugation and left to dry overnight at 50 °C in the oven to obtain the iron (II) octa acyl chloride phthalocyanine.

FeOAClPc: Yield (86.7%)

- FT-IR ($\bar{\upsilon}$, $cm^{-1}$): 2912, 2831, 2325, 2114, 1989, 1734, 1713 (C=O), 1509, 1358, 1308, 1129, 1061, 999, 914, 797, 726, 724, 679 (C-Cl), 638.
- UV-vis ($\lambda_{max}$, nm) (log ε): 342 (4.19), 678 (4.15)
- MS (MALDI-TOF) (m/z): Calculated: 1029.82, Found: 1029.29 $[M - Cl]^+$

### 4.2.4 Electrode pre-modification and immobilization of FeOAClPc, Scheme 4.2

A gold electrode was cleaned following an established procedure [**33**]. Briefly, the gold electrode was polished to a mirror finish on a Beuhler felt pad using an aqueous slurry of 1.0 μm, 0.30 μm and 0.050 μm alumina. The polished electrode was then

ultrasonicated consecutively in ethanol and in water for 5 minutes each. The electrode was etched for 2 minutes in a freshly prepared “Piranha” solution of 3:1 (v/v) 98% $H_2SO_4$:30% $H_2O_2$ to remove organic matter that may be adsorbed. It was then rinsed in copious amounts of deionized water and dried in a stream of nitrogen. Electrochemical cleaning was done in 0.10 M $H_2SO_4$ by cycling the electrode between -0.20 and +1.5 V (versus Ag|AgCl in 3.0 M KCl) at a scan rate of 100 $mV.s^{-1}$, until reproducible voltammograms were obtained. Electrografting of phenylethylamine (PEA) onto the Au electrode was achieved following a previously reported method [**34**]. Briefly, a cleaned electrode was placed in a 5 mL solution of acetonitrile containing 1.0 mM 4-(2-aminoethyl) benzene diazonium (AEBD) salt, synthesized as described in literature [**34**], and 0.10 M $TBABF_4$. Electrografting was conducted between +0.40 V and -0.40 V, at a scan rate of 50 $mV.s^{-1}$. An aryl radical was produced that attached to the Au surface to form a thin film of Au-PEA. **Scheme 4.2** shows electrografting of PEA onto Au electrode and immobilization of FeOAClPc onto the pre-grafted Au-PEA electrode. The immobilization of FeOAClPc was accomplished by the reaction between acyl chloride and amine to form an amide coupling bond. The Au-PEA surface was immersed in a solution of FeOAClPc (1.0 mg, 0.97 µmol) in 1.0 ml dry DMF for 4 hrs, to give a thin monolayer film of FeOAClPc to form Au-PEA-FeOAClPc surface. The Au-PEA-FeOAClPc surface was rinsed with dry DMF to remove any physically adsorbed FeOAClPc. Finally, the Au-PEA-FeOAClPc was rinsed with water and during this step the terminal acyl chloride groups hydrolysed to form carboxylic acid groups.

## 4.3 Results and discussion

### 4.3.1 Synthesis of iron (II) octa acyl chloride phthalocyanine (FeOAClPc, 2)

The FeOAClPc (**2**) was synthesized following a reported method [1], **Scheme 4.1**. The first step was the formation of FeOCAPc (**1**). Synthesis of CoOCAPc is discussed in **Section 3.3.1** and FeOCAPc (**1**) was synthesized following a similar method. The FeOCAPc (**1**) was subsequently converted to acyl chloride derivate by refluxing in thionyl chloride, dry benzene and a few drops of pyridine, used to solubilize the carboxylic acid phthalocyanine.

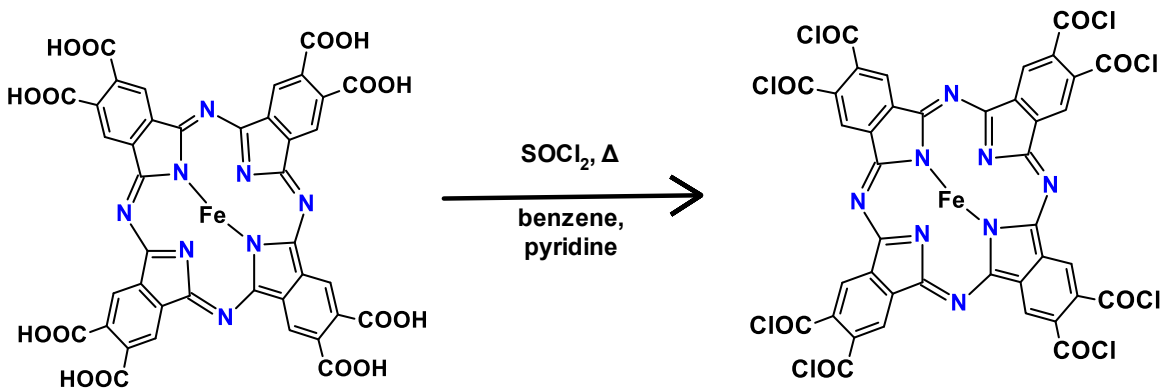


(1) (2)

**Scheme 4.1**: Synthesis of iron (II) octa acyl chloride phthalocyanine (FeOAClPc, **2**)

### 4.3.2 Characterization of FeOCAPc (1) and FeOAClPc (2)

#### 4.3.2.1 FT-IR analysis

The FT-IR spectra of (i) PMDA, (ii) FeOCAPc and (iii) FeOAClPc are shown in **Figure 4.1**. Characteristic vibrational bands at wavenumbers 900 – 1000 $cm^{-1}$ were observed

for the metal phthalocyanines. The broad stretch above 2600 $cm^{-1}$ is related to O-H groups. A vibrational band shift of the carbonyl (C=O) was observed from 1698 $cm^{-1}$ for FeOCAPc to 1713 $cm^{-1}$ for FeOAClPc. The shift is due to chlorine being a highly electronegative halogen element and an electron acceptor. Chlorine weakens the C=O causing the shift in vibrational band to even higher wavenumbers. A vibrational band at 679 $cm^{-1}$ for FeOAClPc was assigned to C-Cl confirming the formation of the FeOAClPc.

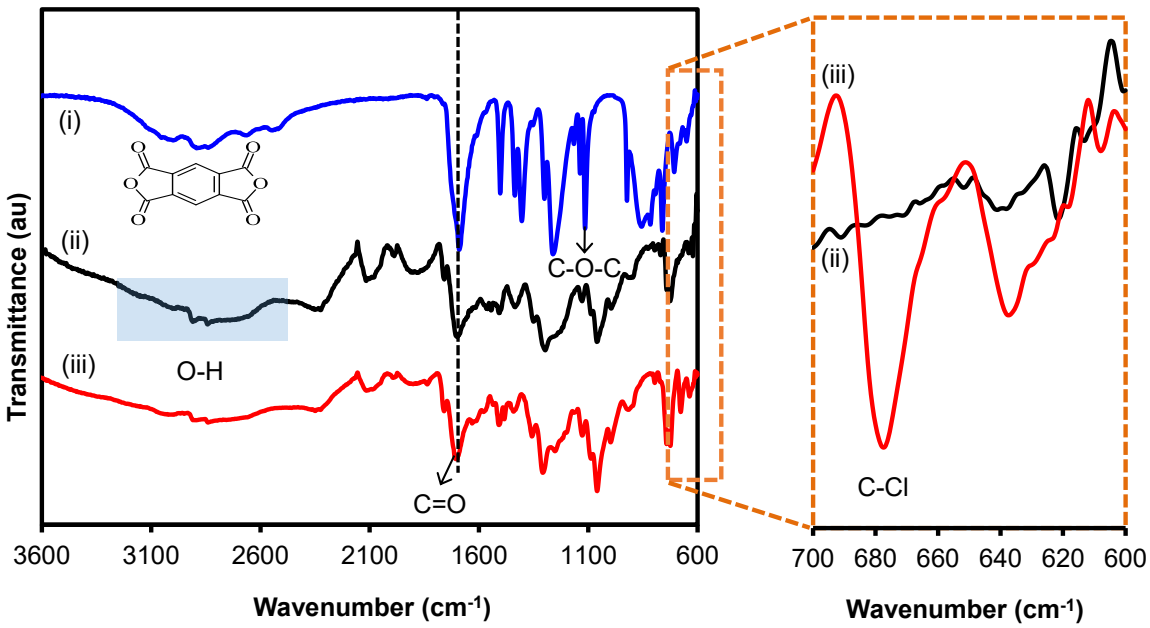


**Figure 4.1**: FT-IR spectra of (i) pyromellitic dianhydride (PMDA), (ii) iron (II) octa carboxylic acid phthalocyanine (FeOCAPc, **1**) and (iii) iron (II) octa acyl chloride phthalocyanine (FeOAClPc, **2**).

### 4.3.2.2 UV-vis and MCD spectroscopy

**Figure 4.2** shows the UV-vis and MCD spectra of (a) FeOCAPc and (b) FeOAClPc in dry DMF. The UV-vis spectra was observed with a strong absorption band in the visible

region called the Q band around 600 – 700 nm and the weak band in the UV region called the B band around 300 – 350 nm, both corresponding to π-π* transitions [35,36]. The MCD spectrum shows the Faraday A1 terms based on Gouterman's 4-orbital model. The B band for FeOCAPc in the UV-vis spectrum has an inflection point in the MCD spectrum at 333 nm while FeOAClPc showed the B band at 342 nm. A shift of the Q band was observed at 678 nm for FeOAClPc as compared to FeOCAPc with the Q band at 677 nm for a Faraday A term. The electronegative Cl at the peripheral acyl chloride functional groups led to the shift in Q band from 677 nm for FeOCAPc to 678 nm for FeOAClPc.

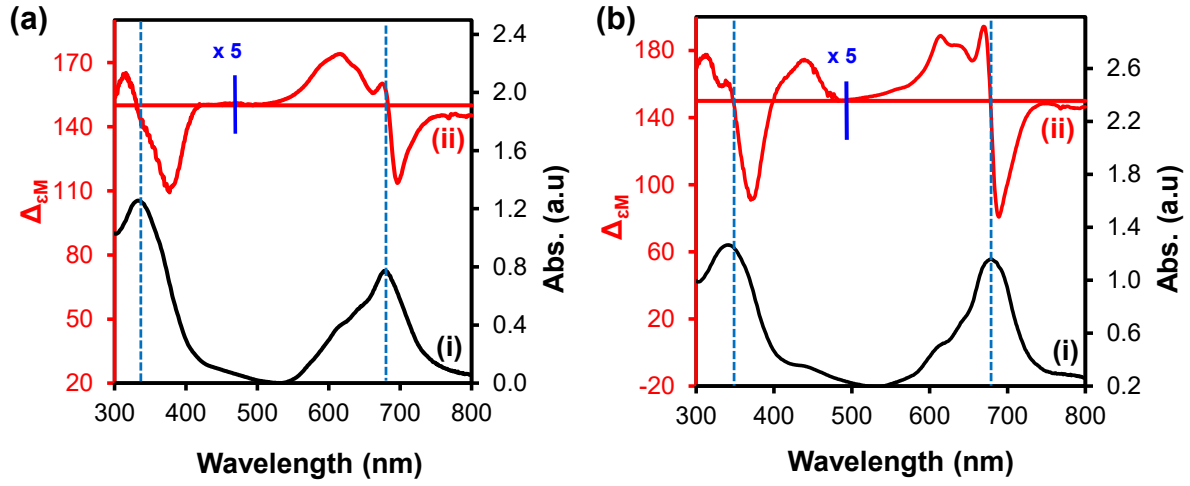


**Figure 4.2**: (i) UV-vis and (ii) MCD spectra for (a) iron (II) octa carboxylic acid phthalocyanine (FeOCAPc) and (b) iron (II) octa acyl chloride phthalocyanine (FeOAClPc) in dry DMF.

#### 4.3.2.3 Mass spectroscopy

The MPc complexes were further characterized using mass spectroscopy. **Figure 4.3** shows the mass spectra of (a) FeOCAPc and (b) FeOAClPc and their corresponding

chemical structures. Mass spectroscopy gives information on the molecular mass of compounds by measuring the ratio of their mass-to-charge (m/z). The intensity of the peak shows the abundance of the ionic species with respective m/z ratio [37]. MPcs degrade with molecular ion peaks corresponding to $[M]^+$, $[M \pm nH]^+$ where n = 1 – 3 [38]. The mass spectroscopy confirmed FeOCAPc and FeOAClPc with peaks corresponding to the molecular ion, m/z = 923.089 and 1029.29 respectively, while the calculated masses are 922.02 and 1029.82 respectively. The obtained mass-to-charge ratio corresponds to $[M + H]^+$ ions for FeOCAPc and $[M - Cl]^+$ for FeOAClPc. The formation of FeOAClPc resulted in higher mass-to-charge ratio much higher due to -COCl functional groups confirming the successful synthesis of FeOAClPc complex.

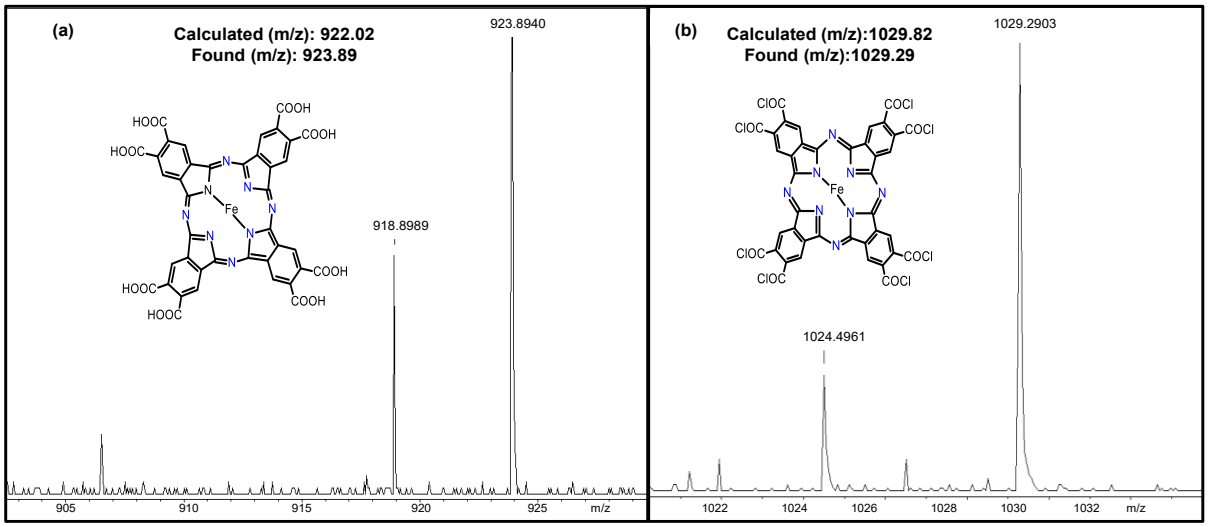


**Figure 4.3**: Mass spectra and corresponding chemical structure of (a) FeOCAPc and (b) FeOAClPc.

#### 4.3.2.4 Raman spectroscopy

**Figure 4.4** shows the Raman spectrum of FeOCAPc. In general, the Raman spectra measured for MPc complexes are sharp and molecularly specific. The spectra are dominated by $A_{1g}$, $B_{1g}$, $B_{2g}$ and $E_g$ modes corresponding to vibrations of the

macrocycle, isoindole moieties and metal-nitrogen bands [39]. The Raman bands observed around 600 - 800 $cm^{-1}$ range are due to $A_{1g}$ and $B_{1g}$ in plane bending of C-N bond. The bands between 800 – 1400 $cm^{-1}$ show either C-N, C-C stretches or C-H bending. A well-defined peak was observed above 1500 $cm^{-1}$, a characteristic G band. The G band is associated with vibrations of C-N-C bridge bonds as well as vibrations of the central Fe atom of the MPc connected to the nitrogen atoms. The FeOAClPc (**2**) was not investigated for Raman analysis as the –COCl undergoes hydrolysis when exposed to moisture.

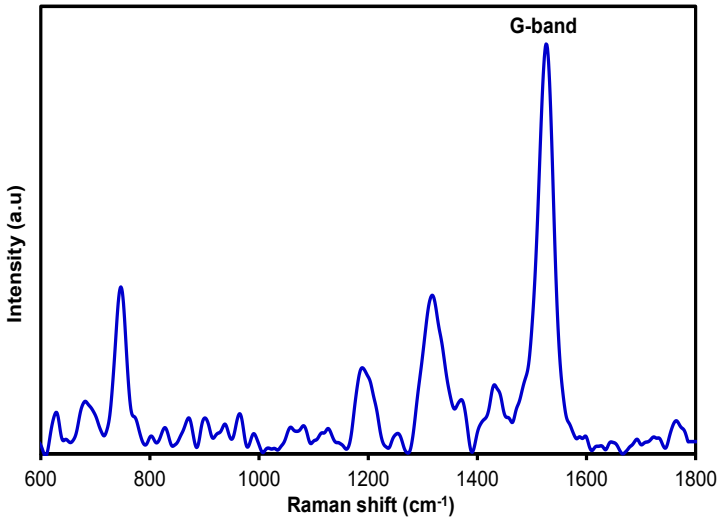


**Figure 4.4**: Raman spectrum of FeOCAPc.

### 4.3.3 Electrode pre-modification of PEA and immobilization of FeOAClPc

The step-by-step modification of the Au surface followed a controlled process for covalent immobilization of FeOAClPc as a thin monolayer film, **Scheme 4.2**. The Au electrode was electrografted following a previous established method [10,21,34]. AEBD salt was used for electrografting the Au electrode surface and this resulted in the surface with terminal amine functional group. The mechanism involves a one

electron reduction of an aryldiazonium salt to produce phenylethylamine (PEA) radical that attaches/grafted onto the gold surface.

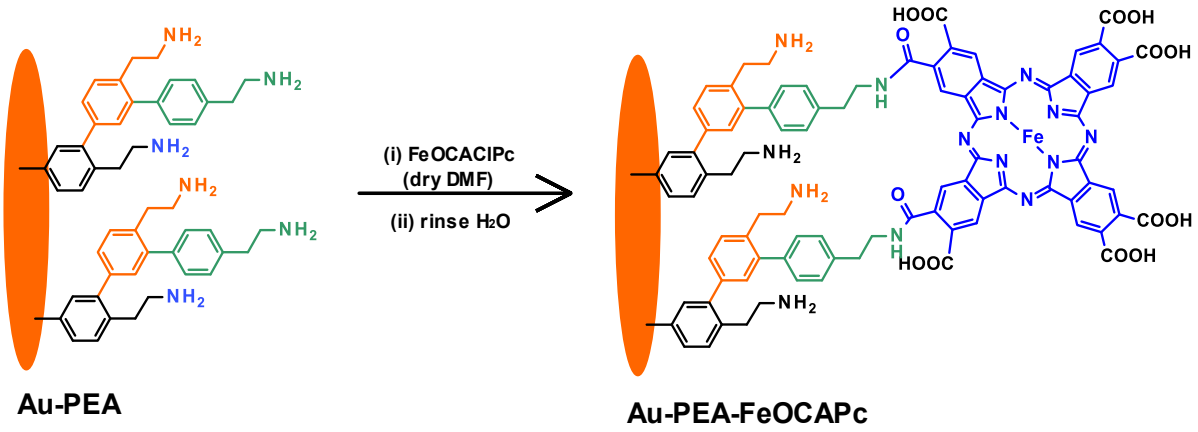


**Scheme 4.2**: Electrografting of AEBD to form Au-PEA and immobilization of FeOAClPc on Au-PEA electrode surface to form Au-PEA-FeOCAPc.

**Figure 4.5** shows a typical cyclic voltammograms (CVs) obtained for the electrografting of the Au electrode by electroreduction of AEBD salt. The electro-reduction of the diazonium salt was confirmed by a reduction peak observed at around 0.18 V on the first scan which results in an $N_2$ (N≡N) group leaving and an aryl radical formation. Scanning to negative potentials results in grafting and attachment of the aryl radical via a carbide (Au-C) bond. On subsequent scans, the reduction current drastically decreased, and the reduction peak disappeared. This was due to the thin insulating organic film that formed on the gold surface and passivating it leading to Au-PEA surface. The resulting modification is very stable due to formation of a covalent Au-C bond between the Au surface and the aryl group [40]. Gold electrode modified with aryl diazonium salt have been shown to have lower capacitance and high rate of electron transfer [41].

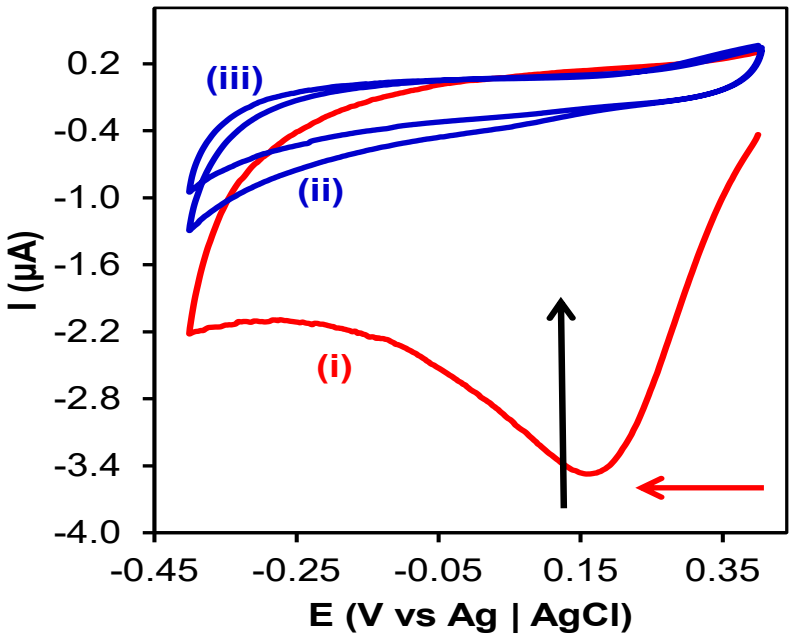


**Figure 4.5**: CVs for the electrografting of 1.0 mM AEBD salt in ACN solution containing 0.10 M $TBABF_4$ onto the Au electrode, from (i) scan 1, (ii) scan 2, and (iii) scan 3. Scan rate = 50 $mV.s^{-1}$.

The FeOAClPc was then immobilized onto the pre-grafted PEA electrode by covalent attachment represented as Au-PEA-FeOAClPc. The acyl chloride functional groups on FeOAClPc spontaneously reacted with amine groups of the PEA forming an amide covalent bond. The Au-PEA-FeOAClPc was first washed in dry DMF to remove any adsorbed metallophthalocyanine, and then exposed to water which hydrolysed the unreacted acyl chloride (-COCl) functional groups to carboxylic acid (-COOH) groups, Au-PEA-FeOCAPc. This is a simple method by which the metallophthalocyanine modified sensor can be fabricated onto a gold surface and is achieved in two steps; (i) the pre-modification of gold electrode with PEA, followed by (ii) spontaneous amidation reaction between the metallophthalocyanine substituents and the amine (-$NH_2$) functional groups of the PEA.

### 4.3.4 Characterization of the bare and modified gold surfaces

Cyclic voltammetry (CV) and electrochemical impedance spectroscopy (EIS) were used to confirm the modification of Au-PEA with FeOAClPc to form Au-PEA-FeOCAPc. Similar studies in the previous **Chapter 3** were carried out using a negative $[Fe(CN)_6]^{3-/4-}$ and a positively charged $[Ru(NH_3)_6]^{2+/3+}$ redox probes. CVs and EIS of Au and Au-PEA were similar to those reported in Chapter 3 and hence not discussed in detail. The Au-PEA-FeOCAPc was discussed in detail. **Figure 4.6** shows CVs and the corresponding EIS of (i) bare Au, (ii) Au-PEA and (iii) Au-PEA-FeOCAPc measured in 2.0 mM (a) $[Fe(CN)_6]^{3-/4-}$ and (b) $[Ru(NH_3)_6]^{2+/3+}$ containing 0.10 M KCl at a scan rate of 50 $mV.s^{-1}$. The pH of both $[Fe(CN)_6]^{3-/4-}$ and $[Ru(NH_3)_6]^{2+/3+}$ solutions was 7.0 adjusted using 0.10 M HCl or 0.10 M NaOH. The oxidation and reduction peaks of $[Fe(CN)_6]^{3-/4-}$ redox couple at Au-PEA-FeOCAPc shifted to high positive and negative values, resulting in an increase in ΔE from 73 ± 4.5 mV to 603 ± 4.1 mV. The peak currents decreased as shown in **Figure 4.6(a)(iii)** confirming the increase in film thickness after the attachment of FeOCAPc and the functional groups (-COOH) repelling the redox probe. The carboxylic groups have a pKa value less than 5 and hence at pH 7.4, -COOH groups are deprotonated ($-COO^-$). The negatively charged carboxyl groups, $-COO^-$ on the Au-PEA-FeOCAPc surface repel the $[Fe(CN)_6]^{3-/4-}$, hindering its redox reaction. The blocking behaviour also confirms the successful immobilization of FeOAClPc onto Au-PEA surface. When the bare Au was exposed to the FeOAClPc, without Au-PEA thin film, the ΔE was 73 mV, confirming that only Au-PEA resulted in the immobilization of FeOAClPc. **Figure 4.6(b)** shows the CVs of (i) Au, (ii) Au-PEA and (iii) Au-PEA-FeOCAPc electrodes in the $[Ru(NH_3)_6]^{2+/3+}$. The Au-PEA-FeOCAPc, **Figure 4.6(b)(iii)** exhibited a slight increase in ΔE to 65.9 ± 4.9 mV indicating the slowed down diffusion process. The negatively charged $[Fe(CN)_6]^{3-/4-}$

was repelled by the negatively charged terminal -$COO^-$ functional group. The positively charged probe, $[Ru(NH_3)_6]^{2+/3+}$ was attracted onto the negatively charged electrode surface. The ΔE decreased from 603 ± 4.1 mV for $[Fe(CN)_6]^{3-/4-}$ to 65.9 ± 4.9 mV for $[Ru(NH_3)_6]^{2+/3+}$.

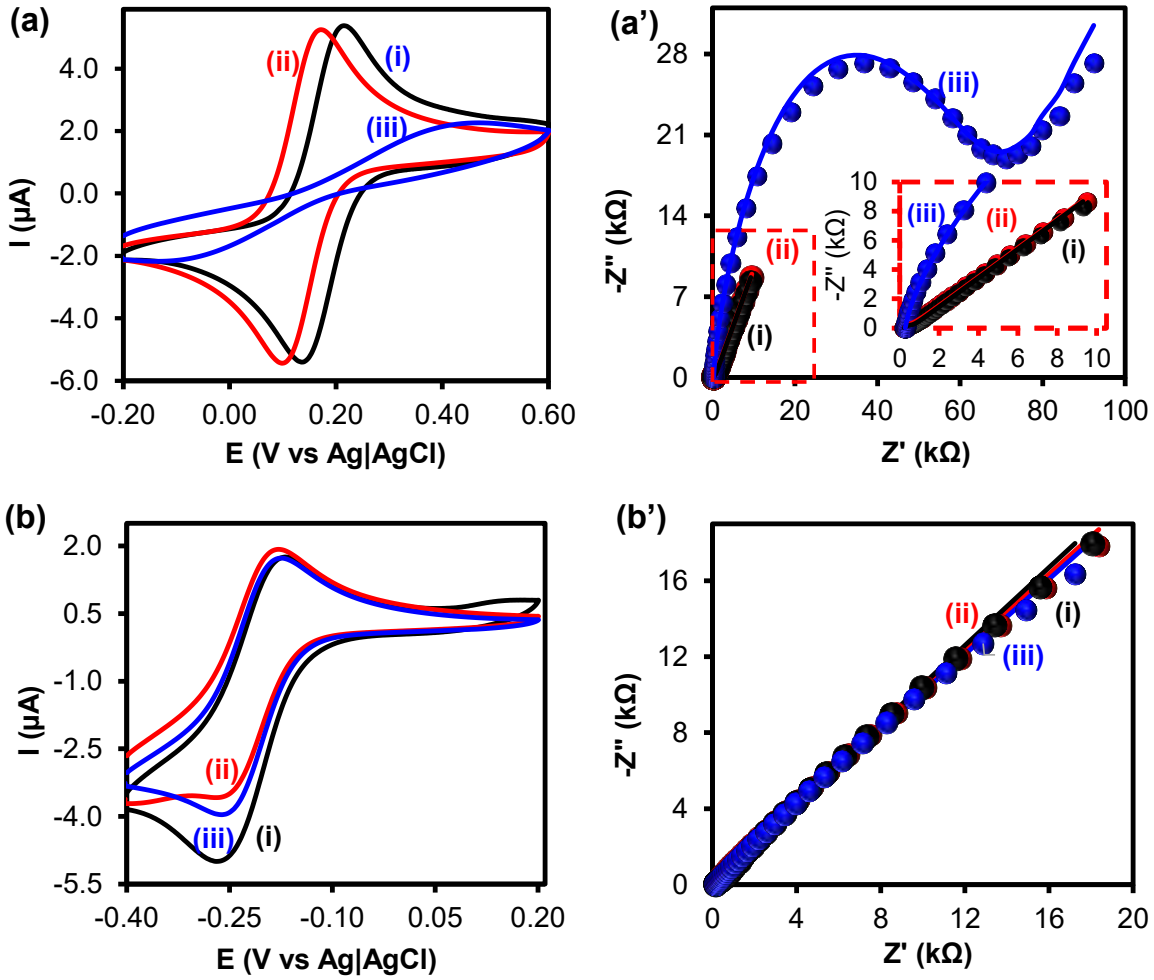


**Figure 4.6**: CVs and Nyquist plots of (i) bare Au, (ii) Au-PEA and (iii) Au-PEA-FeOCAPc measured in 2.0 mM (a) $[Fe(CN)_6]^{3-/4-}$ and (b) $[Ru(NH_3)_6]^{2+/3+}$ containing 0.10 M KCl. Scan rate = 50 $mV.s^{-1}$.

Electrochemical impedance spectroscopy (EIS) was also used to study the electron transfer behaviour of the bare and modified electrode surfaces. The EIS data was represented by Nyquist plots in **Figure 4.6** for (i) bare Au, (ii) Au-PEA and (iii) Au-PEA-

FeOCAPc in 2.0 mM (a') $[Fe(CN)_6]^{3-/4-}$ and (b') $[Ru(NH_3)_6]^{2+/3+}$ both containing 0.10 M KCl. The EIS data in $[Fe(CN)_6]^{3-/4-}$, **Figure 4.6(a')**, was measured at equilibrium potential ($E_{1/2}$ = 148 mV) for the bare electrode. The Randles-Sevcik equivalent circuit, with the topology $R_S(Q[R_{CT}Z_W])$, was used as described before [**42**] to fit the data. $R_S$ is the resistance of the solution, $R_{CT}$ is the resistance of charge-transfer, Q is either a double-layer ($C_{dL}$) or constant phase element (CPE) capacitance and $Z_W$ is the Warburg impedance. The $R_S$ is connected in series to a parallel connection of Q and $R_{CT}$ which is in series with $Z_W$. The raw and fitted data was analysed and represented as the Nyquist plot (-Z″ vs Z'). The fitted data for the bare Au and the modified surfaces is summarized in **Table 4.1**. The semi-circle on the plot at high frequency region signifies a charge transfer process and the extent of the charge-transfer resistance is represented by the diameter of the semi-circle [**1**]. It was observed that both bare Au and Au-PEA exhibited a small semi-circle diameter indicating a rapid electron transfer process. The semi-circle increased for Au-PEA-FeOCAPc. The increase in the diameter also confirmed the modification of the Au-PEA surface with FeOCAPc. Electrode modification resulted in an increase in charge-transfer resistance ($R_{CT}$). The FeOCAPc on Au-PEA-FeOCAPc blocks the surface, hindering electron transfer and hence the bigger $R_{CT}$. A slight increase in $R_{CT}$ was observed from bare Au (0.43 kΩ) to Au-PEA (0.50 kΩ) due to the thin PEA film. A significant increase in $R_{CT}$ was observed from Au-PEA (0.50 kΩ) to Au-PEA-FeOCAPc (129 kΩ). A marked increase in $R_{CT}$ for Au-PEA-FeOCAPc surface was due to electrostatic repulsion of negatively charged $-COO^-$ functional group repelling the negatively charged $[Fe(CN)_6]^{3-/4-}$ redox probe as seen on the CV studies. In the $[Ru(NH_3)_6]^{2+/3+}$ solution in **Figure 4.6(b')**, the applied potential was at $E_{1/2}$ = -218 mV. The $R_{CT}$ increased from 0.011 kΩ of the (i) bare Au to 0.11 kΩ of (ii) Au-PEA. The increase in $R_{CT}$ value was a characteristic of a

thin film of PEA with $NH_3^+$ which resulted in slight repulsion of the $[Ru(NH_3)_6]^{2+/3+}$. On Au-PEA-FeOCAPc, **Figure 4.6(b')(iii)**, the $R_{CT}$ decreased to 0.041 kΩ due to the electrostatic attraction of $[Ru(NH_3)_6]^{2+/3+}$ at negatively charged Au-PEA-FeOCAPc. EIS is an excellent technique to determine the kinetic parameters and surface coverage.

**Table 4.1**: Summary of parameters obtained from EIS in 2.0 mM $[Fe(CN)_6]^{3-/4-}$ containing 0.10 M KCl. RCT values in brackets are for $[Ru(NH_3)_6]^{2+/3+}$.

| Electrode | $R_s$ (kΩ) | $R_{CT}$ (kΩ) | Q (μF.cm$^{-2}$) | n |
|---|---|---|---|---|
| Au | 0.24 | 0.43 (0.011) | 3.00 | 0.85 |
| Au-PEA | 0.21 | 0.50 (0.11) | 0.72 | 0.81 |
| Au-PEA-FeOCAPc | 0.12 | 129 (0.040) | 0.76 | 0.83 |

The surface coverage, $\Theta$ of the modified electrode was calculated using **Equation 3.2**. The surface coverage for Au-PEA-FeOCAPc was found to be 0.997. A surface coverage, $\Theta$ close to 1 ($\Theta$ > 0.90) shows that a completely close-packed stable thin film was formed [43]. This was due to the modification of the electrode by the FeOAClPc.

The EIS data was further used to calculate the apparent electron transfer rate constant, $K_{app}$ using **Equation 3.3** [43]. The $K_{app}$ drastically decreased to 1.0 x 10$^{-7}$ cm.s$^{-1}$ for Au-PEA-FeOCAPc relative to Au and Au-PEA, **Section 3.3.4**. These results suggested that the PEA-FeOCAPc thin film blocked the surface and induced electrostatic repulsion towards the negatively charged redox couple, $[Fe(CN)_6]^{3-/4-}$.

### 4.3.5 Effect of pH of Au-PEA-FeOCAPc towards $[Fe(CN)_6]^{3-/4-}$ and $[Ru(NH_3)_6]^{2+/3+}$

A negative and positively charged redox probes were investigated at pH values ranging from pH 2.0 to pH 8.0. This was done to determine the effect of pH on the rate of electron transfer process of the Au-PEA-FeOCAPc. **Figure 4.7** shows CVs, Nyquist plots of Au-PEA-FeOCAPc measured in 2.0 mM (a) $[Fe(CN)_6]^{3-/4-}$ and (b) $[Ru(NH_3)_6]^{2+/3+}$ containing 0.10 M KCl. The CVs in **Figure 4.7(a)** showed a decrease in peak currents with an increase in pH. At pH values less than 5, the -COOH terminal groups are protonated and neutral and can allow $[Fe(CN)_6]^{3-/4-}$ redox probe to be oxidized and reduced, hence the higher peak current. The mode of mass transport for the redox probes is diffusion. The oxidation peak was also observed to shift from 261 mV to more positive potential values, 503 mV from pH 2.0 to pH 8.0 respectively. In the same manner, the reduction peak shifted from 169 mV to -132 mV, resulting in increasing ΔE. At higher pH, above the pKa value (~5) of carboxylic acid groups, the -COOH terminal groups of the Au-PEA-FeOCAPc are deprotonated and become negatively charged. Electrostatic repulsion between the Au-PEA-FeOCAPc surface and the negatively charged $[Fe(CN)_6]^{3-/4-}$ redox probe from pH 6.0 to 8.0 occurred. This makes the electron transfer difficult. The shape of the voltammograms from pH 6.0 to 8.0 clearly show this effect. In the presence of the positively charged redox probe, $[Ru(NH_3)_6]^{2+/3+}$, **Figure 4.7(b)** there was no significant changes observed in the CVs. There were also negligible changes ΔE as the pH increased from pH 2.0 to pH 8.0. The linear dependence of oxidation peak potential ($E_{pa}$) on pH in **Figure 4.7(c)** is $E_{pa}$ = 0.0579pH + 0.0369 ($R^2$ = 0.997). The slope of 57.9 mV is close to the Nernst value (59.2 mV) for a one proton and one electron transferred electrochemical process.

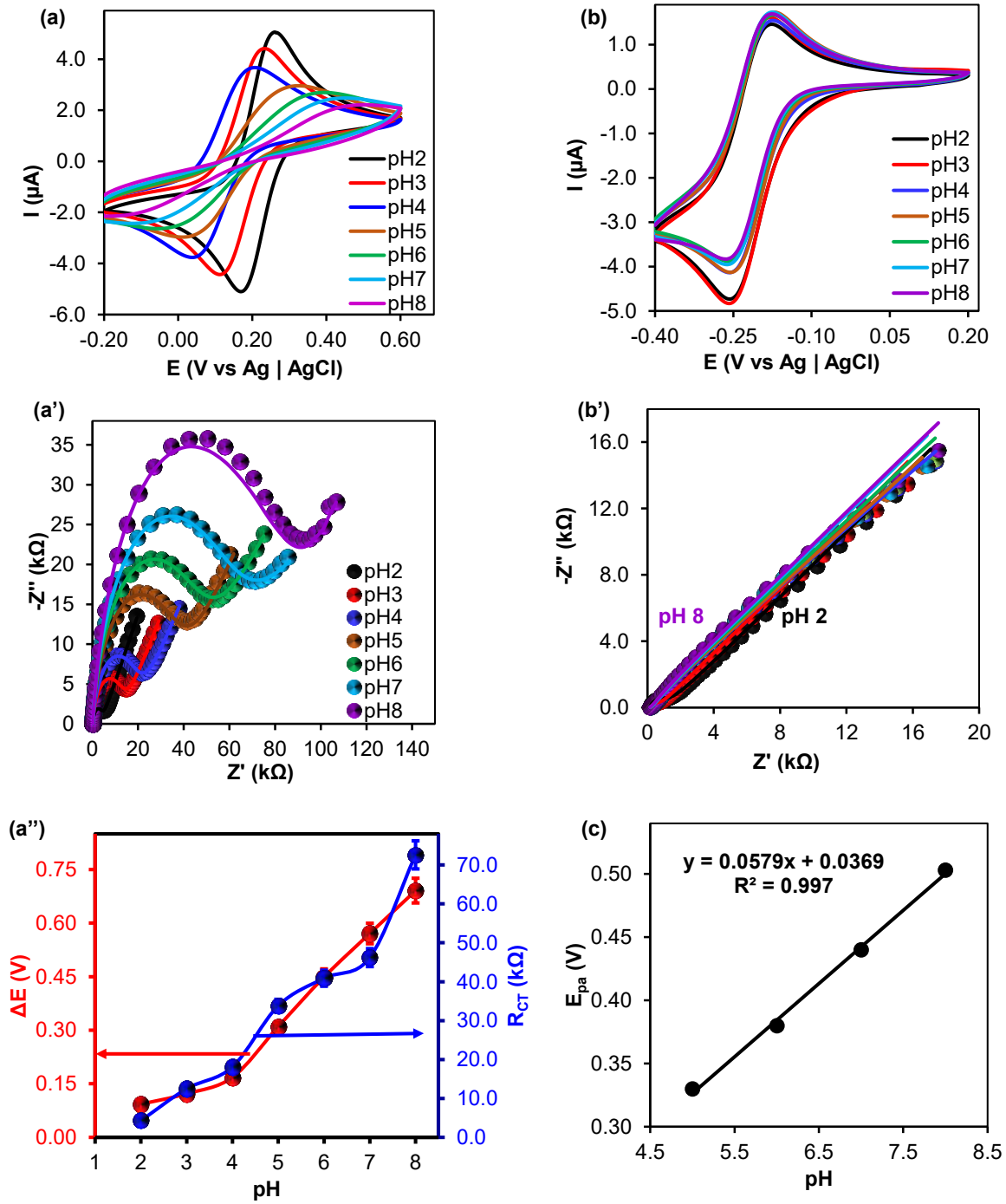


**Figure 4.7**: CVs, Nyquist plots and (a'') correlation of ΔE and $R_{CT}$ vs pH of Au-PEA-FeOCAPc measured in 2.0 mM (a) $[Fe(CN)_6]^{3-/4-}$ and (b) $[Ru(NH_3)_6]^{2+/3+}$ containing 0.10 M KCl in different pH values ranging from (i) 2.0 to (vii) 8.0. (c) $E_{pa}$ vs pH for Au-PEA-FeOCAPc in $[Fe(CN)_6]^{3-/4-}$. Scan rate 50 $mV.s^{-1}$

Towards $[Ru(NH_3)_6]^{2+/3+}$, the diffusion and migration mode of mass transport took place at Au-PEA-FeOCAPc due to charged species. The suppression of a signal is due to electrostatic repulsion between negatively charged ($-COO^-$) thin film of Au-PEA-FeOCAPc and negative redox probe, $[Fe(CN)_6]^{3-/4-}$ confirms the effect of pH on the Au-PEA-FeOCAPc. This phenomenon will play a critical role in the detection of neurotransmitters and screening of ascorbic acid (AA) and uric acid (UA) using pH sensitivity. At neutral pH (7.4), AA exists as an ascorbate anion, UA as a urate anion and $-COO^-$ deprotonated thus repulsion would occur.

The effect of pH on Au-PEA-FeOCAPc was also studied using EIS. Typical Nyquist plots are shown in **Figure 4.7(a')** for $[Fe(CN)_6]^{3-/4-}$ which show increase in $R_{CT}$. There was no significant changes observed in $R_{CT}$ for $[Ru(NH_3)_6]^{2+/3+}$, **Figure 4.7(b')**. A modified Randles-Sevcik equivalent circuit, $R_s(CPE,R_{CT})$ was used to fit the raw data and for analysis. An increase in $R_{CT}$ was observed with an increase in pH for $[Fe(CN)_6]^{3-/4-}$. This was shown by an increase $R_{CT}$ from pH 2.0 to 8.0 in **Figure 4.7(a")**. The inhibition of electron transfer due to pH changes show increase in $R_{CT}$ and $\Delta E$, **Figure 4.7(a")**.

### 4.3.6 Electrochemical detection of the neurotransmitters at Au-PEA-FeOCAPc

The electrocatalysis of Au-PEA-FeOCAPc was investigated towards the detection of catecholamine neurotransmitters. The electrochemical oxidation of the catecholamine neurotransmitters is dependent on pH. **Figure 4.8** shows CVs of Au-PEA-FeOCAPc in the (i) PBS pH 7.4 alone and (ii) PBS pH 7.4 containing 1.0 mM (a) DA, (b) EP, (c) NOR, and (d) overlaid CVs of NTs. The PBS (pH 7.4) solution alone, showed no electrochemical response, **Figure 4.8(i)**. In the presence of 1.0 mM DA, **Figure**

**4.8(a)(ii)**, an intense oxidation peak was observed at 153 mV and a reduction peak at 61.2 mV. For 1.0 mM NOR, the oxidation and reduction peaks were observed at 249 mV and 97.8 mV respectively, **Figure 4.8(b)(ii)** and for 1.0 mM EP, only an oxidation peak at 193 mV was observed with no reduction peak, **Figure 4.8(c)(ii)**. The oxidation peak currents were enhanced with small reduction peaks and this indicates the high electrocatalytic activity of Au-PEA-FeOCAPc towards all the catecholamine neurotransmitters. The potential for electro-oxidation of neurotransmitters shifted slightly in that for DA (153 mV), EP (193 mV) and for NOR (249 mV). Even though the potentials are not clearly separated, there is a 40 mV potential between DA to EP, 96 mV potential between DA and NOR, and 56 mV potential between EP and NOR. In addition, EP has no return (reduction) peak and this can be used to differentiate it from DA and NOR. There is a significant electrocatalytic peak potential overlap in **Figure 4.8(d)** thus making it difficult to discriminate between DA, NOR and EP. The electrode, Au-PEA-FeOACPc will however screen the strong interferents like AA and UA. The work is ongoing to try find methods that will discriminate between the neurotrans-mitters.

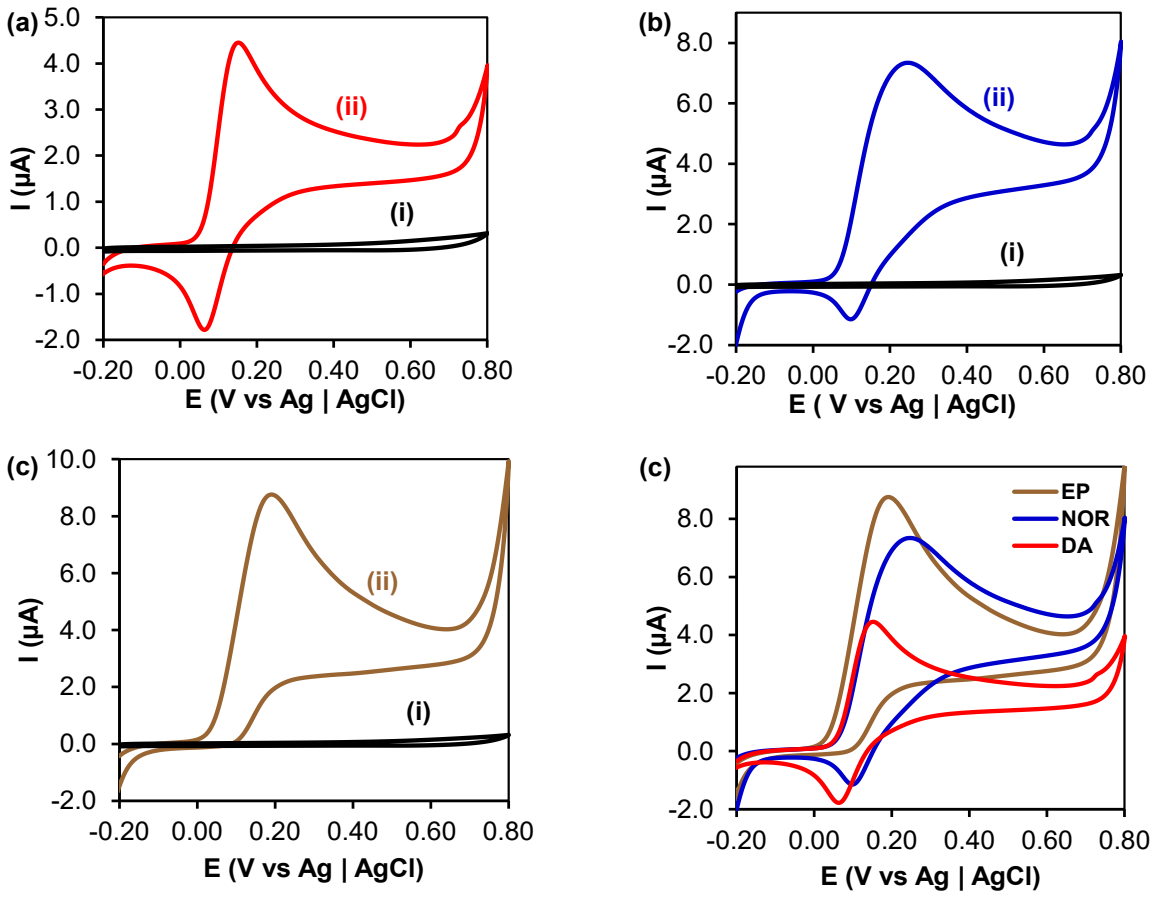


**Figure 4.8**: CVs of Au-PEA-FeOCAPc in (i) PBS (pH 7.4) alone and (ii) PBS (pH 7.4) containing 1.0 mM (a) DA, (b) NOR, (c) EP, and (d) overlaid CVs of NTs. Scan rate = 50 $mV.s^{-1}$.

### 4.3.7 Effect of scan rate on redox probes

The nature of the redox process occurring at the Au-PEA-FeOCAPc surface was studied at different scan rates. **Figure 4.9** shows CVs and linear regression for Au-PEA-FeOCAPc in 0.10 mM of (a) DA, (b) NOR and (c) EP measured at different scan rates. The redox peak current increased with an increase in the scan rate from 25 – 150 $mV.s^{-1}$. A good linearity was seen between anodic peak currents and the square root of scan rates. The results suggest that the nature of the redox process on the Au-PEA-FeOCAPc is a diffusion-controlled process.

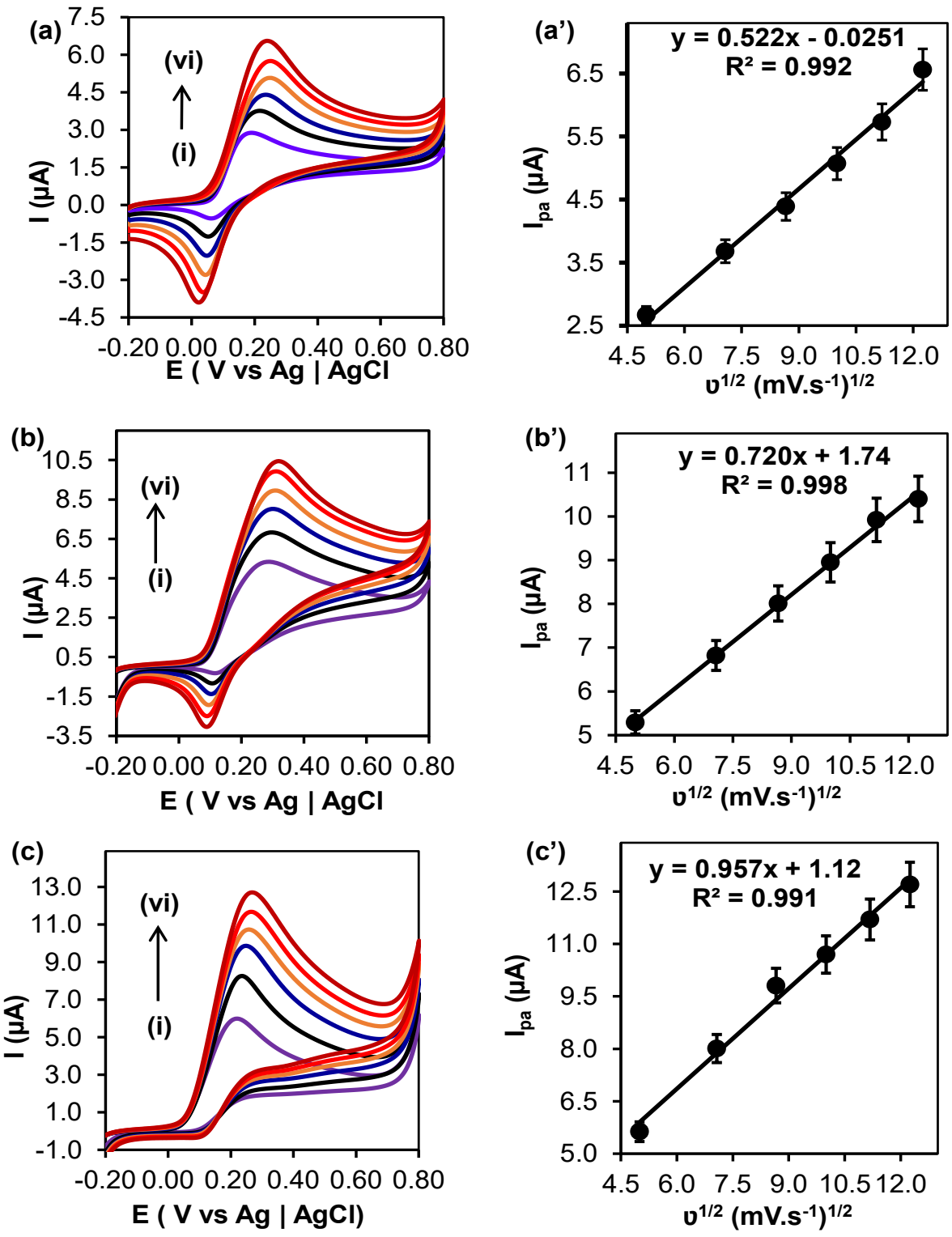


**Figure 4.9**: CVs of Au-PEA-FeOCAPc measured in PBS (pH 7.4) containing 0.10 mM (a) DA, (b) NOR and (c) EP at different scan rates (i) 25 to (vi) 150 $mV.s^{-1}$ and their corresponding linear regression.

### 4.3.8 Screening of the interferents

Ascorbic acid (AA) and uric acid (UA) interferents were both investigated on bare Au, Au-PEA and Au-PEA-FeOCAPc surfaces. **Figure 4.10** shows CVs of (i) bare Au, (ii) Au-PEA, and (iii) Au-PEA-FeOCAPc in (a) 0.10 mM ascorbic acid and (b) 10 µM uric acid. Both AA and UA showed electrocatalytic peaks at (i) bare Au and (ii) Au-PEA surfaces. At Au-PEA-FeOCAPc in **Figure 4.10(iii),** the peaks due to AA and UA were suppressed. This was due to deprotonated -$COO^-$ functional groups of the Au-PEA-FeOCAPc surface at pH 7.4 blocking the ascorbate anions of AA and urate anion of UA. At pH 7.4, the terminal -COOH functional groups of the Au-PEA-FeOCAPc are deprotonated and thus resulted in the electrostatic repulsion of the negatively charged species ($UA^-$ and $AA^-$).

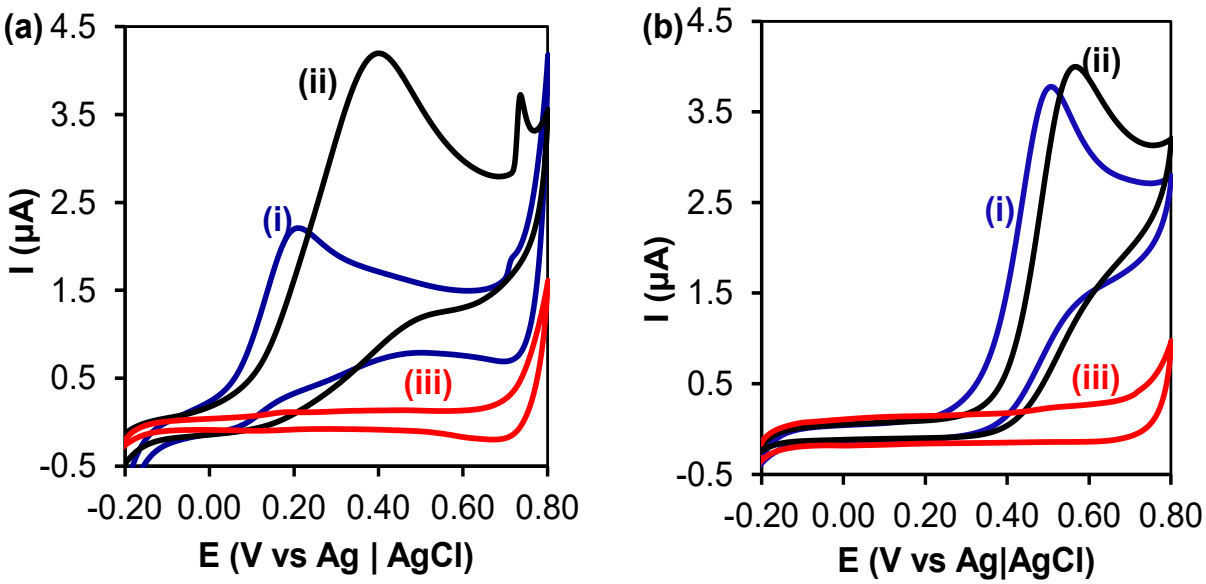


**Figure 4.10**: CVs of (i) bare Au, (ii) Au-PEA and (iii) Au-PEA-FeOCAPc in (a) 0.10 mM AA and (b) 10 µM UA.

### 4.3.9 Effect of AA and UA as interferents

The sensitive electrochemical detection of catecholamine NTs was investigated simultaneously along with ascorbic acid (AA) and uric acid (UA) as the interferents. **Figure 4.11** shows DPVs of Au-PEA-FeOCAPc in PBS (pH 7.4) containing (a) 50 μM DA, (b) 50 μM NOR, (c) 50 μM EP and mixed with 50 μM AA and 50 μM UA. Interference from AA and UA was effectively eliminated and the sensitivity of the Au-PEA-FeOCAPc was excellent towards the catecholamines NTs. Under physiological conditions (pH 7.4), catecholamine NTs are positively charged, DA (pKa 8.9), NOR (pKa 8.6), EP (pKa 8.7) while AA (pKa 4.2) and UA (pKa 5.4) are negatively charged. The negatively charged $-COO^-$ electrode surface attract the cationic species at physiological pH. As a result, an electrostatic repulsion exists between the negatively charged surface and the AA and UA anions. Therefore, electrocatalysis at the electrode surface is blocked, inhibiting the electrochemical response of AA and UA. When mixed with the catecholamine NTs, AA and UA interferents resulted in an insignificant change in the peak current and a small shoulder peak in the high potential region. The oxidation peak height of the individual catecholamine NTs is similar to that in the mixed solutions (NTs + AA + UA), suggesting effective screening of AA and UA.

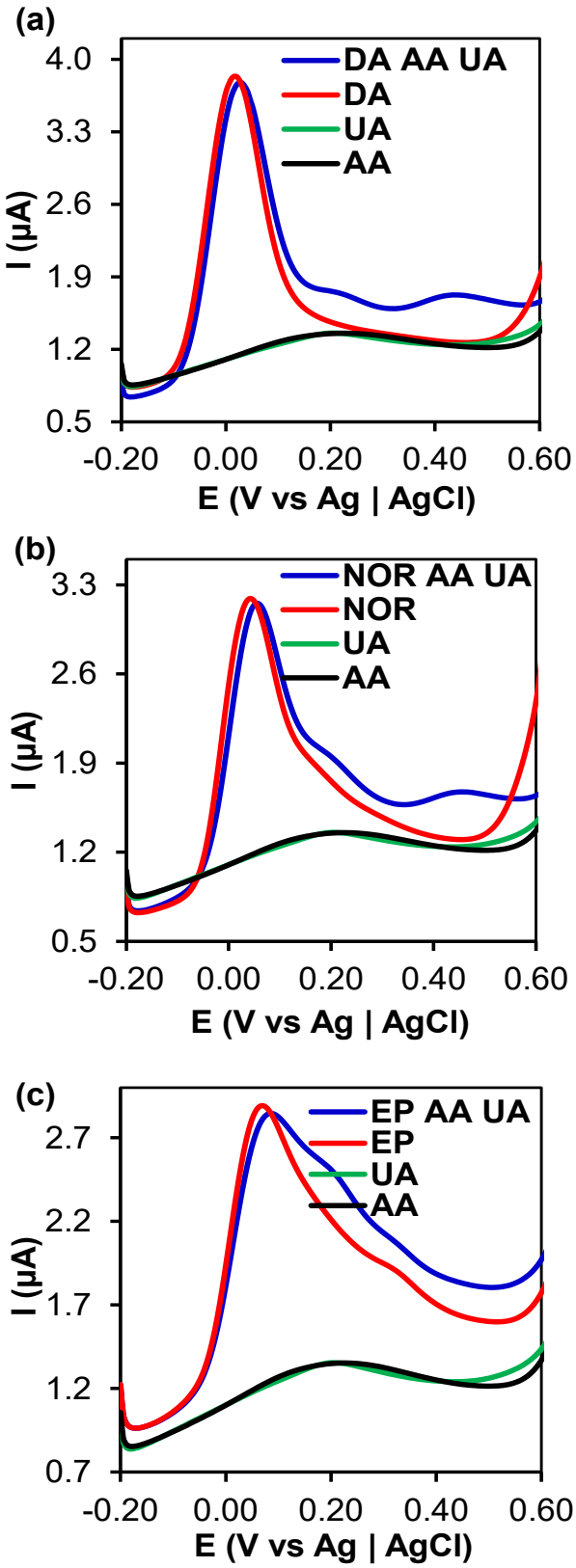


**Figure 4.11**: DPVs of Au-PEA-FeOCAPc in (a) 50 µM DA, (b) 50 µM NOR and (c) 50 µM EP, with 50 µM AA and 50 µM UA in PBS (pH 7.4). Scan rate = 50 $mV.s^{-1}$.

### 4.3.10 Electroanalysis of catecholamine neurotransmitters

Differential pulse voltammetry (DPV) was used to evaluate the effect of different concentrations of the catecholamine NTs because of its higher current sensitivity and better resolution. DPV is a more sensitive electroanalytical technique relative to cyclic voltammetry [**44,45**]. The DPVs of Au-PEA-FeOCAPc (**Figure 4.12**) in PBS (pH 7.4) alone did not show any peaks. In **Figure 4.12**, the presence of 1.0 – 50 μM concentration of (a) DA and (b) NOR and in the presence of 1.0 – 30 μM EP, an excellent electrocatalytic peak was observed at Au-PEA-FeOCAPc electrode towards DA, NOR and EP. An increase in the oxidation peak current was observed with increasing concentrations of the catecholamine NTs. The calibration curves for the oxidation peak currents gave a good linear relationship in the concentration range 1.0 μM – 50 μM for DA and NOR, and 1.0 μM – 30 μM for EP in **Figure 4.12**. The regression coefficient ($R^2$) was found to be 0.99 for all three catecholamine NTs. The limit of detection (LOD) was determined using 3σ/m (where σ is the standard deviation of voltametric blank responses and m is the slope of the linear plot). The LOD of DA and NOR was found to be 0.24 μM and 0.34 μM and a sensitivity of 1.49 $\mu A.\mu M^{-1}.cm^{-2}$ and 1.08 $\mu A.\mu M^{-1}.cm^{-2}$ respectively. Towards EP, limit of detection was found to be 0.45 μM and a sensitivity of 0.81 $\mu A.\mu M^{-1}.cm^{-2}$.

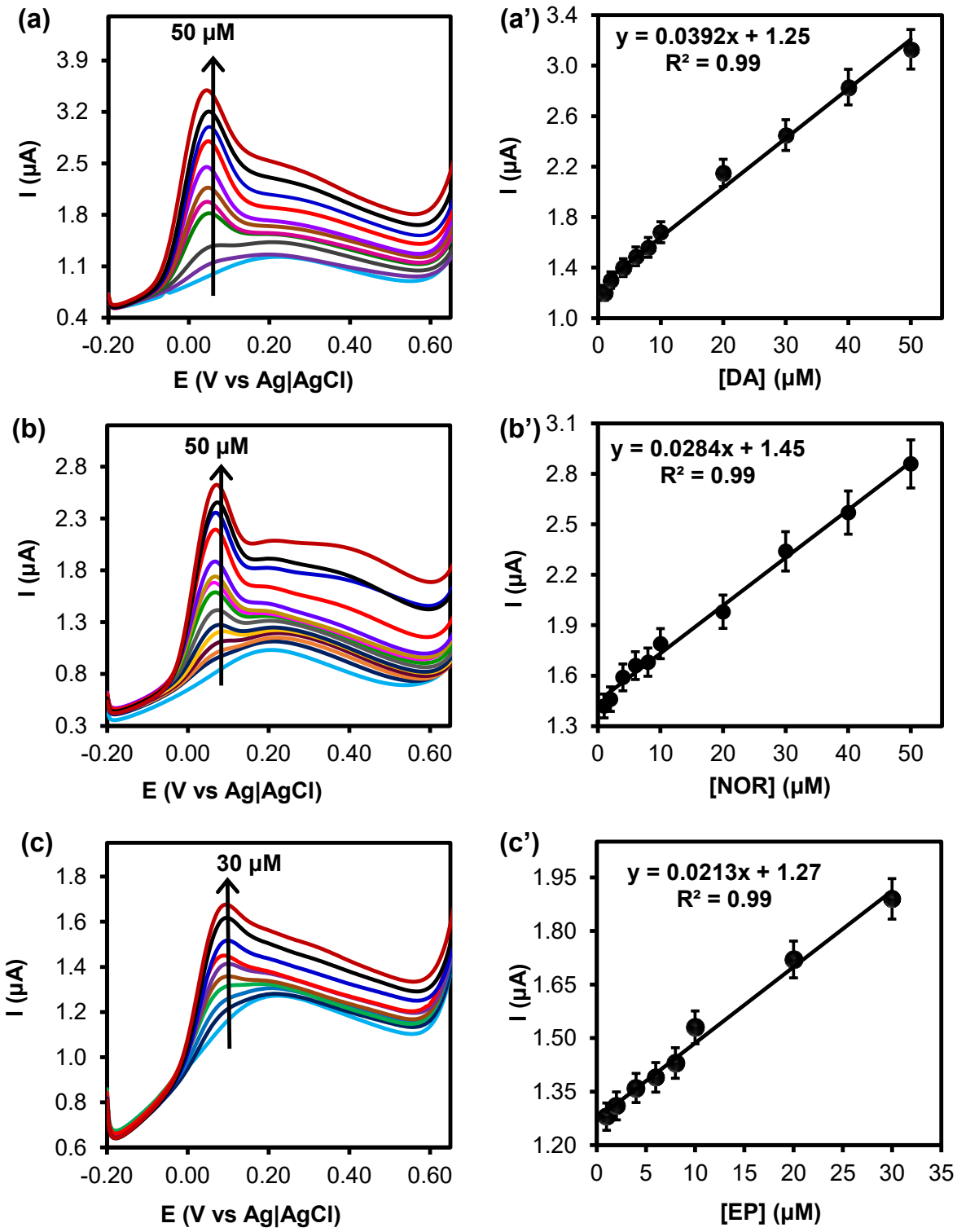


**Figure 4.12**: DPVs and calibration curves of Au-PEA-FeOCAPc in 1.0 – 50 µM of (a) DA, (b) NOR, and (c) 1.0 – 30 µM EP in PBS (pH 7.4). Scan rate = 50 $mV.s^{-1}$.

**Table 4.2** summarizes analytical parameters for Au-PEA-FeOCAPc towards detection of the catecholamine NTs compared with those reported in literature using iron phthalocyanine derivatives, their nanomaterial conjugates as well as gold nanoparticles. It is observed that our results are comparable to the reports [**22,46,47**] on the electrocatalytic detection of the neurotransmitters. The LOD for Au-PEA-FeOCAPc towards DA (0.24 µM) was comparable to the electrode modified with FePc-MWNT and lower than other FePc derivatives [**47,48**], but it was higher than for nanomaterial conjugates [**49,50**]. For NOR, the LOD obtained for Au-PEA-FeOCAPc was lower than electrodes with AuNPs [**46**] and iron oxide doped phthalocyanine [**51**]. The LOD of EP was higher than for cysteamine SAM FePc modified gold electrode [**22**] and lower than FePc/CPE electrode, as well as SAM/AuNPs gold electrode [**46,52**]. Other parameters such as limit of quantification (LOQ), (determined by 10σ/m) and linear concentration range (LCR) were determined and compared to the previously reported in the **Table 4.2**.

**Table 4.2**: Comparison of analytical parameters of electrochemical sensors reported for the detection of DA, EP and NOR.

| Analytes | $E_p$ (mV) | LOD (µM) | LOQ (µM) | LCR (µM) | Sensitivity (µA.µM.cm$^{-2}$) | Ref. |
|---|---|---|---|---|---|---|
| **DA** | 47 | 0.24 | 0.81 | 1.0 - 50 | 1.5 | [**TW**] |
| | [a]130 | 0.29 | - | 2 - 20 | 0.65 | [**47**] |
| | [b]175 | 5.65 | 20.19 | 10 - 60 | 0.40 | [**46**] |
| | [c]167 | 0.21 | - | 0.5 – 8.85 | - | [**48**] |
| | [d]212 | 0.098 | - | 0 - 60 | 0.31 | [**49**] |
| | [e] | 0.02 | - | 0.1 – 1.0 | 0.042 | [**50**] |
| **NOR** | 72 | 0.34 | 1.12 | 1.0 - 50 | 1.1 | [**TW**] |
| | [b]190 | 4.56 | 15.20 | 10 - 60 | 0.35 | [**46**] |
| | [f]208 | 2.2 | - | 7.5 - 48 | - | [**51**] |
| **EP** | 97 | 0.45 | 1.5 | 1.0 - 30 | 0.81 | [**TW**] |
| | [g]200 | 90 nM | 301 nM | 300 – 425 nM | 0.34 nA.M$^{-1}$ | [**22**] |
| | [b]205 | 4.55 | 15.16 | 10 - 60 | 0.79 | [**46**] |
| | [f]167 | 4.6 | - | 7.5 – 48 | 0.048 | [**51**] |
| | [h]401 | 0.5 | - | 1 – 300 | - | [**52**] |

TW (this work), [a]FePc/ED (iron phthalocyanine on indium tin oxide using electrode deposition), [b]Au/SAMs/AuNPs (self-assembled monolayers/gold nanoparticles), [c]FePc-MWCNT (iron phthalocyanine modified multi-walled carbon nanotubes), [d]MWCNT-nanoFeTSPc (multi-walled carbon nanotubes iron tetra-sulfo phthalocyanine), [e]GCE/CNP-FeTCAPc (iron tetracarboxylic acid phthalocyanine/ carbon nanoparticles), [f]MWCNT/$Fe_3O_4$/29H,31H-Pc/GCE (iron oxide doped phthalocyanine/ multi-walled carbon nanotube composite sensor), [g]Au-Cys-FeOCPc (cysteamine self-assembled monolayers-iron octa-carboxy phthalocyanine). [h]Fe-Pc/CPE (iron phthalocyanine modified carbon paste electrodes).

### 4.3.11 Simultaneous and mixed detection of catecholamine NTs

**Figure 4.13(a)** shows the DPV of individual NTs and their mixture. The individual NTs show peak with very small electrocatalytic peak potential differences. The mixture of NTs showed a broad electrocatalytic oxidation peak with increase in electrocatalytic current. NTs cannot be separated using DPV but Au-PEA-FeOCAPc can screen off ascorbic acid and uric acid as shown in **Figure 4.11** above. When the concentration of NOR was increased in the mixture, an increase in the electrocatalytic peak current increased, **Figure 4.13(b)**.

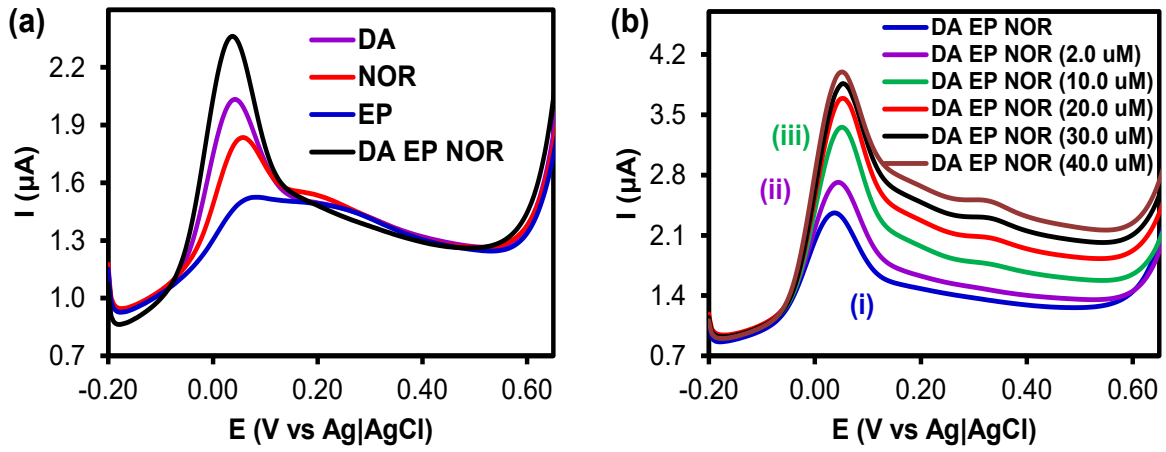


**Figure 4.13**: Simultaneous detection of the 1.0 µM DA and 1.0 µM EP and increasing concentrations of NOR (1.0 – 40.0 µM) in pH 7.4 PBS solution.

### 4.3.12 Real sample analysis

The performance of Au-PEA-FeOCAPc was investigated by detecting the catecholamine NTs in real samples (10% new-born calf serum). The serum samples were spiked with known concentration of DA, NOR, and EP. **Figure 4.14** shows the

DPVs of Au-PEA-FeOCAPc in the concentration range 1.0 µM to 50 µM of (a) DA, (b) NOR and (c) EP in the new-born calf serum, and their corresponding calibration curves. The limits of detection were found to be 0.34 µM for DA, 0.57 µM for NOR and 0.92 µM for EP. The LODs obtained in 10% new-born calf serum analysis were higher than analysis in PBS. **Table 4.3** shows the recoveries of the catecholamine NTs in the 10% new-born calf serum. The relative standard deviation (% RSD) (n = 3) was less than 6.9% showing that the Au-PEA-FeOCAPc has great potential for the determination of DA, NOR, and EP in real sample analysis.

**Table 4.3**: Determination of DA, NOR and EP in 10% new-born calf serum, (n = 3), using Au-PEAFeOCAPc.

| Analyte | Added (µM) | Found (µM) | Recovery (%) | %RSD |
|---|---|---|---|---|
| **DA** | 5 | 5.17 | 105 | 1.5 |
| | 10 | 9.69 | 96.9 | 2.4 |
| | 40 | 40.7 | 102 | 3.2 |
| **NOR** | 5 | 5.01 | 100 | 6.9 |
| | 10 | 9.35 | 93.5 | 1.5 |
| | 40 | 39.7 | 99.3 | 1.7 |
| **EP** | 6 | 6.09 | 102 | 4.1 |
| | 10 | 10.6 | 106 | 1.6 |
| | 40 | 40.6 | 101 | 2.0 |

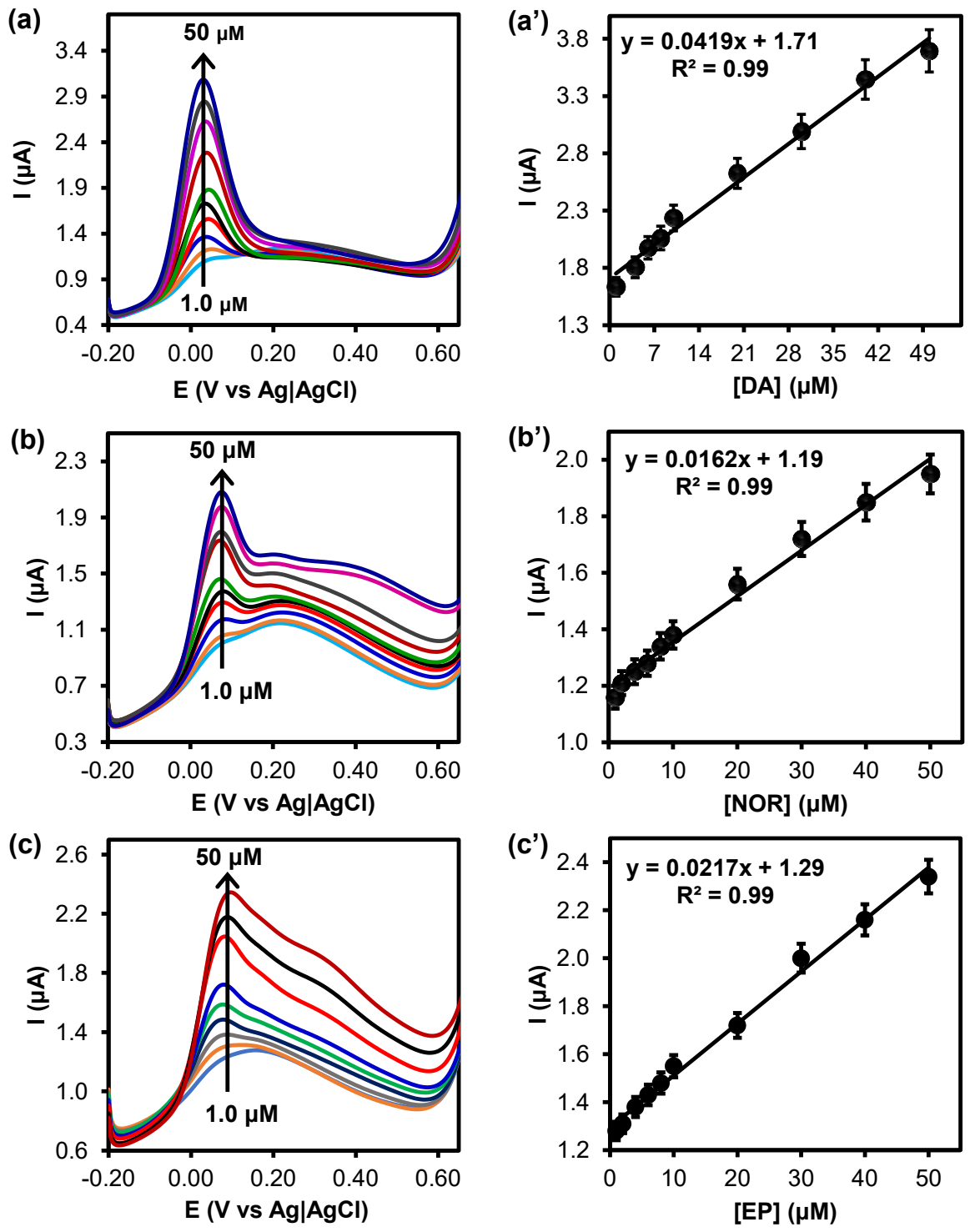


**Figure 4.14**: DPVs and calibration curves of Au-PEA-FeOCAPc in linear range 1.0 µM – 50 µM of (a) DA, (b) NOR and (c) EP in 10% new-born calf serum in PBS (pH 7.4). Scan rate = 50 $mV.s^{-1}$.

### 4.3.13 Mechanism of electrocatalysis

The oxidation potential of the catecholamine neurotransmitters was effectively catalysed at Au-PEA-FeOCAPc. The mechanism involved in electrocatalysis at MPc modified electrode surfaces is a central metal ion-based process and this is due to the potential of NT electro-oxidation peak at the same potential as metal ions [53]. The catecholamine NTs in solution diffused toward the modified Au electrode surface. At potential close to the metal ion, it get oxidized from Fe(II)OCAPc to Fe(III)OCAPc. There is a direct interaction of the hydroxyl groups on the catecholamine NTs with the high oxidation state of Fe(III) of the FeOCAPc leading to the catechol group oxidation [47]. The metal ion is simultaneously reduced back to Fe(II) as the NT is oxidized. Similar work has been reported on catalysis of dopamine and reported the pH mechanism involved [52]. **Equations 4.1** and **4.2** show the mechanism for the electrocatalysis of dopamine (DA) to dopamine-o-quinone (DAq) [54],

$$2Fe^{II}OCAPc \rightarrow 2Fe^{III}OCAPc + 2e^{-} \quad (\mathbf{4.1})$$

$$2Fe^{III}OCAPc + DA \rightarrow 2Fe^{II}OCAPc + DAq + 2H^{+} \quad (\mathbf{4.2})$$

The electrochemical oxidation of dopamine (DA) occurs via a two proton and two-electron process to yield dopamine-o-quinone (DAq). Therefore, two metal complexes are involved. Similar mechanism occurs for epinephrine and norepinephrine [52] and the oxidation occurs to the catechol moiety.

### 4.3.14 Reproducibility, stability, and repeatability

Good reproducibility was found using independently modified electrochemical sensor (Au-PEA-FeOCAPc) following similar procedure. The electrode was modified more than five times and experiments were repeated several times on each electrode. The electrochemical sensor showed excellent repeatability results with a relative standard deviation of < 5%. Ten measurements were recorded on the same Au-PEA-FeOCAPc in PBS (pH 7.4) containing 10 µM DA, **Figure 4.15**, (as a representative of the catecholamine neurotransmitters). The interferents, ascorbic acid and uric acid could not be detected after 30 days of storage of the electrochemical sensor. The results exhibited good stability of the designed electrochemical sensor. This was due to a strong Au-C bond formed through electrografting of the phenylethylamine film and the covalent amide attachment of the FeOCAPc.

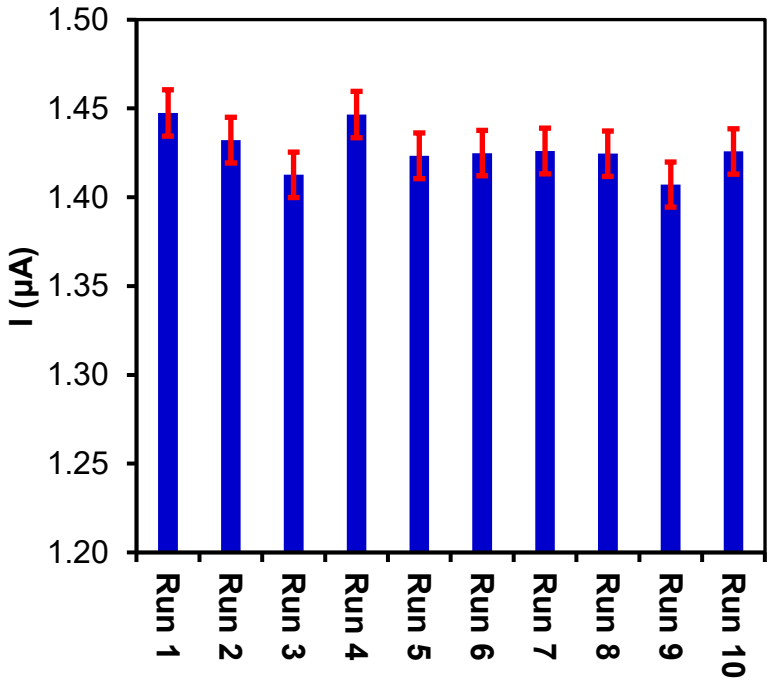


**Figure 4.15**: Variation of peak current of individual DPVs of 10 µM DA in PBS (pH 7.4) at Au-PEA-FeOCAPc.

## 4.4 Conclusions

FeOAClPc was synthesized successfully and covalently immobilized onto PEA pre-grafted gold electrode to form a thin monolayer of Au-PEA-FeOAClPc. Upon hydrolysis, -COCl functional groups were converted to -COOH functional groups on the electrode surface to yield Au-PEA-FeOCAPc. The presence of PEA and PEA-FeOCAPc was confirmed by electrochemical surface characterization using CV and electrochemical impedance spectroscopy (EIS). The -COOH terminal groups at Au-PEA-FeOCAPc are pH sensitive and confirmed by the negatively charged $[Fe(CN)_6]^{3-/4-}$ and a positively charged $[Ru(NH_3)_6]^{2+/3+}$ redox probes. This was a preliminary for cationic and screening of anionic analytes. The Au-PEA-FeOCAPc was investigated for electrocatalytic and electroanalytical properties toward catecholamine neurotransmitters (dopamine, epinephrine, and norepinephrine). The oxidation potentials were 153 mV for DA, 193 mV for EP and 249 mV for NOR using cyclic voltammetry. The ascorbic acid and uric acid could not be detected at Au-PEA-FeOCAPc due to electrostatic repulsion at physiological pH (7.4). Excellent selectivity towards catecholamine neurotransmitters was achieved. The LODs and LOQs (in brackets) for NTs were 0.24 µM (0.81 µM) for dopamine, 0.45 µM (1.5 µM) for epinephrine and 0.34 µM (1.1 µM) for norepinephrine were achieved. The electrode, Au-PEA-FeOCAPc was successfully used to detect the NTs in 10% new-born calf serum in PBS (pH 7.4) as a representative of real and complex sample matrix.

## 4.5 References


[1] P.N. Mashazi, P. Westbroek, K.I. Ozoemena, T. Nyokong, Surface chemistry and electrocatalytic behaviour of tetra-carboxy substituted iron, cobalt and manganese phthalocyanine monolayers on gold electrode, *Electrochim. Acta* 53 (**2007**) 1858–1869. https://doi.org/10.1016/j.electacta.2007.08.044.

[2] L. Tahershamsi, Y. Gerasymchuk, A. Wedzynska, M. Ptak, I. Tretyakova, A. Lukowiak, Synthesis, Spectroscopic characterization and photoactivity of Zr (IV) phthalocyanines functionalized with aminobenzoic acids and their GO-based composites, *C - J. Carbon Res.* 6 (**2019**) 1-13. https://doi.org/10.3390/c6010001.

[3] I. Özçeşmeci, A. Koca, A. Gül, Synthesis and electrochemical and in situ spectroelectrochemical characterization of manganese, vanadyl, and cobalt phthalocyanines with 2-naphthoxy substituents, *Electrochim. Acta* 56 (**2011**) 5102–5114. https://doi.org/10.1016/j.electacta.2011.03.069.

[4] J. Zhang, C. Jiang, J.P. Figueiró Longo, R.B. Azevedo, H. Zhang, L.A. Muehlmann, An updated overview on the development of new photosensitizers for anticancer photodynamic therapy, *Acta Pharm. Sin. B.* 8 (**2018**) 137–146. https://doi.org/10.1016/j.apsb.2017.09.003.

[5] K. Sakamoto, E. Ohno-Okumura, Syntheses and functional properties of phthalocyanines, *Mater. (Basel)* 2 (**2009**) 1127–1179. https://doi.org/10.3390/ma2031127.

[6] S. Arslan, Phthalocyanines: Structure, synthesis, purification and applications, *Batman Univ. J. Life Sci.* 6 (**2016**) 188–197. http://www.yasambilimleridergisi.com/makale/pdf/1466373234.pdf.

[7] I.S. Hosu, Q. Wang, A. Vasilescu, S.F. Peteu, V. Raditoiu, S. Railian, V.

Zaitsev, K. Turcheniuk, Q. Wang, M. Li, R. Boukherroub, S. Szunerits, Cobalt phthalocyanine tetracarboxylic acid modified reduced graphene oxide: A sensitive matrix for the electrocatalytic detection of peroxynitrite and hydrogen peroxide, *RSC Adv.* 5 (**2015**) 1474–1484. https://doi.org/10.1039/c4ra09781e.

[8] E. Demir, H. Silah, B. Uslu, Phthalocyanine Modified Electrodes in Electrochemical Analysis, *Crit. Rev. Anal. Chem.* 52 (**2020**) 1–37. https://doi.org/10.1080/10408347.2020.1806702.

[9] Z. Tavakolian-Ardakani, O. Hosu, C. Cristea, M. Mazloum-Ardakani, G. Marrazza, Latest trends in electrochemical sensors for neurotransmitters: A review, *Sensors* 19 (**2019**) 2037. https://doi.org/10.3390/s19092037.

[10] K. Tshenkeng, P. Mashazi, Covalent attachment of cobalt (II) tetra-(3-carboxyphenoxy) phthalocyanine onto pre-grafted gold electrode for the determination of catecholamine neurotransmitters, *Electrochim. Acta* 360 (**2020**) 137015. https://doi.org/10.1016/j.electacta.2020.137015.

[11] E.S. Bucher, R.M. Wightman, Electrochemical analysis of neurotransmitters, *Annu. Rev. Anal. Chem.* 8 (**2015**) 239–261. https://doi.org/10.1146/annurev-anchem-071114-040426.

[12] J.A. Ribeiro, P.M.V. Fernandes, C.M. Pereira, F. Silva, Electrochemical sensors and biosensors for determination of catecholamine neurotransmitters: A review, *Talanta* 160 (**2016**) 653–679. https://doi.org/10.1016/j.talanta.2016.06.066.

[13] M. Sajid, N. Baig, K. Alhooshani, Chemically modified electrodes for electrochemical detection of dopamine: Challenges and opportunities, *TrAC - Trends Anal. Chem.* 118 (**2019**) 368–385. https://doi.org/10.1016/j.trac.2019.05.042.

[14] J.K. Shashikumara, B.E.K. Swamy, Electrochemical investigation of dopamine in presence of uric acid and ascorbic acid at poly (Reactive Blue) modified carbon paste electrode: A voltammetric study, *Sensors Int.* 1 (**2020**) 100008. https://doi.org/10.1016/j.sintl.2020.100008.

[15] X. Wang, J.I.N. Baokang, L.I.N. Xiangqin, In-situ FTIR spectroelectrochemical study of dopamine at a glassy carbon electrode in a neutral solution, *Anal. Sci.* 18 (**2002**) 931–933. https://doi.org/10.2116/analsci.18.931.

[16] W.J. Barreto, S. Ponzoni, P. Sassi, A Raman and UV-vis study of catecholamines oxidized with Mn(III), *Spectrochim. Acta - Part A Mol. Biomol. Spectrosc.* 55 (**1998**) 65–72. https://doi.org/10.1016/S1386-1425(98)00164-4.

[17] V. Carrera, E. Sabater, E. Vilanova, M.A. Sogorb, A simple and rapid HPLC-MS method for the simultaneous determination of epinephrine, norepinephrine, dopamine and 5-hydroxytryptamine: Application to the secretion of bovine chromaffin cell cultures, *J. Chromatogr. B Anal. Technol. Biomed. Life Sci.* 847 (**2007**) 88–94. https://doi.org/10.1016/j.jchromb.2006.09.032.

[18] K.E. Secor, T.E. Glass, Selective amine recognition: Development of a chemosensor for dopamine and norepinephrine, *Org. Lett.* 6 (**2004**) 3727–3730. https://doi.org/10.1021/ol048625f.

[19] L.A. Kartsova, A.A. Sidorova, V.A. Kazakov, E.A. Bessonova, A.Y. Yashin, Determination of catecholamines by capillary electrophoresis and reversed-phase high-performance liquid chromatography, *Zhurnal Anal. Khimii.* 59 (**2004**) 826–831. https://doi.org/1061-9348/04/5908-0737.

[20] Y. Wei, Y. Liu, Z. Xu, S. Wang, B. Chen, D. Zhang, Y. Fang, Simultaneous detection of ascorbic acid, dopamine, and uric acid using a novel electrochemical sensor based on palladium nanoparticles/reduced graphene

oxide nanocomposite, *Int. J. Anal. Chem.* 2020 (**2020**). https://doi.org/10.1155/2020/8812443.

[21] O.K. Adeniyi, P.N. Mashazi, Stable thin films of human P53 antigen on gold surface for the detection of tumour associated anti-P53 autoantibodies, *Electrochim. Acta* 331 (**2020**) 135272. https://doi.org/10.1016/j.electacta.2019.135272.

[22] B.O. Agboola, K.I. Ozoemena, Efficient electrocatalytic detection of epinephrine at gold electrodes modified with self-assembled metallo-octacarboxyphthalocyanine complexes, *Electroanal.* 20 (**2008**) 1696–1707. https://doi.org/10.1002/elan.200804240.

[23] S. Alwarappan, G. Liu, C.Z. Li, Simultaneous detection of dopamine, ascorbic acid, and uric acid at electrochemically pretreated carbon nanotube biosensors, Nanomedicine Nanotechnology, *Biol. Med.* 6 (**2010**) 52–57. https://doi.org/10.1016/j.nano.2009.06.003.

[24] A. Liu, M. Wei, I. Honma, H. Zhou, Biosensing properties of titanate-nanotube films: Selective detection of dopamine in the presence of ascorbate and uric acid, *Adv. Funct. Mater.* 16 (**2006**) 371–376. https://doi.org/10.1002/adfm.200500202.

[25] Y. Li, J. Du, J. Yang, D. Liu, X. Lu, Electrocatalytic detection of dopamine in the presence of ascorbic acid and uric acid using single-walled carbon nanotubes modified electrode, *Colloids Surfaces B. Biointerf.* 97 (**2012**) 32–36. https://doi.org/10.1016/j.colsurfb.2012.03.029.

[26] K. Ozoemena, P. Westbroek, T. Nyokong, Cyclic voltammetric studies of octabutylthiophthalocyaninato-cobalt (II) and its self-assembled monolayer (SAM) on gold electrode, J*PP.* 6 (**2002**) 98–106.

https://doi.org/10.1142/S1088424602000130.

[27] K.I. Ozoemena, T. Nyokong, P. Westbroek, Self-assembled monolayers of cobalt and iron phthalocyanine complexes on gold electrodes: Comparative surface electrochemistry and electrocatalytic interaction with thiols and thiocyanate, *Electroanal.* 15 (**2003**) 1762–1770. https://doi.org/10.1002/elan.200302753.

[28] B.O. Agboola, K.I. Ozoemena, Self-assembly and heterogeneous electron transfer properties of metallo-octacarboxyphthalocyanine complexes on gold electrode, *Phys. Chem. Chem. Phys.* 10 (**2008**) 2399–2408. https://doi.org/10.1039/b800611c.

[29] K.I. Ozoemena, T. Nyokong, Comparative electrochemistry and electrocatalytic activities of cobalt , iron and manganese phthalocyanine complexes axially co-ordinated to mercaptopyridine self-assembled monolayer at gold electrodes, *Electrochim. Acta* 51 (**2006**) 2669–2677. https://doi.org/10.1016/j.electacta.2005.08.007.

[30] J. Nackiewicz, M. Kliber, Synthesis and selected properties of metallo and metal-free 2,3,9,10,16,17,23,24-octacarboxyphthalocyanines, *Arkivoc* 2015 (**2015**) 269–299. https://doi.org/10.3998/ark.5550190.p008.923.

[31] E.A. Kuzmina, T. V. Dubinina, N.E. Borisova, L.G. Tomilova, Octachloro- and hexadecafluoro-substituted lanthanide (III) phthalocyaninates: Synthesis and spectral properties, *Macroheterocycles* 10 (**2017**) 520–525. https://doi.org/10.6060/mhc171253d.

[32] K. Sakamoto, E. Ohno, Synthesis and electron transfer property of phthalocyanine derivatives, *Prog. Org. Coatings* 31 (**1997**) 139–145. https://doi.org/10.1016/S0300-9440(97)00029-5.

[33] W. Ma, Y.L. Ying, L.X. Qin, Z. Gu, H. Zhou, D.W. Li, T.C. Sutherland, H.Y. Chen, Y.T. Long, Investigating electron-transfer processes using a biomimetic hybrid bilayer membrane system, *Nat. Protoc.* 8 (**2013**) 439–450. https://doi.org/10.1038/nprot.2013.007.

[34] S. Griveau, D. Mercier, C. Vautrin-Ul, A. Chaussé, Electrochemical grafting by reduction of 4-aminoethylbenzenediazonium salt: Application to the immobilization of (bio)molecules, *Electrochem. Commun.* 9 (**2007**) 2768–2773. https://doi.org/10.1016/j.elecom.2007.09.004.

[35] A. Kalkan, Z.A. Bayir, Phthalocyanines with rigid carboxylic acid containing pendant arms, *Polyhedron* 25 (**2006**) 39–42. https://doi.org/10.1016/j.poly.2005.06.056.

[36] F. Hacivelioğlu, M. Durmuş, S. Yeşilot, A.G. Gürek, A. Kiliç, V. Ahsen, The synthesis, spectroscopic and thermal properties of phenoxycyclotriphosphazenyl-substituted phthalocyanines, *Dye. Pigment* 79 (**2008**) 14–23. https://doi.org/10.1016/j.dyepig.2007.12.010.

[37] T.O. Nicolescu, Interpretation of Mass Spectra (Fourth Edition), (**2018**) 350. https://doi.org/http://dx.doi.org/10.5772/intechopen.68595.

[38] P. Mashazi, E. Antunes, T. Nyokong, Probing electrochemical and electrocatalytic properties of cobalt(II) and manganese(III) octakis(hexylthio)phthalocyanine as self-assembled monolayers, *JPP.* 14 (**2010**) 932–947. https://doi.org/10.1142/S108842461000277X.

[39] A. Kumar, D. Naumenko, L. Cozzarini, L. Barba, A. Cassetta, M. Pedio, Influence of substrate on molecular order for self-assembled adlayers of CoPc and FePc, *J. Raman Spectrosc.* 49 (**2018**) 1015–1022. https://doi.org/10.1002/jrs.5344.

[40] D. Bélanger, J. Pinson, Electrografting: A powerful method for surface modification, *Chem. Soc. Rev.* 40 (**2011**) 3995–4048. https://doi.org/10.1039/c0cs00149j.

[41] J.J. Gooding, Advances in interfacial design for electrochemical biosensors and sensors: Aryl diazonium salts for modifying carbon and metal electrodes, *Electroanal.* 20 (**2008**) 573–582. https://doi.org/10.1002/elan.200704124.

[42] P. Mashazi, T. Nyokong, Electrocatalytic studies of covalently immobilized metal tetra-amino phthalocyanines onto derivatized screen-printed gold electrodes, *Microchim. Acta* 171 (**2010**) 321–332. https://doi.org/10.1007/s00604-010-0438-6.

[43] S. Khene, D.A. Geraldo, C.A. Togo, J. Limson, T. Nyokong, Synthesis, electrochemical characterization of tetra- and octa-substituted dodecyl-mercapto tin phthalocyanines in solution and as self-assembled monolayers, *Electrochim. Acta* 54 (**2008**) 183–191. https://doi.org/10.1016/j.electacta.2008.08.018.

[44] S. Banerjee, S. McCracken, M. Faruk Hossain, G. Slaughter, Electrochemical detection of neurotransmitters, *Biosens.* 10 (**2020**) 101. https://doi.org/10.3390/bios10080101.

[45] C. Luhana, I. Moyo, K. Tshenkeng, P. Mashazi, In-sera selectivity detection of catecholamine neurotransmitters using covalent composite of cobalt phthalocyanine and aminated graphene quantum dots, *Microchem. J.* 180 (**2022**) 107605. https://doi.org/10.1016/j.microc.2022.107605.

[46] S. Ramirez, N. Silva, M.P. Oyarzun, J. Pavez, J.F. Silva, Gold nanostructures on self-assembled monolayers activity for epinephrine, noradrenaline and dopamine, *J. Electroanal. Chem.* 799 (**2017**) 349–357.

https://doi.org/10.1016/j.jelechem.2017.06.040.

[47] C.S. Martin, P. Alessio, F.N. Crespilho, C.M.A. Brett, C.J.L. Constantino, Influence of the supramolecular arrangement of iron phthalocyanine thin films on catecholamine oxidation, *J. Electroanal. Chem.* 836 (**2019**) 7–15. https://doi.org/10.1016/j.jelechem.2019.01.029.

[48] D. Patrascu, I. David, V. David, C. Mihailciuc, I. Stamatin, J. Ciurea, L. Nagy, G. Nagy, A.A. Ciucu, Selective voltammetric determination of electroactive neuromodulating species in biological samples using iron (II) phthalocyanine modified multi-wall carbon nanotubes paste electrode, *Sensors Actuators, B Chem.* 156 (**2011**) 731–736. https://doi.org/10.1016/j.snb.2011.02.027.

[49] O.O. Fashedemi, K.I. Ozoemena, A facile approach to the synthesis of hydrophobic iron tetrasulfophthalocyanine (FeTSPc) nano-aggregates on multi-walled carbon nanotubes: A potential electrocatalyst for the detection of dopamine, *Sensors Actuators, B Chem.* 160 (**2011**) 7–14. https://doi.org/10.1016/j.snb.2011.06.085.

[50] C.P. Keshavananda Prabhu, M. Nemakal, S. Aralekallu, I. Mohammed, M. Palanna, V.A. Sajjan, D. Akshitha, L.K. Sannegowda, A comparative study of carboxylic acid and benzimidazole phthalocyanines and their surface modification for dopamine sensing, *J. Electroanal. Chem.* 847 (**2019**) 113262. https://doi.org/10.1016/j.jelechem.2019.113262.

[51] N.G. Mphuthi, A.S. Adekunle, E.E. Ebenso, Electrocatalytic oxidation of epinephrine and norepinephrine at metal oxide doped phthalocyanine/MWCNT composite sensor, *Sci. Rep.* 6 (**2016**) 1–20. https://doi.org/10.1038/srep26938.

[52] S. Shahrokhian, M. Ghalkhani, M.K. Amini, Application of carbon-paste electrode modified with iron phthalocyanine for voltammetric determination of

epinephrine in the presence of ascorbic acid and uric acid, *Sensors Actuators, B Chem.* 137 (**2009**) 669–675. https://doi.org/10.1016/j.snb.2009.01.022.

[53] T.F. Kang, G.L. Shen, R.Q. Yu, Voltammetric behaviour of dopamine at nickel phthalocyanine polymer modified electrodes and analytical applications, *Anal. Chim. Acta* 356 (**1997**) 245–251. https://doi.org/10.1016/S0003-2670(97)00383-8.

[54] J. Oni, T. Nyokong, Simultaneous voltammetric determination of dopamine and serotonin on carbon paste electrodes modified with iron(II) phthalocyanine complexes, *Anal. Chim. Acta* 434 (**2001**) 9–21. https://doi.org/10.1016/S0003-2670(01)00822-4.

# Chapter 5

## 5 Discussions

### 5.1 Electrografting

The two electrochemical sensors, Au-PEA-CoOCAPc and Au-PEA-FeOCAPc, were developed by modifying a gold electrode by electrografting an aryl diazonium salt, aminoethyl benzene diazonium salt (AEBD). Electrografting has been the subject of great research interest due to the strong covalent bond that forms between the aryl derivative radical and the substrate. This results in a more stable layer compared to alkanethiol-SAMs [1,2]. The research has led to (i) demonstration of covalent bonding of the aryl groups on gold and on carbon [3,4], (ii) reasonable control of the films that are formed on surfaces, and (iii) description of mechanisms involved in the electrochemical grafting reaction and in the further growth of the film [1]. A less time-consuming approach is grafting the electrode in-situ where the aryl diazonium salt is generated onto the surface in an acidic aqueous solution. However, the challenge is that the exact concentration of the diazonium salt in solution cannot be known which is a very important parameter in the control of the film [5]. In the present study, AEBD salt was synthesized and then used for electrografting on Au electrode. The benefit of this approach is that the amount of the diazonium salt can be controlled. The synthesized salt can be stored for later use, which saves both reagents and time. Two mechanisms are involved in the electrografting process. Firstly, the formation of an aryl radical by electrochemical reduction of aryl diazonium ion and then covalent attachment of the radical on the surface. A strong and stable covalent bond was formed through electrografting of AEBD on Au yielding a thin monolayer of phenylethylamine (PEA).

## 5.2 pH sensitivity of the electrochemical sensors

Ascorbic acid and uric acid co-exist with catecholamine neurotransmitters in real samples. They are strong interferents because they are oxidized at potentials close to those of the catecholamine neurotransmitters, resulting in the overlapping of voltammetric response. A preliminary study was done to investigate the effect of pH in the detection of the catecholamine neurotransmitters and screening of the interferents. Both ascorbic acid and uric acid were detected on bare Au and Au-PEA surfaces. **Table 5.1** shows a summary of the oxidation potentials ($E_{pa}$) of AA and UA at bare Au and Au-PEA surfaces.

**Table 5.1**: Summary of oxidation potentials of AA and UA.

| **Surface** | **AA ($E_{pa}$ / mV)** | **UA ($E_{pa}$ / mV)** |
|---|---|---|
| Au | 213 | 505 |
| Au-PEA | 403 | 566 |
| Au-PEA-CoOCAPc | - | - |
| Au-PEA-FeOCAPC | - | - |

No oxidation of ascorbic acid and uric acid was observed on both Au-PEA-CoOCAPc and Au-PEA-FeOCAPc. This was attributed to the pH sensitive -COOH functional groups of the electrochemical sensors which are deprotonated at pH 7.4. Under physiological conditions (pH 7.4), the interferents are negatively charged, AA (pKa 4.2) and UA (pKa 5.4) while the surface of the electrochemical sensor is also negatively charged ($-COO^-$). An electrostatic repulsion effect was experienced between the negatively charged surface and the anionic ascorbate and urate ions. Therefore, an

electron transfer at surface of the sensor was blocked and AA and UA were effectively screened off with no electrochemical response.

## 5.3 Detection of catecholamine NTs at Au-PEA-CoOCAPc and Au-PEA-FeOCAPc

Detection of the catecholamine neurotransmitters at Au-PEA-CoOCAPc and Au-PEA-FeOCAPc was investigated at physiological conditions. The catecholamine neurotransmitters have pKa values above 8.0 and possess a net positive at pH 7.4 charge due to ($-NH_3^+$). The surface of the sensors is deprotonated bearing negatively charged carboxyl functional groups ($-COO^-$). An electrostatic attraction resulted between the negatively charged $-COO^-$ terminal functional groups of either Au-PEA-CoOCAPc or Au-PEA-FeOCAPc and the protonated amino functional group ($-NH_3^+$) of the catecholamine neurotransmitters. An electron transfer process occurred, and the catecholamine neurotransmitters were oxidized. Catecholamine neurotransmitters are oxidized in region for metal oxidation and hence the oxidation mechanism is a metal-based process. The redox potentials for the oxidation of the catecholamine neurotransmitters at Au-PEA-CoOCAPc and Au-PEA-FeOCAPc are summarized in **Table 5.2**.

**Table 5.2**: Comparison of electrocatalysis of Au-PEA-CoOCAPc and Au-PEA-FeOCAPc towards the detection of DA, NOR and EP.

| | **AuPEA-CoOCAPc** | | **Au-PEA-FeOCAPc** | |
|---|---|---|---|---|
| | $E_{ox}$ (mV) | $E_{red}$ (mV) | $E_{ox}$ (mV) | $E_{red}$ (mV) |
| **DA** | 193 | 12.4 | 153 | 61.2 |
| **EP** | 241 | - | 193 | - |
| **NOR** | 246 | 90.5 | 249 | 97.5 |

First row transition metal complexes have over the years shown to be excellent electrocatalysts due to their interesting redox properties [6–8]. The catalytic detection of DA, EP and NOR was observed to exhibit comparable oxidation and reduction potentials between the two electrochemical sensors. Literature has reported iron phthalocyanine complexes having faster rate of electron transfer [9] relative to cobalt phthalocyanine complexes. Iron is more easily oxidized than cobalt Pcs [10] and hence FePc is expected to lower the oxidation potential. In this study, DA was detected at less energy values at Au-PEA-FeOCAPc by 40 mV than at Au-PEA-CoOCAPc. An improved electrocatalytic effect of FeOCAPc was also observed for EP, oxidized at much lower potential, a potential difference of 48 mV when compared to Au-PEA-CoOCAPc. However, NOR was oxidized at similar potential at either Au-PEA-CoOCAPc or Au-PEA-FeOCAPc. A similar trend was observed for the oxidation potentials, NOR > EP > DA for both the electrochemical sensors.

## 5.4 References


[1] D.M. Shewchuk, M.T. McDermott, Comparison of diazonium salt derived and thiol derived nitrobenzene layers on gold, *Langmuir* 25 (**2009**) 4556–4563. https://doi.org/10.1021/la8040083.

[2] S. Kesavan, S.B. Revin, S.A. John, Fabrication, characterization and application of a grafting based gold nanoparticles electrode for the selective determination of an important neurotransmitter, *J. Mater. Chem.* 22 (**2012**) 17560–17567. https://doi.org/10.1039/c2jm33013j.

[3] J.J. Gooding, Advances in interfacial design for electrochemical biosensors and sensors: Aryl diazonium salts for modifying carbon and metal electrodes, *Electroanal.* 20 (**2008**) 573–582. https://doi.org/10.1002/elan.200704124.

[4] A.L. Gui, G. Liu, M. Chockalingam, G.L. Saux, J.B. Harper, J.J. Gooding, A comparative study of modifying gold and carbon electrode with 4-Sulfophenyl diazonium salt, *Electroanal.* 22 (**2010**) 1283–1289. https://doi.org/10.1002/elan.200900615.

[5] J. Pinson, F. Podvorica, Attachment of organic layers to conductive or semiconductive surfaces by reduction of diazonium salts, *Chem. Soc. Rev.* 34 (**2005**) 429–439. https://doi.org/10.1039/b406228k.

[6] K. De Wael, A. Adriaens, Comparison between the electrocatalytic properties of different metal ion phthalocyanines and porphyrins towards the oxidation of hydroxide, *Talanta* 74 (**2008**) 1562–1567. https://doi.org/10.1016/j.talanta.2007.09.034.

[7] K. Ozoemena, P. Westbroek, T. Nyokong, Long-term stability of a gold

electrode modified with a self-assembled monolayer of octabutylthiophthalocyaninato-cobalt(II) towards L-cysteine detection, *Electrochem. Commun.* 3 (**2001**) 529–534. https://doi.org/10.1016/S1388-2481(01)00213-2.

[8] P. Mashazi, T. Nyokong, Electrocatalytic studies of covalently immobilized metal tetra-amino phthalocyanines onto derivatized screen-printed gold electrodes, *Microchim. Acta* 171 (**2010**) 321–332. https://doi.org/10.1007/s00604-010-0438-6.

[9] K.I. Ozoemena, T. Nyokong, Comparative electrochemistry and electrocatalytic activities of cobalt , iron and manganese phthalocyanine complexes axially co-ordinated to mercaptopyridine self-assembled monolayer at gold electrodes, *Electrochim. Acta* 51 (**2006**) 2669–2677. https://doi.org/10.1016/j.electacta.2005.08.007.

[10] B. Agboola, T. Nyokong, Comparative electrooxidation of nitrite by electrodeposited Co(II), Fe(II) and Mn(III) tetrakis (benzylmercapto) and tetrakis (dodecylmercapto) phthalocyanines on gold electrodes, *Anal. Chim. Acta* 587 (**2007**) 116–123. https://doi.org/10.1016/j.aca.2007.01.031.

# Chapter 6

## 6 Conclusions and future perspectives

### 6.1 Conclusions

The synthesis of cobalt and iron octa acyl chloride phthalocyanines (CoOAClPc, FeOAClPc) was successfully achieved. The synthesized MPc complexes were confirmed by FT-IR spectroscopy, UV-vis spectroscopy, MCD, and mass spectroscopy. CoOAClPc and FeOAClPc were each immobilized onto a PEA pre-grafted gold electrode surface, Au-PEA, by amidation to yield Au-PEA-CoOAClPc and Au-PEA-FeOAClPc respectively. The amine functional groups on PEA reacted with the acyl chloride functional groups to form an amide bond. On hydrolysis of the unreacted acyl chloride terminal functional groups, carboxylic acid functional groups were formed, yielding Au-PEA-CoOCAPc and Au-PEA-FeOCAPc. Electrochemical methods (cyclic voltammetry and electrochemical impedance spectroscopy) were used to characterize the sensing electrodes, Au-PEA-CoOCAPc and Au-PEA-FeOCAPc. The X-ray photoelectron spectroscopy conclusively showed the successful immobilization of the MPcs onto the PEA surface. Two redox species were used for preliminary studies, a negatively charged $[FeCN_6]^{3-/4-}$ and a positively charged $[Ru(NH_3)_6]^{2+/3+}$ probes. The sensing electrodes exhibited pH selectivity and sensitivity towards the redox probes. The electrocatalytic and electroanalysis studies towards the detection of DA, EP, and NOR were investigated using sensing electrodes at pH 7.4. The modification process exhibited good reproducibility and the modified electrodes showed excellent sensitivity, electrocatalytic and electroanalytical properties towards the catecholamine NTs. The electroanalytical parameters obtained from differential pulse voltammetry exhibited good limits of detection. A good linearity was observed

for the studied concentration range up to 50 μM. The LOD was found to be 64 nM for DA, 0.22 μM for EP and 0.17 μM for NOR using Au-PEA-CoOCAPc. At the Au-PEA-FeOCAPc, the LOD was found to be 0.24 μM for DA, 0.45 μM for EP and 0.34 μM for NOR. The sensors blocked the signal due to GA, AA, and UA as strong interferents. The Au-PEA-FeOCAPc was evaluated for its potential application in real sample analysis, and it showed good percentage recoveries. The systems studied in this work show promising methods and results and may be used for the detection of catecholamine NTs and screen off interferents.

## 6.2 Future perspectives

The designed electrochemical sensors do not discriminate between the catecholamine neurotransmitters. The catecholamine NTs were detected individually and the difference in the potential is not enough to detect them simultaneously. A future study of these systems is to explore the incorporation of polymers and/or molecular-imprinted polymers and their effect on the electrocatalytic signal when integrated with phthalocyanine complexes. Measurement of NTs is a brain analysis, therefore future work would require the use of ultra-microelectrodes with small (μm) diameter which can act as probes. Increasing sensitivity of the electrodes is also another area of interest. Incorporating nanomaterials with MPcs is a subject that needs to be pursued further.